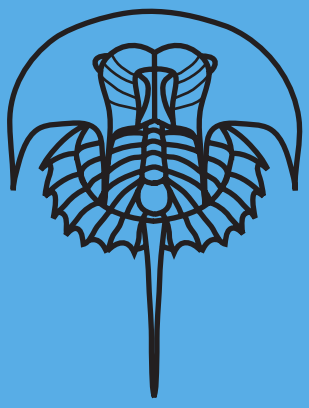

TREATISE ONLINE

Number 182

Part T, Revised, Volume 1
Anatomy of Internal Organs: Crinoidea

Thomas Heinzeller and Bernard Ruthensteiner

2024

KU PALEONTOLOGICAL INSTITUTE
The University of Kansas

Lawrence, Kansas, USA
https://journals.ku.edu/treatiseonline

PART T, REVISED, VOLUME 1, TREATISE ONLINE 182

ANATOMY OF INTERNAL ORGANS

Thomas Heinzeller[1] and Bernhard Ruthensteiner[2]

[1,2]SNSB-Bavarian State Collection of Zoology, Munich, Germany, heinzeller@lrz.uni-muenchen.de; ruthensteiner@snsb.de]

Dedicated to Nicholas Holland, Professor Emeritus of Marine Biology at University of California San Diego, in recognition of his pioneering work on crinoid morphology.

I. RETROSPECT AND GOAL

During the late nineteenth century, light microscopes had been developed with greatly improved resolution. This resulted in a boost in structural light microscopic studies throughout biology. Echinoderm research also benefited from this, and fundamental insights into the internal organization of crinoids were gained by several scientists. The early studies, such as those of P. H. Carpenter (1884) or Hamann (1889), to name just a few examples, still form the basis of present knowledge on crinoid soft part anatomy. These and later structural studies were compiled in review articles, perhaps the most significant of which were those by Chadwick (1907), A. H. Clark (1921), Cuénot (1948), Hyman (1955), and Nichols (1967).

At the time when Breimer (1978) wrote his chapter on the anatomy of crinoids for Treatise, Part T, Vol. 2, only this traditional knowledge was available. At the same time, extended light microscopic methods, for example immunohistochemistry and electron microscopy, were increasingly applied for the analysis of crinoid anatomy; among the earliest were Goyette (1967) and Holland (1969). The knowledge gained in the studies of the following three decades led to a clearer understanding and reevaluation of the structures previously reported by conventional light microscopists. The change in perspective is one of three-dimensional (3D) analysis, which is readily accessible today through computer technology, which greatly facilitates spatial understanding of the structures. Another reason for the change in perspective was mentioned by Breimer himself when he wrote: "The section on anatomy is largely based on literature data, taken from older works on the subject." He also complained about the limitation to a single species: "the species *Antedon bifida* has developed in literature … as a model crinoid for zoologists," and he called for a "special emphasis on stalked forms belonging to the Isocrinida, Millericrinida, Bourgeticrinida, and Cyrtocrinida" (Breimer 1978, p. 10).

The aim of this article is to provide as up-to-date and comprehensive an overview as possible on the anatomy of the entire group of recent crinoids. To this end, we studied, first, a variety of feather star species and, second, several species of the isocrinid, bourgeticrinid, and cyrtocrinid groups.

MATERIAL

This article presents 3D organ models of four specimens (Fig. 1), two of which represent the feather star group and one each for the bourgeticrinid and isocrinid group. More precisely, these four animals are a *Leptometra* sp. juvenile—already free swimming, a juvenile *Metacrinus* sp., as well as adult specimens of *Dorometra nana* (Hartlaub, 1890) and *Democrinus chuni* (Döderlein, 1907). This material was chosen for its small size; the specific name "*nana*" of *Dorometra* marks

Treatise Online is a publication of The University of Kansas, Paleontological Institute,

Cite: Heinzeller, Thomas, & Bernard Ruthensteiner. 2024. Part T, Revised, Volume 1, Anatomy of Internal Organs: Crinoidea. Treatise Online 182:1–81, 80 fig. [https://doi.org/10.17161/to.vi.22577]

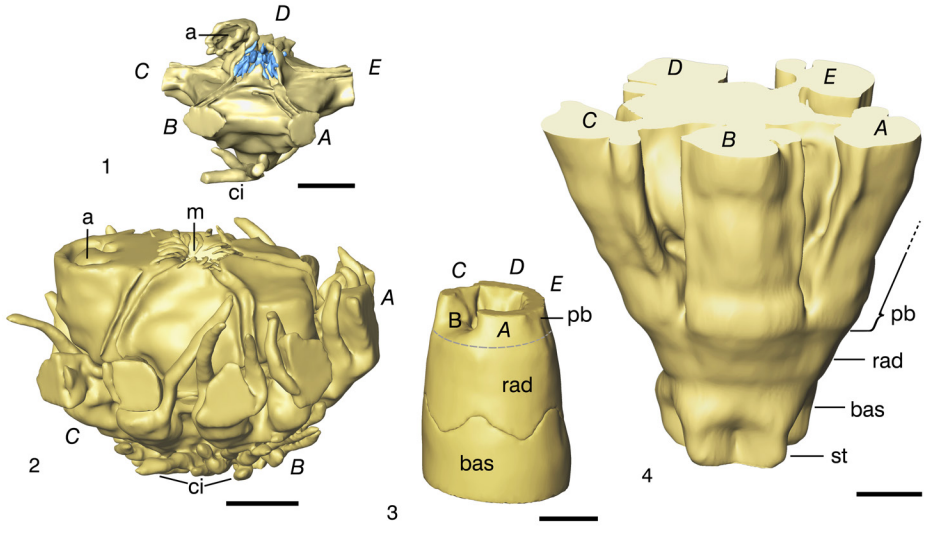

Fig. 1. 3D models of external view of the specimens. *1, Leptometra* sp. (mouth tentacles blue to distinguish tentacles and valves). *2, Dorometra nana* (Hartlaub, 1890). *3, Democrinus chuni* (Döderlein, 1907). *4, Metacrinus* sp. (although the boundaries of ossicles become blurred in decalcified specimens, the position of some ossicles is indicated in *3* and *4*). All scale bars 0.5 mm. Labels: *A–E* =rays, a=anal opening, ci=cirri (truncated), m=mouth opening with tentacles. bas=basal, rad=radial, pb=series of primibrachials, st=stalk. Images new, by authors.

this species as a dwarf among crinoids. This allowed the preparation of complete histological section series oriented horizontally and extending from the aboral end of the body to the tegmen in *Leptometra* and *Dorometra*. The *Bathycrinus* specimen included an oral portion of the basals, the radials, and the initial segments of the primibrachials. In *Metacrinus* sp., the series of sections extended from the very first columnals to the level of the esophagus. This was the basic material for the creation of various organ models using the 3D analysis software system AMIRA. The external aspects of these preparations are shown in Fig. 1.

In addition to these four species, material of the following crinoid taxa (general classification after Messing, 2023; concerning the Suborder Bathycrinina after H. Hess, C. G. Messing, & W. I. Ausich, 2011) is used here to examine specific questions.

These include: Order Comatulida, non-bourgeticrinid: (genera listed only): *Antedon* de Fréminville, 1811; *Capillaster,* A. H. Clark, 1909a; *Clarkcomanthus* Rowe & others, 1986; *Comactinia* A. H. Clark, 1909b; *Comatella* A. H. Clark, 1908a; *Comatula* Lamarck, 1816; *Davidaster* Hoggett & Rowe, 1986; *Dorometra* A. H. Clark, 1917, *Himerometra* A. H. Clark, 1907; *Isometra* A. H. Clark, 1908b; *Leptometra* A. H. Clark, 1908b; *Oligometra* A. H. Clark, 1908b; *Promachocrinus* P. H. Carpenter, 1879; and *Anthometrina* Eléaume, Hess, & Messing, 2011. Suborder Bourgeticrinina: *Bathycrinus* Thomson, 1872; *Caledonicrinus* Avocat & Roux in Améziane-Cominardi & others, 1990; and *Democrinus* Perrier, 1883. Order Cyrtocrinida: *Cyathidium* Steenstrup, 1847; and *Neogymnocrinus* Hess, 2006. Order Isocrinida: *Endoxocrinus* A. H. Clark, 1908b; *Metacrinus* P. H. Carpenter, 1884; *Neocrinus* Thomson, 1864; and *Saracrinus* A. H. Clark, 1923.

Histotechnical annotation: All sections that are stained with Toluidin blue were embedded in resine and cut 1 µm thick. All others are wax preparations and cut 5–7 µm thick. Unless noted otherwise, all figures are new and were generated by the authors, T. Heinzeller and B. Ruthensteiner.

ACKNOWLEDGEMENTS

Our thanks go to Professor Dr. Gerhard Haszprunar for providing the facilities and equipment of the SNSB—Bavarian State Collection of Zoology. Likewise, it is gratefully acknowledged that the far-sighted staff of this institution prevented the destruction of valuable histological material that has now become the basis of this article. We are also indebted to Maria Byrne, whose critical comments on the manuscript were particularly helpful. A special thanks from Thomas Heinzeller goes to Professor Ulrich Welsch for the introduction to the crinoid topic and the years of fruitful joint research work. And even if it was a long time ago, the tireless histotechnical work of Beate Aschauer should also be mentioned with great appreciation.

II. COELOMIC SYSTEM

Coelom is generally understood to be well-defined spaces within the connective tissue lined with a coelothelium containing coelomoc fluid. Each type of coelom derives from four larval vesicles (hydrocoel, axocoel, left and right somatocoel) that develop before reaching the doliolaria stage. The main lines of development of the crinoid coelom were already described in the nineteenth century by several authors, for example Bury (1888). A general, relatively schematic—and ingeniously simple—overview was given by Holland (1991). A very detailed study specifically addressing the development of coelomic spaces in *Antedon bifida* Pennant 1777 was completed by Engle (2013).

Nevertheless, the relationship between larval and fully developed coelomatic spaces and structures remains unclear in several respects. This is especially true for the axocoel and the two embryonic somatocoelia, because these three vesicles merge into a common space before further differentiation takes place. Consequently, the application of embryological terms (hydro-, axo-, somatocoel) to adult coelomic spaces as used here (Fig. 2) has some likelihood of validity but remains to be considered with reservation.

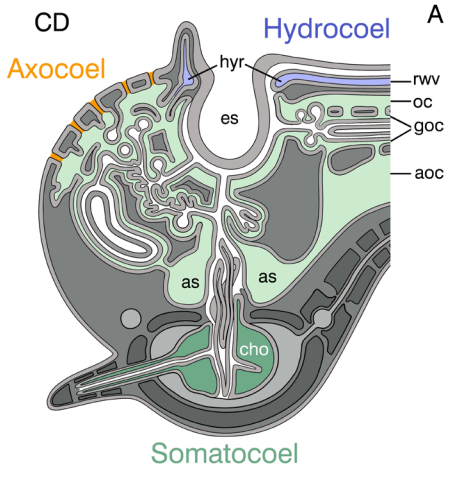

Fig. 2. Schematic drawing of the main coelomic compartments, vertical section with the A ray on the right and the CD interray on the left, axocoel in orange, hydrocoel in light blue, somatocoel in green, more precisely: above the rosette in light green, below in darker green. Labels: aoc=aboral canal, as=axial sinus, cho =chambered organ, es=esophagus, goc=gonocoel, hyr =hydrocoelomic ring, oc=oral canal, rwv=radial water vessel (modified from original drawing in Heinzeller & Welsch, 1994, fig. 10A).

HYDROCOEL: THE WATER VASCULAR SYSTEM

General features

The distinctive structures of the water vascular system are ontogenetically derived from the hydrocoel (e.g., Seeliger, 1893; Mortensen, 1920). At the latest in the cystidean stage, the ends of the horseshoe-shaped anlage of the water vascular system fuse, forming a closed ring canal; the fusion point marks the CD interray, which differs in several aspects from the other four interrays. At this stage, the ring canal surrounds the mouth opening. Later, in the pentacrinoid larva, five radial arm canals emanate from the ring. Branches from the initial radial canals grow into the gradually formed pinnules. Offshoots in tentacles arise from pinnular canals. Because the ends are closed, a certain pressure can be maintained in the entire, flow-filled canal system. This internal pressure is controlled, in part, by the activity of the muscles of the canal walls.

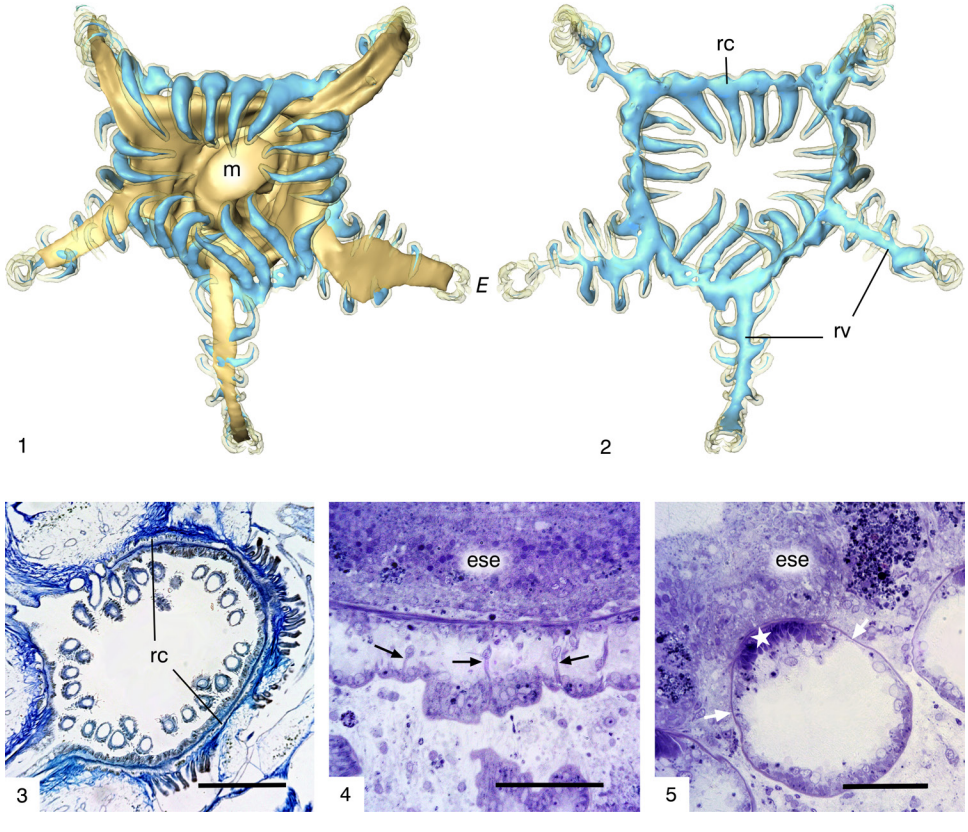

Fig. 3. Hydrocoel, circumoral organization. *1–2*, *Dorometra nana* (Hartlaub, 1890), 3D model. *1,* Oral aspect of the mouth with inclining mouth tentacles (*bright blue*) and with proximal food grooves (*bright gold*), m =mouth opening, *E*=E ray. *2*, Aboral aspect, note the bulbous widenings of the ring canal at the base of each tentacle, rc= ring canal, rv=radial vessel. *3, Cyathidium foresti* Cherbonnier & Guille 1972, horizontal section of the ring canal (rc), scale bar 500 µm. *4* and *5*, *Antedon bifida* Pennant, 1777, horizontal sections; *4*, myoepithelial cells (*arrows*) cross the lumen of the ring canal, ese=esophageal epithelium, scale bar 50 µm; *5*, cross-sectioned mouth tentacle with intensely stained inner cells (star), *arrows* point to the thickened basal lamina, ese=esophagus, scale bar 50 µm. Staining: Azan in *3*, Toluidin blue in *4* and *5.* Images new, by authors.

The water vascular system is made of epithelial tubes. Depending on their fluid content, these tubes can reach a width of up to 100 µm. Juvenile animals regularly have 20 tentacles arranged around the mouth opening; their number may increase with growth, commonly at the expense of pentagonal symmetry. Ring and radial canals are adjacent to a hemal lacuna on the side of the epithelium of the upper esophagus or of the food groove. The basal lamina of the tube can usually be discerned by light microscopy because it is strengthened by collagen fibrils (Fig. 3.5, Fig. 4.1). The epithelium is squamous to columnar, it is sparsely ciliated, and it can be very different in height on opposite sides of tubes. In addition, the proximal portions of the radial canals have a high columnar epithelium, which becomes lower in the periphery and is lowest in the pinnular canals.

Myoepithelial cells are the predominent cell type in the hydrocoelomic epithelium. These myoepithelial cells contain contractile filaments in their basal processes and are typically oriented parallel to the axis of the tube. Cells of this type allow hydrocoelomic tubes to contract and tentacles to swing out in any direction. However, bending toward the food groove or mouth opening may

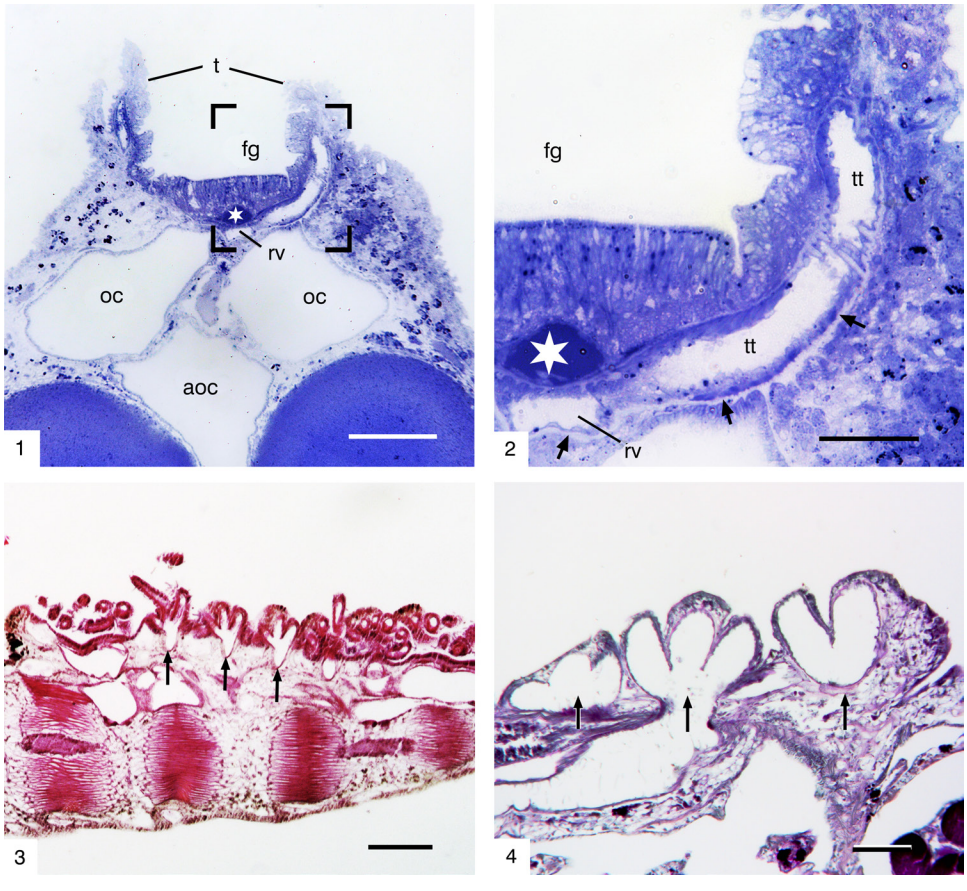

Fig. 4. Hydrocoel, canals in arms and pinnules. *1*, *Antedon mediterranea* (Lamarck, 1816), arm in cross section, *white asterisk* marks the hemal lacuna, *rv*=radial vessel, oc=oral somatocoelomic canal, aoc=aboral somatocoelomic canal, fg=food groove, t=tentacle, scale bar 200 µm. *2,* Higher magnification of area marked in *1*, white asterisk marks the hemal lacuna, arrows point to typically thickened basal membrane, fg=food groove, rv=radial vessel, tt=coelomic tube of the tentacle, scale bar 50 µm. *3, Dorometra nana* (Hartlaub, 1890), longitudinal, section of a pinnule slightly lateral to the midline with three roots of tentacle tube triads (*arrows*), scale bar 100 µm. *4, Cyathidium foresti* Cherbonnier & Gille 1972, longitudinal section of an arm with three roots of tentacle tube triads (arrows), scale bar 100 µm. Staining: *1,* Toluidin blue, *2,* Hemalum-Eosin, *3,* PAS-Hemalum. Images new, by authors.

be their strongest activity, caused by cells concentrated on the inner side of the tube (Fig. 3.5), which are particularly rich in myofilaments (asterisk in Fig. 3.5). In the ring canal, myoepithelial cells of the inner wall can contract the ring and, thus, also the mouth opening. Another myoepithelial cell type is spindle-shaped and crosses the tube from side to side (Fig. 3.4). All these muscle cells stabilize the system and help to maintain the internal water pressure.

The water canals follow all the branching of the arms. In addition, the water canals give off one pinnular canal per vertebra, alternating to each side. Finally, the water canals in the arms and pinnules bear regularly arranged dilatations forming small atria. From each of these, a triad of finger-shaped outgrowths rises to the edges of the food grooves. Each outgrowth of a triad supplies one tube foot (Fig. 4.2–4.3). Such triads are located along the entire food groove of arms and pinnules.

During ontogeny, the ring canal forms another type of tubular outgrow, the stone canals. These canals intrude into the subteg-

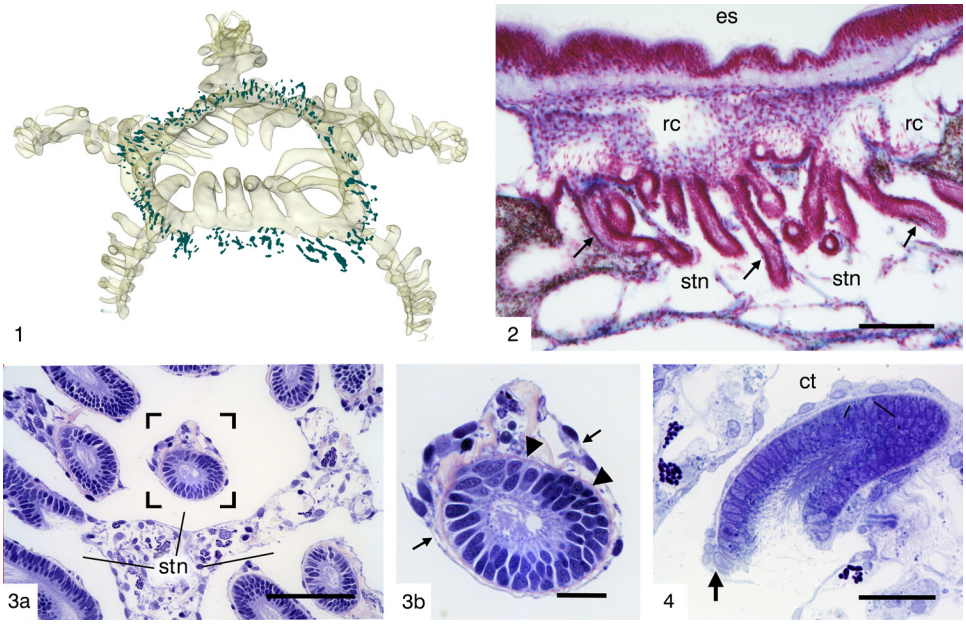

Fig. 5. Hydrocoel, stone canals. *1–2*, *Dorometra nana* (Hartlaub, 1890); *1,* 3D-model of the oral region, slightly oblique aboral view, stone canals in dark green; *2,* horizontal section, arrows point to stone canals, es=esophagus, rc=ring canal, stn=subtegminal net, scale bar 50 µm. *3a* and *3b*, *Metacrinus levii* (Améziane-Cominardi in Améziane-Cominardi & others, 1990); *3a,* cross sectioned stone canals, stn=subtegminal net, scale bar 50 µm; *3b,* higher magnification of the area marked in *3a,* showing a stone canal with numerous kinocilia inside the lumen, arrows point to the surrounding coelothelium, arrowheads to the basement membrane, scale bar 10 µm. *4, Himerometra robustipinna* P. H. Carpenter, 1881a, opening of a stone canal into the coelomic cavity, *arrow* points to the transition between somatocoelium and hydrocoelium, ct=coelothelium, scale bar 20 µm. Staining: Hemalum-Eosin in *2,* Toluidine blue in *3–5.* Images new, by authors.

minal net of the somatocoel and open into the latter by forming an orifice at their tip. The earliest (primary) stone canal (Fig. 6) appears in the CD interray of early cystideans. Successively, a large number of secondary stone canals are formed all along the ring canal, in *Antedon,* approximately 30 per interray. Stone canals serve to replace leaked water (see Fig. 16, p. 15).

Stone canals

As mentioned above, the stone canals run between the hydrocoelomic ring canal and the subtegminal net of the body cavity is (Fig. 5.2). ~15–30 µm, and the mean length is ~100 µm, depending in part on the size of the animal. The stone canals lie close together on the ring canal (Fig. 5.1) (in contrast to the madrepores, which are absent in the CD interray). The epithelium of the stone canals is identical to that of the ring canal, and as in the latter, the basal lamina is thickened (Fig. 5.3). Myoepithelial cells enable the closure of the canal. The predominant cell type is high-prismatic, each with a kinocilium with an oblique root. In the lumen, the kinocilia together form an undulating flame (Heinzeller & Welsch 1994), transporting water from the somatocoelomic space into the hydrocoelomic ring canal. At the site where the stone canals enter the somatocoelomic space, they are externally sheathed by the coelothelium. As a result, the distal parts of the stone canals consist of an inner and an outer epithelium with a delicate connective tissue lamella between them (Fig. 5.4).

Primary Stone Canal

The course of the primary stone canal differs from that of the secondary stone canals. In the young *Leptometra* sp., the

primary stone canal arises from the ring canal in the CD interray (Fig. 6.1). According to Engle (2013), it terminates in a small coelomic space, the so-called small ventral coelom—initially axocoelomic, characterized by the orifice of the primary madreporic canal (Fig. 8).

MADREPORIC CANALS, AXOCOELOMIC REMNANTS

Most authors agree that crinoids miss a right axocoel (summarized by Scriba, 2015) and that the left axocoel fuses with both left and right somatocoelia to form the main body cavity around the digestive tract (Hyman, 1955; Holland, 1991). Apart from this agreement, the assignment of some developed segments of the coelom to embryonic sources remains controversial. This concerns, for example, the origin of the madreporic canals, also termed tegminal ducts.

Hydropore, the primary madreporic canal

Embryological studies on late doliolarian larvae, for example by Seeliger (1893), on *Antedon rosacea* (currently identified as *A. bifida bifida* Pennant, 1777), reveal an outgrowing edge of the axocoel, the later small ventral coelom that subsequently breaks through the integument. This opening is called the hydropore and represents the first open connection of the coelomic space with the overlying sea water. In young animals, the hydropore is located in the CD interray next to the anal cone (Fig. 7.1b). The tubular connection of the superficial opening with the small ventral coelom is called the primary madreporic canal (Fig. 7.2, Fig. 6.2b).

Madreporic canals, the tegminal ducts

In addition to the primary madreporic canal, four other ducts can be observed crossing the tegmen in juvenile feather stars. Each of them opens on the surface of the tegmen in the interradial axis, except CD, exactly at the base of the valves—triangular remnants of the former roof of the vestibulum, which disappear during

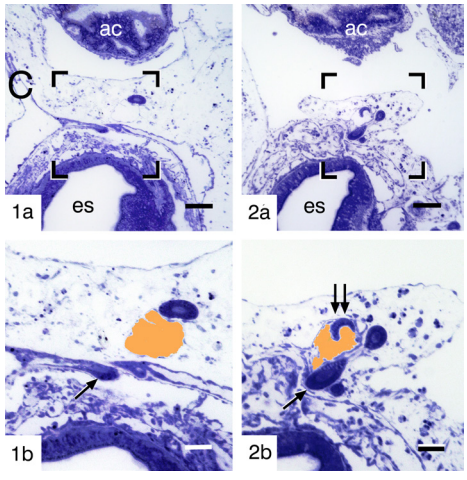

Fig. 6. Hydrocoel, primary stone canal. *1a*, Juvenile *Leptometra celtica* M'Andrew & Barrett, 1857, horizontal section just below the tegmen, ac=anal cone, es=esophagus, C=C ray, scale bar 100 µm. *1b*, Area marked in *1a* at higher magnification, arrow points to the origin of the primary stone canal; orange patch is axocoelomic small ventral coelom, scale bar 50 µm. *2a*, Horizontal section, approximately 20 µm aboral to *1a,* ac=anal cone, es=esophagus, scale bar 100 µm. *2b,* Area marked in *2a* at higher magnification; the primary stone canal (*arrow*) runs from level 1 to level 2 both outward and toward ray D. Continuing upward, it changes direction again before extending downward and eventually (*double arrow*) opening into the axocoelomic small ventral coelom (*orange*), scale bar 50 µm. Images new, by authors.

further development. Below the tegmen, the ducts open into the body cavity, the subtegminal net, oralmost part of the axial sinus. During further growth, these trans-tegminal ducts multiply. In large feather stars, their number increases to several hundred, and the tegmen as well as the oral side of proximal arm segments become sprinkled with their orifices (Fig. 8.5). The lumina of these ducts are ~10 µm wide, with ampulla-like parts near the orifice that can be up to 30–40 µm wide. In the ampulla, the epithelium is high, rich in apical microvilli, and each cell bears a long flagellum. These flagella point outward (see Fig. 16). The part of the duct below the ampulla is lined with a very flat epithelium. Its length varies greatly.

It has been debated—and remains highly controversial—whether the multiplicity of tegminal ducts derives from a cleavage

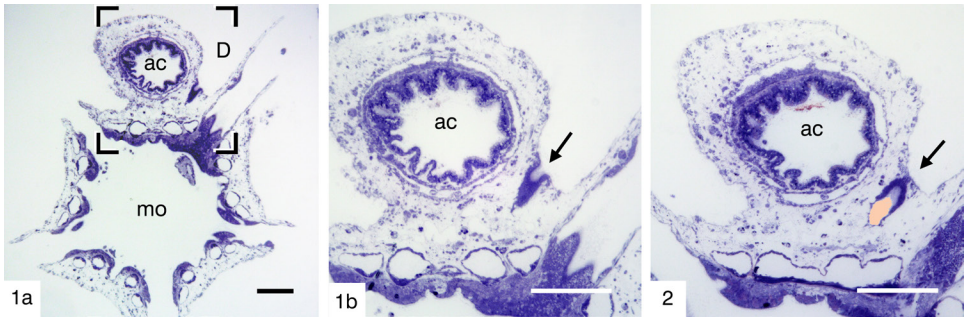

Fig. 7. Axocoel, hydropore. *1a–b,* Juvenile *Leptometra celtica* M'Andrew & Barrett, 1857. *1a,* Horizontal section at the base of the anal cone, ac=anal cone, mo=mouth opening, D=D ray, scale bar 200 µm. *1b,* Area marked in *1a* at higher magnification, arrow points to the hydropore, ac=anal cone, scale bar 200 µm. *2,* Section a few microns aborally than *1a,* showing the junction of the hydropore (*arrow*) with the axocoelomic small ventral coelom (*orange*), ac=anal cone, scale bar 200 µm. Staining: Toluidine blue. Images new, by authors.

of the primary madreporic canal (Balser & Ruppert 1993) or represents a *de novo* formation (Engle 2013). The large distance between the primary madreporic duct and the secondary ducts argues against the split hypothesis. Furthermore, assuming that the subtegminal network is indeed derived from the axocoel, it seems justified to consider the secondary madreporic canals extending from the subtegminal network to the surface as rudiments of the axocoel.

Possible further axocoelomic remnants

In isocrinids, a coelomic pouch extends between the axial tubular organ and the Reichensperger's organ (see Section IV), which is aborally closed but orally in open continuity with the oral axial sinus. This coelomic space (Fig. 9.1) has been interpreted as axocoelomic by Holland, Grimmer, and Wiegmann (1991), an attribution strongly supported by the embryological work of Engle (2013).

Most crinoids are free spawners releasing their gametes by rupturing the overlying tissue layers (see Section VI). In contrast, in the cyrtocrinid *Cyathidium foresti* Cherbonnier & Gille 1972, gonoducts are used for this purpose (Fig. 9.1, Fig. 9.3). Based on their location and structure, these ducts correlate with the madreporic canals and can also be considered axocoelomic remnants.

SOMATOCOEL

In the following, the terms oral and aboral are used exclusively in the anatomical descriptive sense for the reasons already mentioned in the introduction and do not represent references to homology of embryonic structures of the same name.

In the arms and calyx a complex system of coelomic cavities exists, either as a collection of narrow slits in the connective tissue bounded by the coelothelium or as wide cavities. The entire system contains a watery, typically cell-free fluid that flows rapidly, at least in larger cavities (see *Circuit of the Somatocoelomic Fluid*, p. 16).

ORAL SOMATOCOEL IN ARMS

General features

In the arms and pinnules, there are typically three superimposed coelomic ducts. The uppermost is hydrocoelomic, as explained previously. The canal immediately below it is called the oral somatocoelomic canal, and the lowest is the aboral somatocoelomic canal. The two somatocoelomic ducts are seemingly separated by a horizontal septum, but there are numerous widely spread openings through which the somatocoelomic canals communicate with each other, (and also with the gonocoel, see p. 11). These canals branch into arms and pinnules and decrease in size proportionally toward the

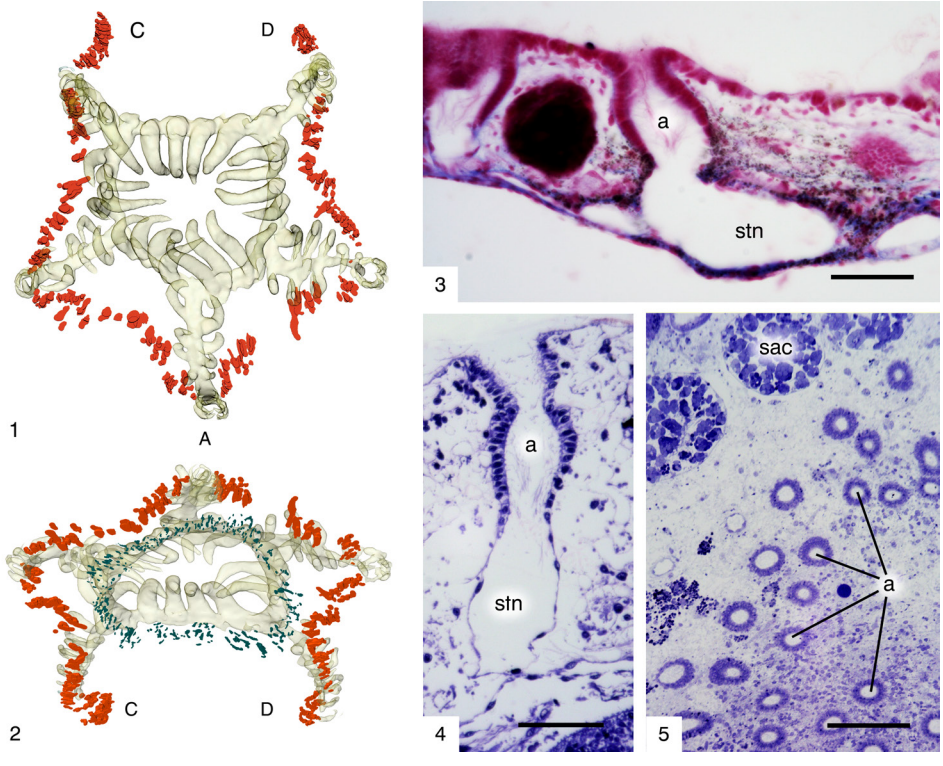

Fig. 8. Axocoel, madreporic canals. *1–2*, *Dorometra nana* (Hartlaub, 1890), 3D model of mouth region, tentacles transparent *gray*, madreporic canals *red*, stone canals *green*. *1*, Oral view. *2*, Aboral view, slightly oblique; note that there are no madreporic canals in the CD interray. *3*, Tegminal plate, vertical section with madreporic canal opened longitudinally, a=ampulla, stn=subtegminal net, scale bar 50 µm. *4*, Juvenile *Metacrinus* sp., madreporic canal showing varying types of epithelium in the ampulla (a) and the connecting duct to the subtegminal net (stn), scale bar 50 µm. *5*, *Promachocrinus kerguelensis* P. H. Carpenter, 1879, tangential section through the tegmen, sacculi (sac) mark the edge of the food groove, a=ampullae of madreporic canals. Scale bar 100 µm. Staining: *3*, Hemalum-Eosin, *4* and *5*, Toluidine blue. Images new, by authors.

tip. The horizontal septum does not extend to the tips, so near the tip, the lumen of both canals is continuous. The oral canal may also be subdivided by a middle vertical septum in some places; subdivisions of the aboral canal were not present anywhere. In cross section, the elliptical canal appears more-or-less oval in profile, or is divided into two circular canals, whereas the aboral canal is wedge-shaped where it is constricted by the flexor muscles (Fig. 10.1–10.2)

Ciliated pits

All somatocoelomic arm canals are lined by a cuboidal epithelium whose phagocytotic function has been demonstrated (Grimmer & Holland, 1979). On the luminal surface, the cells bear a fringe of microvilli and a single kinocilium each. In the aboral midline of the aboral canal, there are well-defined pits at regular intervals. Within the pits, the cells bear one kinocilium each, but because of the high number of these very slender cells, the pit is remarkably densely ciliated (Fig. 11.3). In cooperation with the numerous kinocilia distributed throughout the canal epithelium, these ciliated pits presumably generate the flow of the coelomic fluid (Grimmer & Holland, 1979).

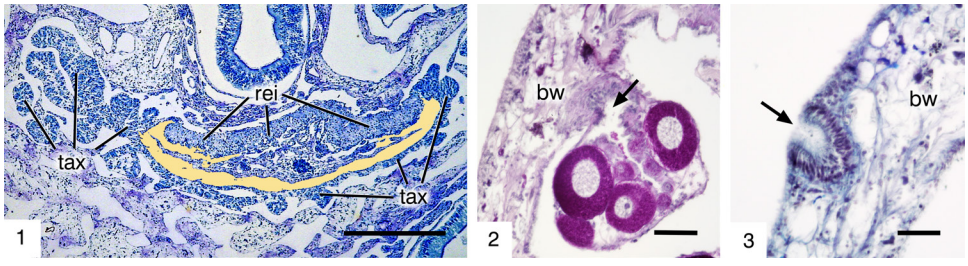

Fig. 9. Axocoelomic remnants. *1, Metacrinus levii* (Améziane-Cominardi in Améziane-Cominardi & others, 1990), horizontal section. The space between the tubular axial organ (tax) and the Reichensperger's organ (rei) is marked in ochre, scale bar 200 µm. *2* and *3, Cyathidium foresti* Cherbonnier & Gille 1972, proximal arm sections containing an ovary with purple stained oocytes. Short duct (arrow in *2*) from the ovary through the body wall (bw) with opening at the surface (*arrow* in *3*), scale bars in *2* and *3*, 25 µm. Staining: *1,* Hemalum, *2,* Azan, *3,* Alcian blue. Images new, by authors.

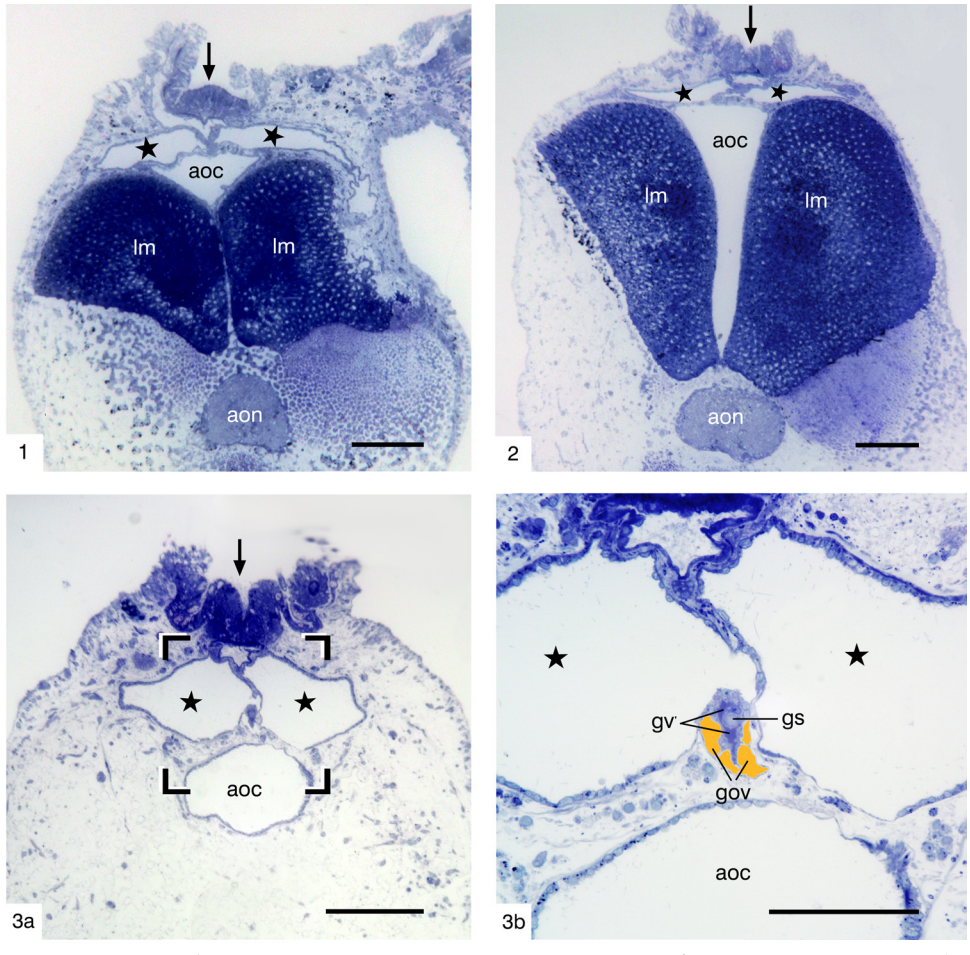

Fig. 10. *Leptometra celtica* M'Andrew & Barrett, 1857, transverse sections of arms. *1–2*, section near articulation showing prominent longitudinal flexor muscles (lm), *arrows* point to the food groove, asterisks mark the oral somatocoelomic canal, aoc=aboral somatocoelomic canal, aon=aboral nerve, scale bars each 100 µm; *3a,* section in the middle between two joints, *arrow* points to food groove, *stars* mark oral somatocoelomic canal, aoc=aboral somatocoelomic canal, scale bar 100 µm; *3b* area marked in *3a*, *stars* in the oral somatocoelomic canals; aoc=aboral somatocoelomic canal, gs=genital strand, gv=genital vessel, goc=gonocoel (*orange*), scale bar 50 µm. Staining: Toluidine blue. Images new, by authors.

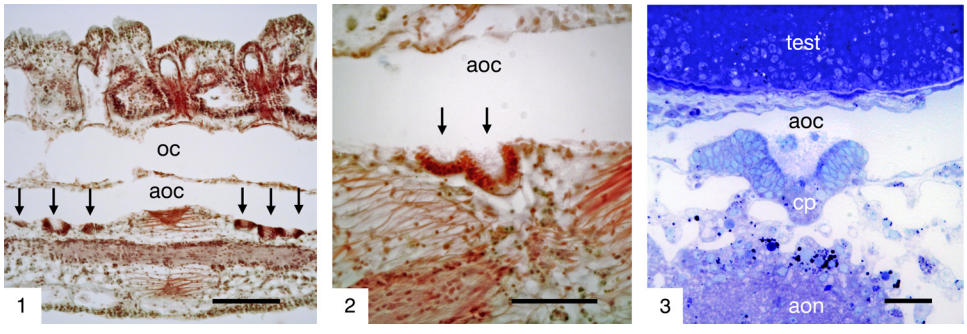

Fig. 11. Ciliated pits in pinnules. *1, Comatella nigra* P. H. Carpenter, 1888, longitudinal section of a pinnule showing two series of ciliated pits (*arrows*), scale bar 100 µm. *2,* Close-up of two pits similar to *1,* scale bar 50 µm. *3, Antedon bifida* Pennant 1777, transverse section through a genital pinnule showing a large ciliated pit (cp) with dense ciliation, aoc=aboral canal, aon=aboral nerve, oc=oral canal, test=testis, scale bar 100 µm. Staining: Hemalum-Eosin in *1* and *2,* Toluidine blue in *3.* Images new, by authors.

Gonocoel, genital coelom

Certain sections of arms and pinnules contain a genital cord (termed a rachis, see Section VI, p. 52). This cord and the hemal vessel surrounding it lie in a separate coelom, the gonocoel. This coelom occupies the middle of the horizontal septum and, if the oral canal is divided, the aboral edge of the vertical septum (Fig. 10.1–10.2).

Tracing the gonocoel from the arms back to the midbody shows that the gonocoel splits off from the oral canal at the base of the arm and runs separately within the calyx wall, eventually entering less well-defined somatocoelomic regions in the CD interray (see Section VI, Fig. 58). During the breeding season, the gonocoel completely encases the full-grown ovaries or testes (Section VI, see Fig. 60, Fig. 61).

Oral somatocoel in the calyx

It is very likely that all somatocoelomic cavities in the calyx are in open contact with each other. Therefore, the definition of compartments is artificial, at least to some extent, but facilitates the understanding of the complex system.

Overall, the shape of the somatocoel in the calyx of a feather star can be compared to a sketch of a Roman oil lamp with a central filling hole (mouth) and eccentric wick hole (anus) (Fig. 12.2). The base and lid of the lamp are formed by aboral (deep) and high oral (subtegminal) parts of the axial sinus. The walls consist all-around of a broad, hollow, girdle-like structure, the perivisceral coelom. The interior (the oil reservoir of the lamp) houses the coiled intestine, and in its spindle the mesentery as well as in the various mesentery coelomic cavities that constitute the central part of the axial sinus. To complete the overview, the connection to the arm canals must also be considered. An overview of the entire structure (Fig. 12) is a 3D model of the somatocoel of *Dorometra nana*. Further, closer examination of this model reveals the following details:

Axial sinus

The oral part of the axial sinus (Fig. 12.1b) is the subtegminal net comprising mostly small lacunae arranged around the esophagus. The target caverns of the madreporic canals and the stone canals contribute to this net. At its margin, the subtegminal net is connected to both the perivisceral coelom and to the oral arm canals (Fig. 12.3). The middle, central part consists of several more-or-less tubular, more-or-less coaxial, more-or-less voluminous cavities, one of which contains the axial organ (Fig. 13.5; see Section IV). The most voluminous of these cavities is of central importance for fluid circulation (central mesenteric cavity in Fig. 16). The most aboral, deep part of the axial sinus (Fig. 12.1b) is located on the oral side of the rosette. The aboral arm canals originate from this part. Differences of the

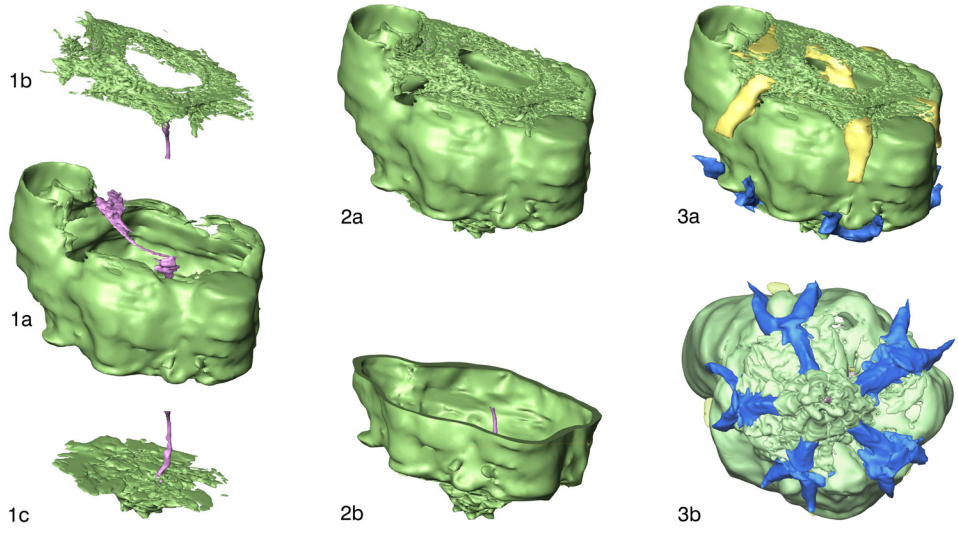

Fig 12. Somatocoel of *Dorometra nana* (Hartlaub, 1890), 3D model, slightly oblique oral view. *1–3*, Three (of four) components separated: *1a*, perivisceral coelom; *1b*, subtegminal net; *1c,* deep part of the axial sinus (axial organ in *1a, 1b,* and *1c* in *purple*); *2a*, total model; *2b,* aboral half after horizontal crop; *3a,* arm canals added (oral arm canals in *yellow*); *3b,* aboral view (aboral arm canals in *blue*). Images new, by authors.

axial sinus in groups other than feather stars are treated separately (see p. 14).

Perivisceral coelom

A girdle-like coelomic space surrounds the viscera, which mainly contains intestine and axial organs (Fig. 12.1a) and lies immediately underneath the body wall. Its thickness is remarkably constant, probably due to the numerous cell bridges tying the outer and inner epithelia to each other. The outer coelothelium covers the inner surface of the body wall, and the inner coelothelium covers the outer surface of the gut. The inner wall adjacent to the gut merges into the mesentery.

Mesentery

The mesentery (Fig. 13) is a connective tissue plate inside the intestinal coil; its connective tissue is disrupted in many places by the somatocoelomic cavities of the central axial sinus. The mesentery extends from the basal axial sinus orally up to the subtegminal net. Between the C and D ray, it is connected to the body wall, including a connection of the mesenteric coelom with the perivisceral coelom (Fig. 13.1–13.3). From an oral view, the mesentery rotates counterclockwise, from the outside to the inside (Fig. 13.2–13.3, Fig. 13.6), performing a full rotation in *Dorometra nana,* a species with endocyclic arrangement. The mesentery contains the axial sinus with the axial organ, which shifts from a central position in the basal axial sinus to an eccentric position in the subtegminal net near the root of the anal cone (Fig. 13.1–13.5) resulting from the rotation of the mesentery. The shape of the mesenteric somatocoelomic caverns varies from slits to bulbs to tubes. In total, the cavities form a bridge between the influx region of the oral arm canals and the basal axial sinus. In *Dorometra nana,* the oral-aboral connection is formed by a single prominent tube. In most other taxa, multiple cavities appear to contribute to this connection, which plays an important role in the circuit of the coelomic fluid (see p. 16).

Anal cone coelom

In the anal cone, the anal duct mucosa is completely surrounded by the somatocoelomic anal cone coelom. The outer two-

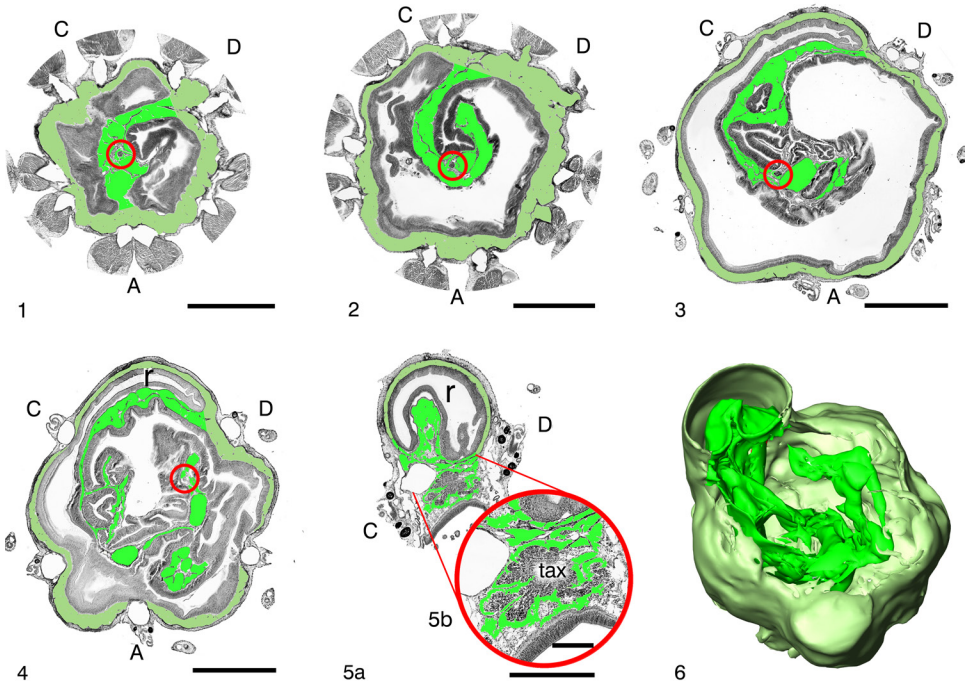

Fig. 13. *Dorometra nana* (Hartlaub, 1890), somatocoelomic cavities in mesentery. *1–5,* Ascending horizontal sections with *gray* tissue, somatocoelomic spaces in mesentery in *light green*, perivisceral coelom in *olive green*, capital letters mark rays. In *1*, the mesentery rests on the deep part of the axial sinus and forms bridges to the perivisceral coelom in the A and D rays. Further orally (*2–4*) there is only the bridge to the D ray. In *4–6,* note the mesenteric contribution to the anal cone coelom (see Fig. 14), r=rectum. In *5*, the mesenteric coelom enters the subtegminal net embedding the oral parts of the tubular axial organ (*tax*, circled in *red* in *1–5*), higher magnified in *5b*. *6,* 3D model of mesenteric coelomic spaces, subtegminal net omitted for clarity. Scale bars 500 µm in *1–5*, and 100 µm in *5b*. Images new, by authors.

thirds of the anal cone coelom appears to represent the continuation of the perivisceral coelom, and the inner third is contributed by the mesentery (Fig. 13.5–13.6; Fig. 14.1). At the tegminal level, this somatocoelomic sheath is indented by a bulge created by the stomach, whereas at higher levels it is elliptical to circular. In *Dorometra nana,* this coelomic sheath looks similar to the perivisceral coelom with some cellular bridges (Fig. 14.2). In *Comaster schlegelii* P. H. Carpenter, 1881b, respective cellular bridges are numerous and of considerable size (Fig. 14.3), probably due to the storage of mucus.

Arm Canals

The oral arm canals (Fig. 12.3a–12.3b) enter the body at the subtegminal level. They supply both the subtegminal net and the central part of the axial sinus (Fig. 15; Fig. 16). The aboral arm canals emerge from the deep axial sinus just above the rosette. They extend toward the arm roots from where they run together with the oral canals toward the periphery.

Supplementary notes to the axial sinus

Feather stars. At the level of the ring commissure (Fig. 15.1–15.2), i.e., between the radial ossicles, the axial sinus consists mainly of vesicular to tubular caverns of similar size. Further orally, where the coelomic space widens between the primibrachials, the axial sinus caverns vary in shape and size (Fig. 15.3). It is likely that the details of the axial sinus of feather stars vary considerably among species or even within species depending on size and age.

Fig. 14. Anal cone coelom. *1*, *Dorometra nana* (Hartlaub, 1890), 3D model of the coelomic walls of the lower anal cone, oblique oral view. The outer (*green*) compartment arises from the perivisceral coelom, the inner (*blue*) from the mesenteric coelom (see Fig. 9.6). *2, Dorometra nana,* histological section corresponding to *1*, arrows point to myoepitheial cells crossing the coelomic cleft, hs=horn of stomach, tax=tubular axial organ, scale bar 200 µm. *3a*, *Comaster schlegeli* P. H. Carpenter, 1881b, horizontal section, the coelothelial cells bridging the coelom are swollen, scale bar 250 µm; *3b*, higher magnification of the area marked in *3a*, arrows point to swollen myoepithelial cells, the star marks the specific connective tissue replacing the hemal lacuna (see Section V), scale bars 100 µm. Staining: Hemalum-Eosin in *2*, Azan in *3*. Images new, by authors.

Bourgeticrinina. In *Democrinus chuni,* the somatocoel of the calyx is relatively simply formed. It does not have clear compartmentalization (Fig. 18.2–18.4), but it apparently consists of a common space between the body wall and the intestine, which sends five extensions into the arms. The somatocoelomic space below the gut ends blind aborally (Fig. 18.5a). Only in the middle does a narrow somatocoelomic cleft surrounding the tubular axial organ penetrate the sclerite (Fig. 18.5b). In contrast to the isocrinids, the oral somatocoel does not descend until the chambered organ (Fig. 19; Fig. 22.5); where its most oral apex is located inside the basals in *Democrinus chuni* (see Bohn & Heinzeller, 1999).

Isocrinida. Unlike the feather stars, there is no rosette separating the deep axial sinus from the chambered organ in isocrinids,

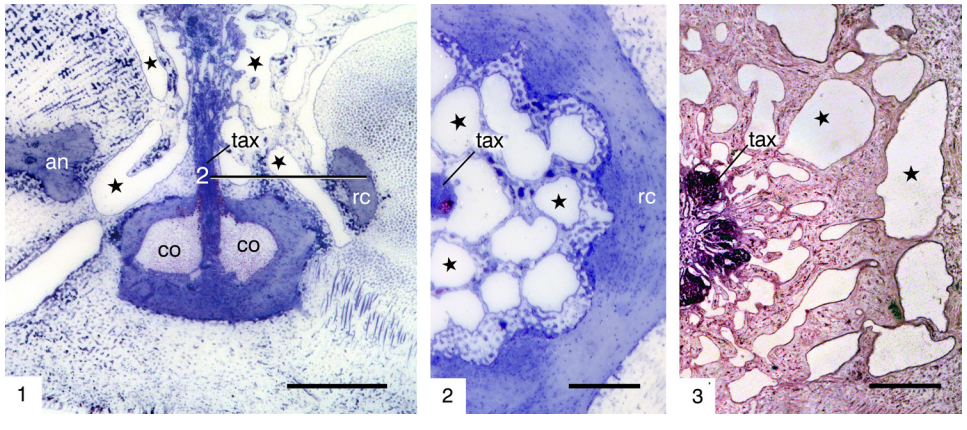

Fig. 15. Axial sinus of feather stars. *1, Clarkcomantus albinotus* Rowe, Hoggett, Birtles, & Vail, 1986, sagittal section, *stars* mark some caverns of the axial sinus, co=chambered organ, tax=tubular axial organ, an=arm nerve, rc=ring commissure. Number 2 marks plane of section *2*, scale bar 400 µm. *2, Clarkcomanthus littoralis* P. H. Carpenter, 1888, horizontal section, *stars* mark caverns of the deep axial sinus, tax=tubular axial organ, rc=ring canal, scale bar 200 µm. *3, Promachocrinus kerguelensis* P. H. Carpenter, 1879, horizontal section slightly oral of the ring commissure, tax=tubular axial organ, scale bar 400 µm. Staining: Toluidine blue in *1* and *2*, PAS and Hemalum in *3*. Images new, by authors.

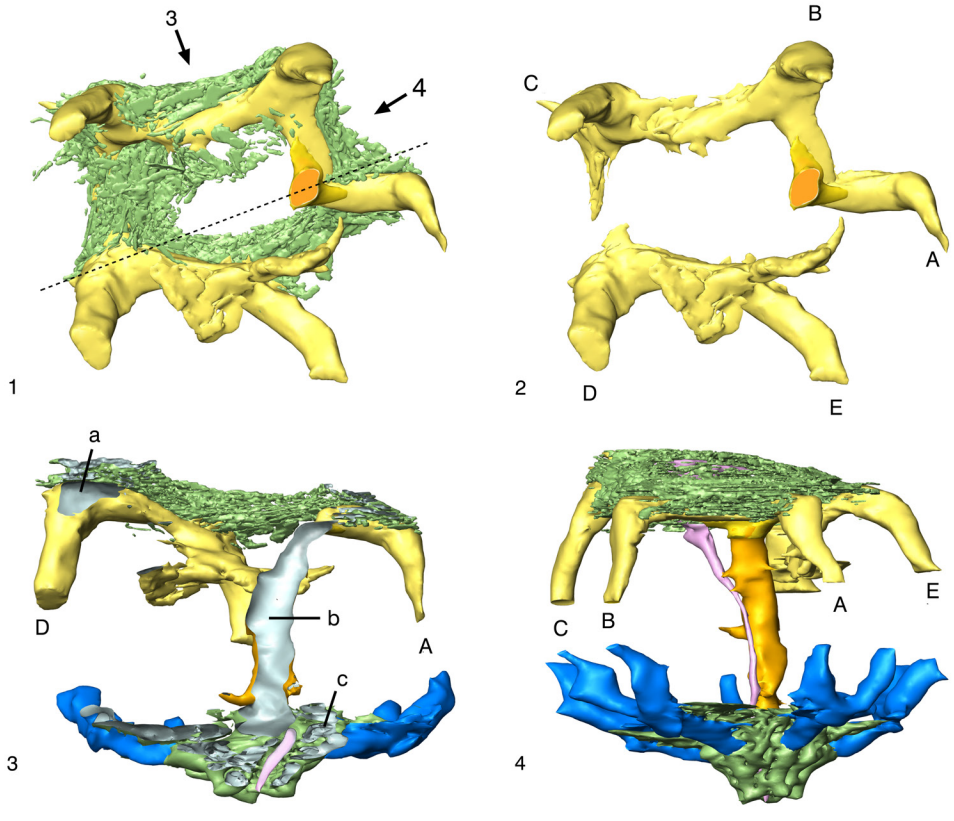

Fig. 16. *Dorometra nana* (Hartlaub, 1890), 3D model. *1,* Aboral view of the oral arm canals (*yellow*) converging within the subtegminal network (*light green*), central mesenteric cavity (*orange*) originates in the AB interray. *2*, Same as *1* with subtegminal network omitted. *3,* Model cropped in the plane indicated by the *dashed line* in *1*, viewing direction corresponding to arrow "3" in *1*, letters mark the sites where the model is cropped: a=oral curvature of the arm canal in D ray, b=descending central mesenteric cavity, c=transition from the deep axial sinus (*dark green*) to the aboral arm canal (*blue*). *4,* Viewing direction corresponding to arrow 4 in *1*. A–E=rays, counted counterclockwise in *2* as seen aborally. The *pink* structures in *3* and *4* represent the tubular axial organ. Images new, by authors.

which are represented here by *Metacrinus levii* (Améziane-Cominardi in Améziane-Cominardi & others, 1990). Thus, the chambered organ projects orally far beyond the basalia, and the axial sinus extends aborally until the radial-basal boundary.

Cyrtocrinida. In cyrtocrine crinoids, there is a coelomic cavity surrounding the gut aborally and laterally, similar to the axial sinus in other crinoid groups (Fig. 20). However, this cavity lacks any oral-aboral compartmentation, despite some structuring by connective tissue strands. Furthermore, because there is no trace of a chambered organ, the present axial sinus could be called an oral somatocoel.

In cyrtocrinids there are also some peculiarities concerning the arm coelom. In the embryonic stage of *Cyathidium foresti,* only a single somatocoelomic canal extends into each arm, in contrast to the two canals (one oral and one aboral) of other crinoids. However, proximal gonochoric arm regions of adult animals have three floors: a middle one containing the gonads, an oral one above, and an aboral one below. These are

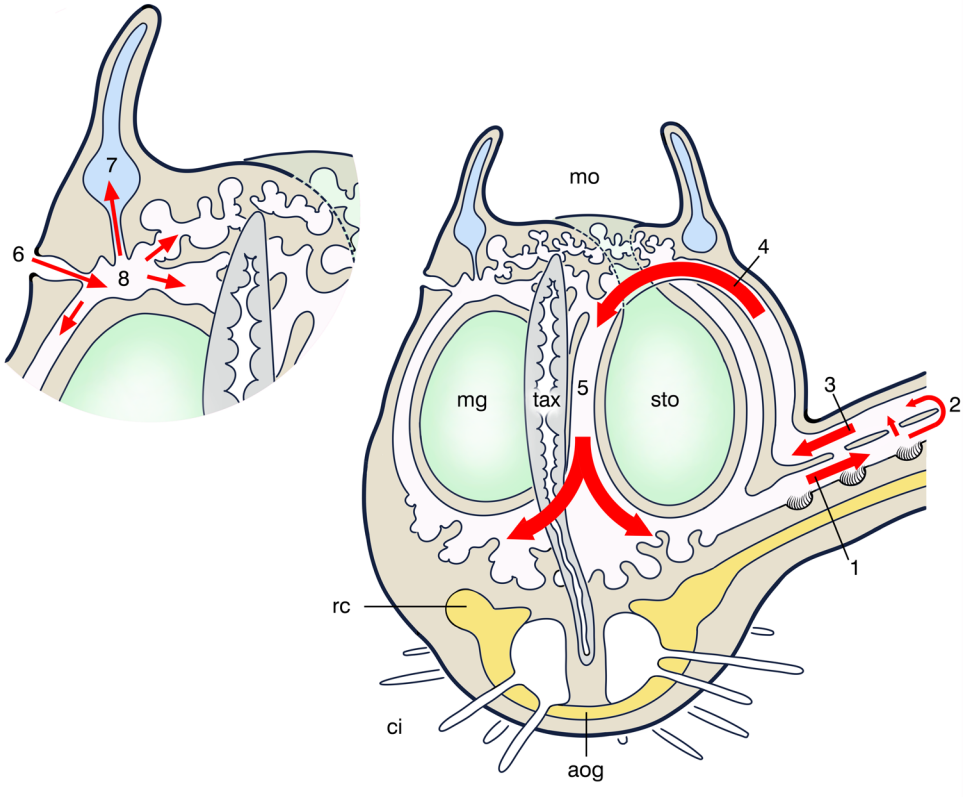

Fig. 17. Schematic drawing of the coelomic water circuit in crinoids. mo=mouth opening, sto=stomach, mg=midgut, tax=tubular axial organ, aog=aboral ganglion, rc=ring commissure, ci=cirri. 1=aboral arm canal, 2= tip of arm or pinnule, 3=oral arm canal, 4=ransition of oral arm canal into axial sinus (5). Enlarged section top left: 6=madreporic canal, 7=hydrocoelomic ring canal, 8=cavern of the subtegminal net. *Red arrows* trace the direction of flow. Image new, by authors.

separated by septa, which may represent specific (secondary) formations of the Cyrtocrinoidea.

CIRCUIT OF SOMATOCOELOMIC FLUID

The current directions of fluids had been assessed by the life observation of rapidly transported beads (Grimmer & Holland, 1979). The circuit can also be inferred from morphological data as presented herein for recent species or by Saulsbury (2019) for fossil material.

For the pattern of the circuit, consult Fig. 17. The numbers in brackets in the following description refer to the numbers in the figure, and red arrows trace the direction of the flow. Coelomic fluid is driven outward by kinocilia in the aboral arm canal [1]. It enters the oral canal through leaks in the horizontal septa and at the tips of arms and pinnules where the two canals converge [2]. In the oral canal, it flows inward [3]. From there, the fluid is transmitted [4] to the descending caverns of the axial sinus [5], from where it flows back into the aboral arm canals.

The somatocoelomic fluid is in mutual exchange with the hydrocoelomic fluid as well as with the external environment. The stone canals pump water from subtegminal caverns [8] into the hydrocoelomic ring canal [7] and, thus, stabilize the water pressure required for tentacle movements. The

madrepores [6] are wider than the stone canals and their kinocilia are less dense. Therefore, the direction of water transport in the madrepores cannot be clearly deduced from morphology. One function may be postulated, i.e. the compensation of water loss through various leaks. Overall, it seems clear that the axocoelomic, hydrocoelomic, and somatocoelomic compartments work together to maintain body fluid balance.

Consideration on functions

The flow of coelomic fluid between the arms and calyx can be interpreted in terms of adequate distribution of nutrients or oxygen. At contact with the gut, the fluid may be loaded with absorbed nutrients. As it travels to the periphery, it comes into close contact with arm muscles that require energy sources. Conversely, the fluid in the oral canals originates from areas near the surface where gas exchange may take place. Thus, it may support respiration in the core areas of the calyx, at least in large animals. Identical conclusions were drawn by Saulsbury (2019) from studies of fossils of the cretaceous feather star *Decameros ricordeanus* Rasmussen, 1961.

ABORAL SOMATOCOEL

Chambered organ in general

The chambered organ is a unique crinoid structure, formed by the aboral coelom. The complete absence of this organ has been demonstrated only in cyrtocrinids, for instance in *Holopus rangii* d'Orbigny 1837 (see Grimmer & Holland, 1990) and in two species of *Cyathidium* (Heinzeller & Fechter, 1995; Heinzeller & others, 1996). The organ roughly consists of coaxial tubes of the aboral coelom, usually five in number (Fig. 21.1), but there are exceptions. In *Capillaster multiradiatus* (Linnaeus 1758), for example, one can count 15 tubes (Fig. 21.1–21.2). As a rule, however, chambered organs are pentamerous. All five tubes are closed at both ends.

In isocrinids, the oral end of these tubes lay at the level of the radials, from where they run aborally, reach the stalk, and continue for some distance. In the nodals, side branches of the tubes extend into the cirri. In feather stars, the five tubes lie below the rosette and terminate in the centrodorsal cavity, at the base of the bowl-shaped aboral ganglion. As in isocrinids, branches extend from the tubes into the cirri.

Two main compartments of the chambered organ can be distinguished. The oral one is characterized by conspicuous bubble-like swellings traditionally referred to as chambers (or herein, the bulbous compartment of the chambered organ). The compartment supplying the cirri is located farther aborally. In isocrinids, these parts are confined to the nodals of the stalk. In feather stars, all cirrus supplying parts are concentrated in a confined space in the aboral ganglion, aborally of the bulbous chambered organ. This tight concentration of structures can be understood as if several nodal parts were pushed into each other. This compartment of the chambered organ will be referred to as labyrinthic. Bulbous and labyrinthic compartments together constitute the entire chambered organ of feather stars (Fig. 21.3).

In all chambers, the coelothelium produces a homogenous substance that stains metachromatically blue in hues ranging from light pink to dark purple when stained with Toluidine blue. The substance is present either in fine-grained dispersion or in the form of spherules released from the secretory coelothelium (Fig. 21.3–21.6). This material is present exclusively in the chambered organ, even in its finest extensions, which, for example, cross the rosette or extend into the cirri. Although these conspicuous spherules were observed by several early microscopists (e.g., Perrier 1873; Reichensperger, 1905) and also analyzed histochemically (Holland, 1968), their function remains unclear.

Chambered organ in detail

Isocrinids. In isocrinids, as observed in the juvenile *Metacrinus* sp., the bulbous chambers vary in size and are loosely arranged. They mark the oral ends of the aboral

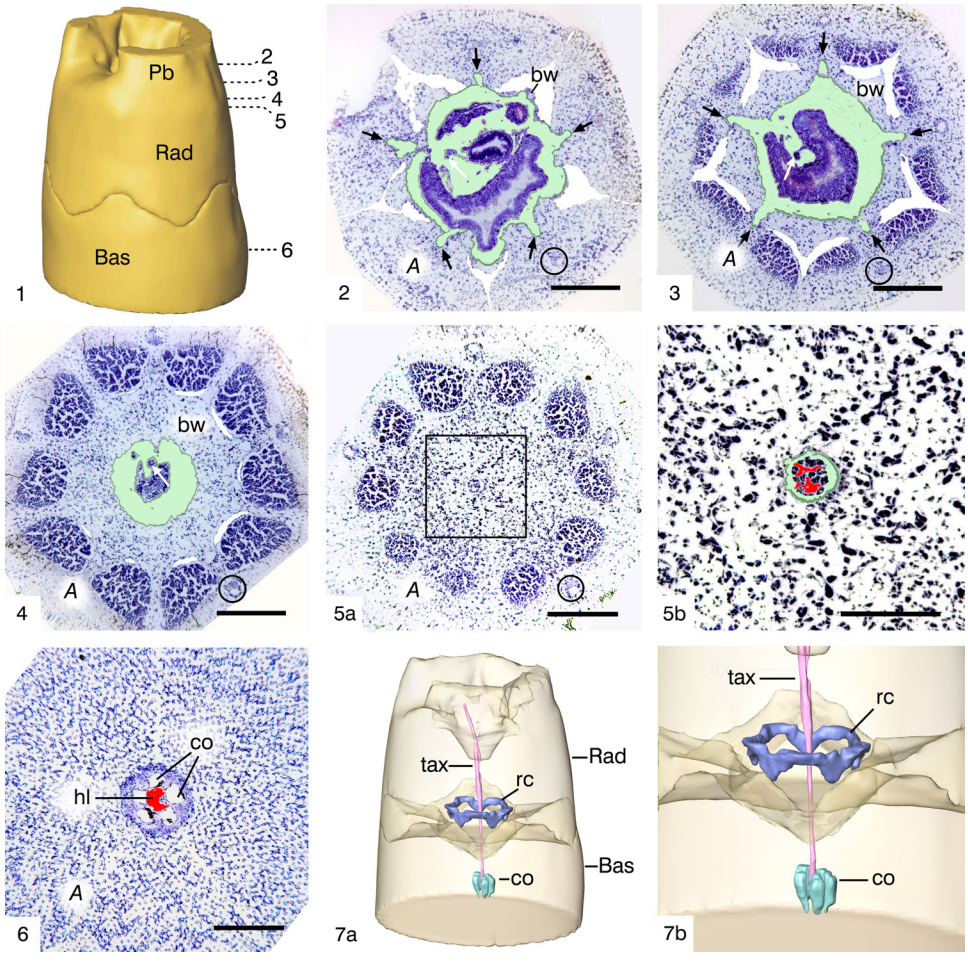

Fig. 18. *Democrinus chuni* (Döderlein, 1907). *1*, 3D model of specimen with one primibrachial (B) damaged, oblique oral view, Pb=primibrachial, Rad=radial, Bas=basal ossicle. Labels 2–6 indicate approximate level of cross sections. In *2–5,* the primibrachials appear almost fused; *bright white:* space between arms and the body wall (bw) of the calyx that communicates far orally with the external environment; *2, 3,* and *4,* the oral somatocoel (*green*) extends into the arms (*black arrows*), *white arrows* point to the tubular axial organ, *black circles* mark the arm nerve of the E ray, A=A ray, bw=body wall, scale bars each 200 µm. *5a,* The central area (magnified in *5b* shows the hemal lumen (hl) within the tubular axial organ surrounded by a very narrow somatocoelomic space (*green*), scale bar 200 µm, *5b,* 50 µm; 6 and *7*, chambered organ; *6,* cross section through basal ossicles; A =A ray, co=chambered organ, hl=hemal lacuna of the tubular axial organ, scale bar 200 µm. *7a*, 3D model with transparent body wall, oblique oral view, Rad=radial, Bas=basal ossicles, rc=ring commissure, co=chambered organ, tax=tubular axial organ; *7b,* detail at higher magnification. Images new, by authors.

somatocoelomic tubes and are surrounded by caverns of the axial sinus. In the calyx, the aboral end of the swellings of the chambered organ is at the level of the deepest cavities of the axial sinus (Fig. 22.2). In the oral direction, the swellings end a considerable distance below the level of the ring commissure. Laterally, the chambers keep their distance from each other (Fig. 22.7–22.9), so that the central hemal space is alternately bounded by the chambers and by caverns of the axial sinus (Fig. 38.3, see p. 36). Below the axial sinus, the tubes taper and move close together (Fig. 22.7, 22.10). In their middle, they enclose the central hemal space with the embedded axial tubules (Fig.

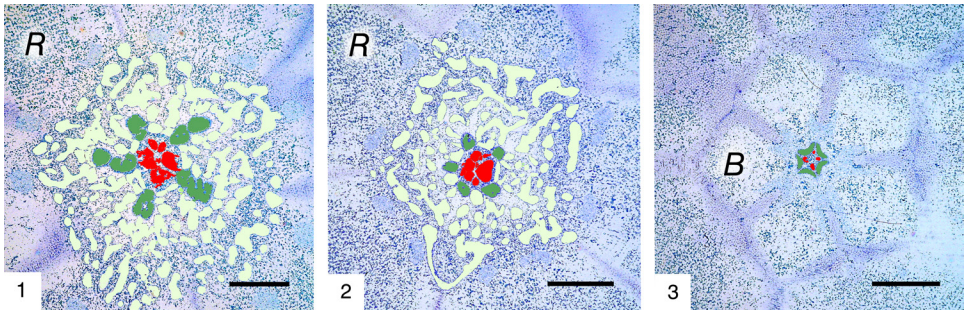

Fig. 19. Deep axial sinus of the isocrinid *Metacrinus levii* (Améziane-Cominardi in Améziane-Cominardi & others, 1990), cross sections; axial sinus is light green, chambered organ is dark green, hemal vessel embedding the axial tubules is red. *1*, Level of the radials (*R*), scale bar 200 µm. *2*, Deepest caverns of the axial sinus, *R*=radial, scale bar 200 µm. *3*, Level of basals (*B*), the tubes of the chambered organ are the only remaining coelomic structures, scale bar 200 µm. Staining: Toluidine blue. Images new, by authors.

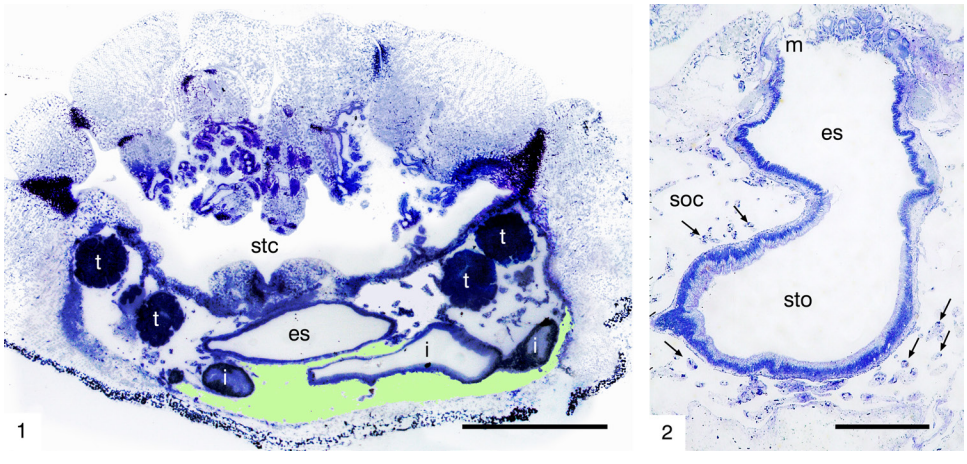

Fig. 20. *Cyathidium plantei* Heinzeller & others, 1996. *1*, Sagittal section of a whole animal showing the curled arms and their tangle of tentacles covering the suprategminal cavity (stc), es=esophagus, i=intestine t=testes in gonocoelic cavities. The *light green* space between the intestine and the aboral body wall can be considered as equivalent of the axial sinus, scale bar 1 mm. *2*, Sagittal section through mouth (m), esophagus (es), and stomach (sto); *arrows* point to trabeculae in the somatocoel (soc), scale bar 200 µm. Staining: Toluidine blue. Images new, by authors.

22.5–22.7). The coelomic tubes branch when reaching the stalk, which grows out by the formation of new columnals, namely nodals, each of which forms five, still-short cirri (Fig. 22.2–22.5, 22.7, 22.10).

Feather stars: Bulbous part. In feather stars, the entire chambered organ is positioned aboral to the axial sinus, immediately below the rosette. The chambers are radially oriented and lie close together but do not exhibit interconnections. All five are the same size and are roughly onion-shaped, and as a group they resemble a garlic bulb. The oral tip of each chamber continues as a thin tube. These tubes traverse the rosette and enter the axial sinus where they terminate blindly (Fig. 21.4). In the center of the outer wall of each bulb sits a pointed projection or cusp. Between the chambers are connective tissue septa that appear star-shaped in cross-section (Fig. 23.7). The septa are rich in hemal lacunae. These lacunae originate in the central hemal column, which lies centrally between the chambers and encloses the tubular axial complex (Fig. 23.8).

Feather stars: Labyrinthic part. At the aboral edge, the walls of the chambers fold and form intermediate floors, either horizontal

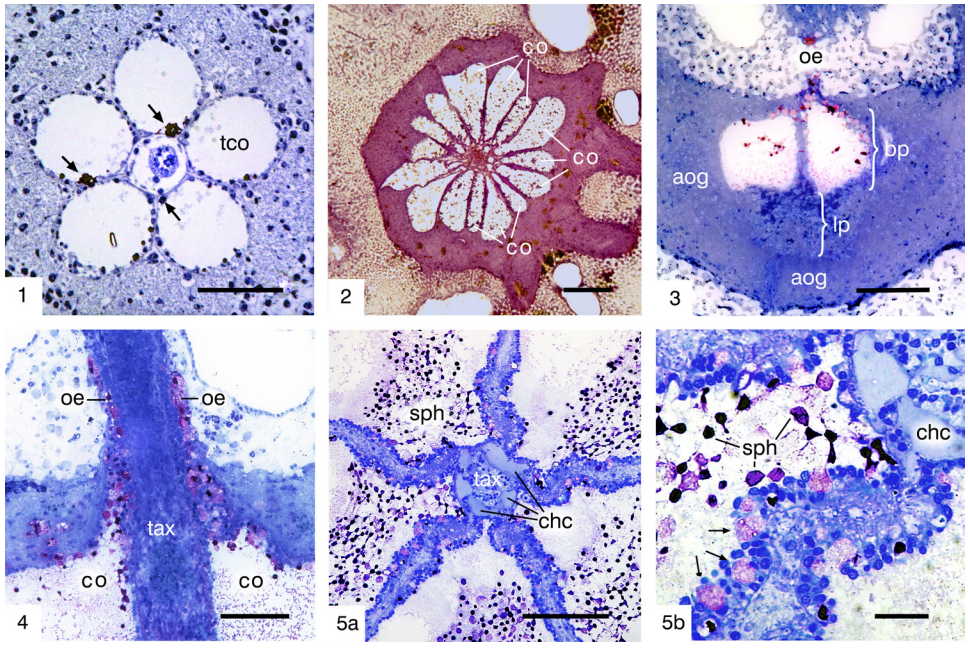

Fig. 21. Chambered organ. *1, Metacrinus sp.*, juvenile specimen, cross section through stalk with coelomic tubes, arrows point to secretory cells, tco=tubes of chambered organ, scale bar 50 µm. *2, Capillaster multiradiatus* (Linnaeus 1758), cross section, chambered organ deviating from usual pentamery, co=chambers, scale bar 200 µm. *3, Oligometra serripinna* P. H. Carpenter, 1881b, sagittal section showing the two compartments of the chambered organ, the bulbous part (bp) with the oral extensions (oe) and the labyrinthic part (lp), aog=aboral ganglion, scale bar 100 µm. *4, Clarkcomanthus albinotus* Rowe, Hoggett, Birtles, & Vail, 1986, sagittal section, oral extensions (oe) of the chambers traverse the rosette together with the tubular axial organ (tax), co=chambers, scale bar 50 µm. *5a–5b*, *Comatella nigra* P. H Carpenter 1888, cross section through the chambered organ with five septa radiating from the center, which contains the tubular axial organ (tax) and the central hemal column (chc). Note the purple secretory globules (sph) accumulated in the lumina of the chambers may also be found within the coelotelium at higher magnification (*5b*), scale bars 100 µm in *5a,* 10 µm in *5b*. Staining: Toluidine blue in *1, 3, 4* and *5a–b*, Hemalum-Eosin in *2*. Images new, by authors.

or sloping toward the periphery. The narrow coelomic spaces between the floors are all connected to the main lumen of their bulb and correspond in number to the generations of cirri that developed before. The folding of the bulb occurs primarily on its outer wall on both sides of the cusp. The folds lace off as coelomic tubes and contribute to the construction of a new cirrus at the cusp. This occurs iteratively, resulting in a confusing pattern of clefts beneath the bulb in histologic sections. Overall, this aboral region of the chambered organ may be referred to as the labyrinth (Fig. 23.9).

CIRRI

The internal structure of the cirrus (Fig. 24.1) is the same in isocrinids and feather

Fig. 22. Chambered organ of an isocrinid (on facing page). *Metacrinus sp.*, juvenile specimen. *1–7,* Three-dimensional models. *1,* External aspect of specimen, rad=plane of radials, bas=plane of basals, st=stalk, scale bar 1 mm. *2,* Body surface transparent with *gray* chambered organ. *3,* Region of chambered organ showing the oral swellings, five longitudinal tubes, and cirral canals (cic) supplying the two youngest sets of cirri *in statu nascendi*, at higher magnification. *4,* Chambered organ isolated, italic numbers show the levels of transverse sections *8–10*. *5,* The base of the axial sinus (*copper colored*) marks the level orally of which the tubes swell to bulbs. *6* and *7,* relationship between the chambered organ and the tubular axial complex (*green*). *8–10,* Transverse sections at the levels indicated in *4*. Staining: Toluidine blue, scale bars in *4–10* each 200 µm. Images new, by authors.

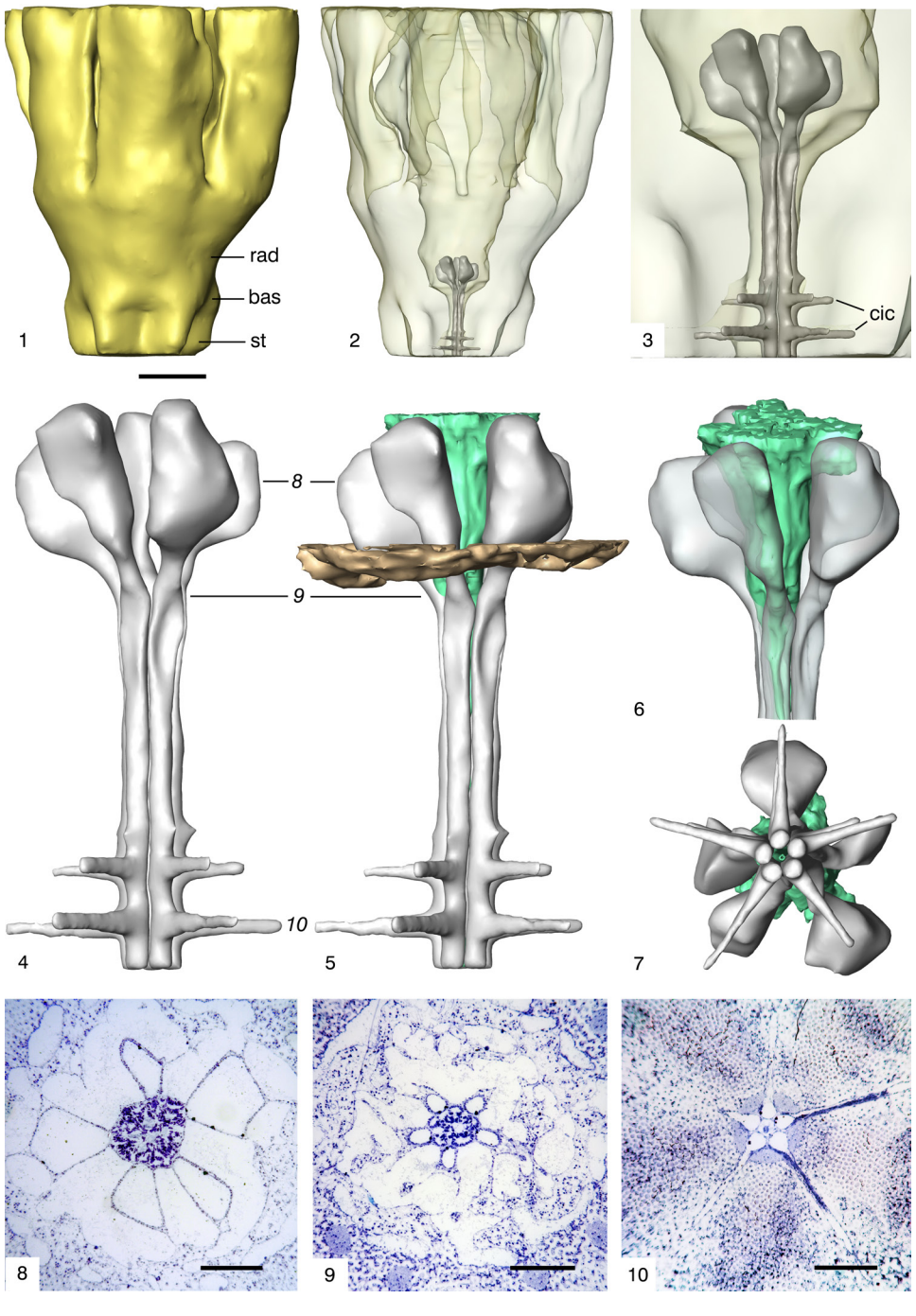

Fig. 22. Chambered organ of an isocrinid. See explanation on facing page.

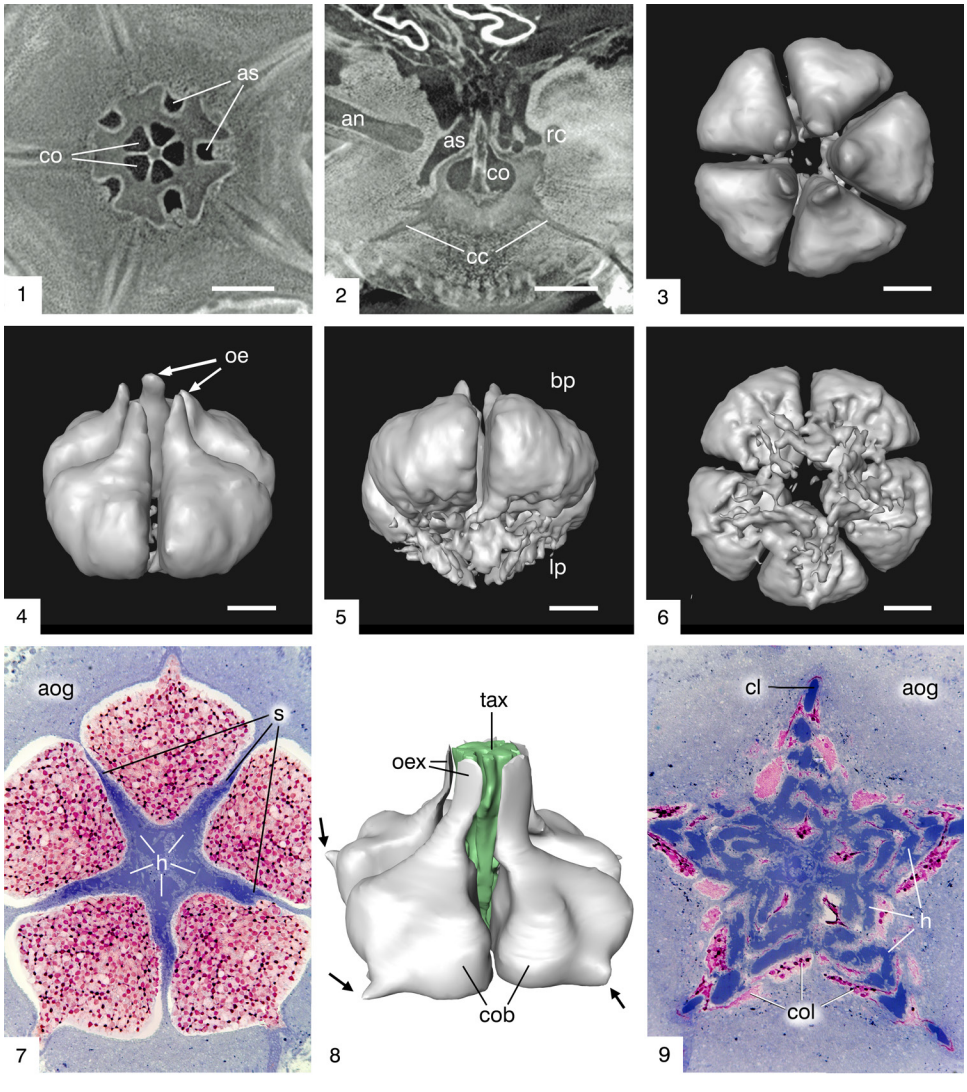

Fig. 23. Chambered organ of feather stars. *1–6, Antedon bifida* Pennant 1777. *1–2*, Ortho slices of the calyx of µCT data. *1*, Horizontal section at the level of the radials, as=axial sinus, co=chambers of the chambered organ. *2,* Sagittal section, radial on the left side, an=arm nerve, cc=canals of cirral nerves, rc=ring commissure. *3–6*, 3D models from µCT data; *3,* oral view; *4,* Slightly oral view, oe=oral extensions. *5,* Lightly obliquely aboral view, bp=bulbous part of chambers, lp=labyrinthic part of chambers. *6,* Aboral view with the labyrinthic part in a less detailed version. *7–9, Leptometra celtica* M'Andrew & Barrett, 1857, *7* and *8,* bulbous part. *9,* Labyrinthic part. *7,* Horizontal section showing five chambers at their maximum extension, embedded in the aboral ganglion (aog), separated from each other by septa (s) containing dark blue stained hemal lacunae (h). The chambers are unusually densely filled with secretory spherules that stain red by metachomasia. *8,* 3D model, viewed slightly obliquely from oral, arrows point to the cusps of the bulbs, cob=chambered organ bulbous part, oex=oral extentions, tax=tubular axial complex. *9,* Horizontal section of the labyrinthic part, showing numerous baton-like continuations of the septal tissue with dark blue hemal lacunae (h) alternating with aboral folds of the chambers marked by the red secretion, col=chambered organ labyrinthic part, cl=prospective cirral lacuna. Staining: Toluidine blue. All scale bars 100 µm. Images new, by authors.

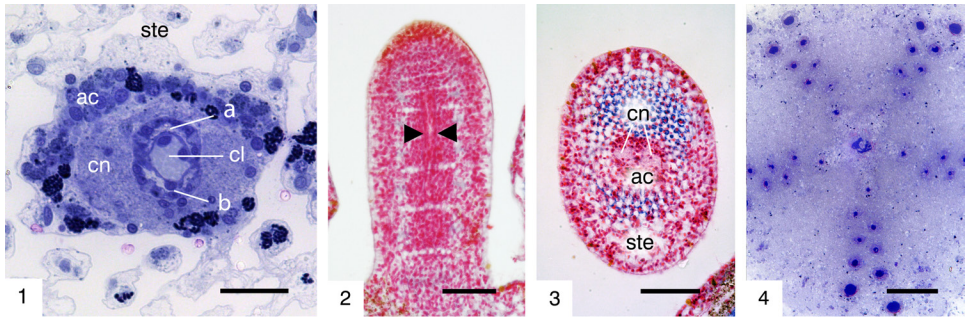

Fig. 24. Feather star cirri. *1, Himerometra robustipinna* P. H. Carpenter, 1881a, transverse section through a cirral bundle crossing the centrodorsal stereom (ste), cn=cirral nerve, cl=cirral lacuna, a and b=coelomic tubes, scale bar 20 µm. *2–3, Dorometra nana* (Hartlaub, 1890). *2*, Longitudinal section through a budding cirrus, cirral bundle between arrowheads, scale bar 50 µm. *3,* Transverse section through a cirrus near an articulation, the cirral nerve (cn) and the amebocytes (ac) are most conspicuous, scale bar 50 µm. *4, Leptometra celtica* M'Andrew & Barrett, 1857*,* horizontal section through the aboral ganglion below the chambered organ with double tracks of central cirral units, scale bar 100 µm. Staining: Toluidin blue in *1* and *4*, Azan in *2* and *3*.

stars, regardless of their radiation from an isocrinid nodal or from a feather star centrodorsal. A hemal lacuna runs internally and is bounded by two celomic tubes, one of which is typically oral and the other aboral. This combination of three tubes forms the central cirral unit. This is sheathed by the cirrus nerve; together they form the cirrus bundle (Fig. 24.1). In proximal regions, the hemal lacuna typically occurs with a wide lumen, whereas there is no internal space in the periphery. Amebocytes occur in high density in places on the surface of the cirral nerves (Fig. 24.1, 24.3) but rarely in the lacuna.

Cirral roots

Isocrinida. The fine structure of cirrus rooting was analyzed by Grimmer, Holland, & Hayami (1985) using *Metacrinus rotundus* P. H. Carpenter & L. von Graf, 1885 as an example. These will be briefly presented here, together with an illustration of *Endoxocrinus* (*Diplocrinus*) *sibogae* (Döderlein, 1907) (Fig. 25). The cirrus articulates at the nodal ossicle; this is also the level where the aforementioned cirral bundles radiate from internal structures of the stalk. The hemal lacuna is in continuity with the central hemal column. Both coelomic tubes arise from the same aboral somatocoelomic tube. On their way out, tubes and lacuna cross the stalk nerves, from which its branches give rise to the actual cirral nerves.

Not shown in the figure, on the side opposite to the hemal lacuna, the coelothelia are enriched with neurons and nerve fibers and form a considerable intraepithelial nerve plexus in addition to the external cirral nerve.

At the aboral margin of the basalia, new nodalia develop even after maturation. There, the outgrowth of coelomic tubes can be observed (Fig. 22.4–22.5, Fig. 25.10).

Feather stars. In feather stars, the labyrinthic part of the chambered organ is the source of new cirri. At the cusp of a bulb (Fig. 29.7–29.8), pairs of new central cirral units form. In the 3D model presented here (Fig. 26), the pairs were tracked along their hemal lacunae, which have recognizable lumina from the beginning (although they appear as solid red strands in the model, see Fig. 31.3, p. 30). In the specimen of *Leptometra celtica* M'Andrew & Barrett, 1857 examined here, all and even tiny coelomic lumina could be tracked because of the presence of the metachromatically staining secretion used.

There are further details observed in this species. The developing coelomic tubes initially are compressed with a minute flat lumen and become only secondarily provided with a distinct lumen. The two

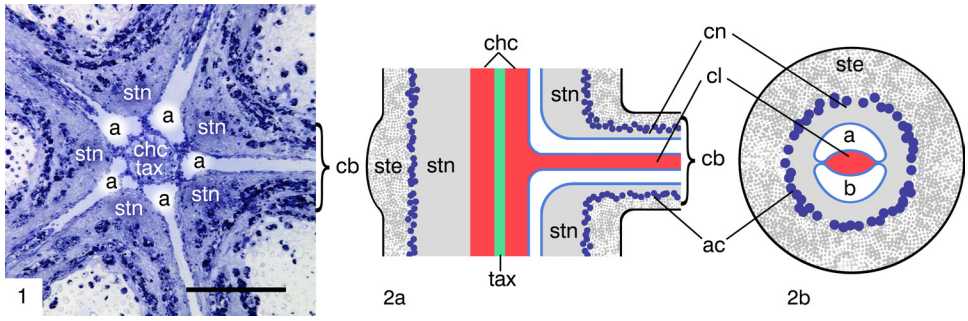

Fig. 25. Cirri of isocrinid crinoids. *1, Endoxocrinus sibogae* (Döderlein, 1907), cross section of the stalk at a nodal level with five radiating cirral bundles, a=tubes of the chambered organ, scale bar 200 µm. Staining: Toluidine blue. *2a*, Schematic longitudinal section of the stalk. *2b,* Cross section of a cirrus. Abbreviations: a=oral coelomic tube, b=aboral coelomic tube, ac=accumulated amebocytes, cb=cirral bundle, chc=central hemal column, cl=cirral lacuna, cn=cirral nerve, ste=stereom, stn=stalk nerve, tax=tubular axial complex, blue line=coelothelium (modified from Grimmer, Holland, & Hayami, 1985, fig. 1,D–E).

central cirral units look similar to twins arising from slightly different planes in the oral-aboral direction (Fig. 26.5). Furthermore, the coelomic lumina of level "b" (in Fig. 26) belong to the aboral tube of the oral central cirral unit and simultaneously to the oral tube of the aboral central cirral unit. After emergence from the bulb, one central cirral unit (CCU) turns to the right, the other to the left. Thus, in horizontal sections through the deep aboral ganglion, the central cirral units have a staggered double track pattern (Fig. 24.4).

Function of cirri. The function of cirri in both isocrinids and feather stars is locomotion and/or holding the animal to the substratum. Video recordings (Birenheide & Motokawa, 1995) showed that active cirrus movements can be triggered by irritation of the animal. Because no muscle cells can be detected in a cirrus, various mechanisms for the active movement have been suggested (reviewed by Baumiller & Janevski, 2011), including hydraulic pressure in the coelomic tubes (Teuscher, 1876). Most substantial, however, is the assumption of neural control of the mutual connective tissue in the ligaments (Birenheide, Yokoyama, & Motokawa, 2000), see Section VII.

III. HEMAL SYSTEM

Like other echinoderms, crinoids have a hemal system (Fig. 27), but circulating blood is missing. However, true circulation is possible—and actually takes place—in fluid filled coelomic spaces (see *Somatocoel* in Section II, p. 8. In addition, a system of interconnected spaces exists in crinoids called the hemal system, which contains its own matrix.

The hemal matrix consists mainly of a fine, granular glycoprotein substance with a lipid component and also collagen fibrils. In addition, various types of amebocytes (comparable to blood cells) are present. The viscosity of the matrix is assumed to be too high to be kept moving in the small lumina of the lacunae and vessels. However, the hemal net provides a conduit for amebocytes to travel to almost all parts of the body. According to Grimmer and Holland (1979), this should be assumed to be the main function of the hemal spaces of crinoids (but there may be other functions, which are discussed at the end of this section).

The entire connective tissue space, skeleton included, is bordered all around by the basal laminae of various epithelia or coelothelia—this also applies to each hemal space, with minor exceptions. Therefore, hemal spaces may be regarded as a special part of the connective tissue—also due to the rare places where hemal space and connective tissue meet directly.

Both hemal lacunae and hemal vessels lack an inner cell layer comparable to the

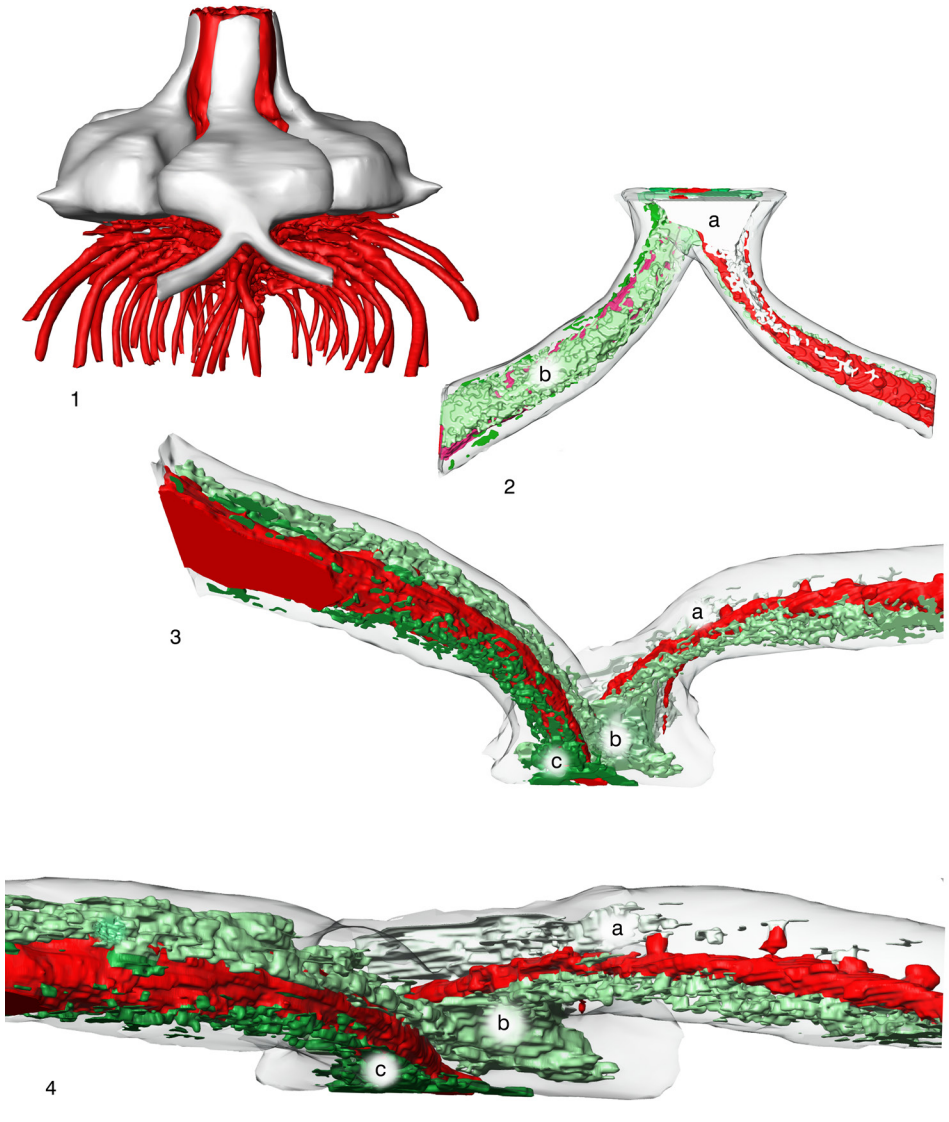

Fig. 26. Roots of two new cirri in *Leptometra celtica* M'Andrew & Barrett, 1857, 3D model. *1*, Lateral view of the five bulbs around the central hemal column (note that the anterior bulb started to form new cirri). *2–4,* Closer look at internal structures through the transparent *gray* coelothelium, coelomic lumina in shades of green, the more aboral, the *darker green*, hemal lacunae *red*; a, b, and c=levels of coelomic lumina. *2,* Oral view; *3,* oblique aboral view; *4*, horizontal view showing superjacent levels of coelomic lumina and hemal lacunae. Images new; by authors.

endothelium of mammalian blood vessels. Lacunae are typically connective tissue spaces bounded by basal laminae of two or more epithelia or coelothelia (Fig. 28.1–28.2), or in some places they merge directly into connective tissue. Vessels are formed only by eversions of the coelothelium and lie freely in somatocoelomic caverns. In some places, a tiny stalk connects the vessel to the wall of the cavern (Fig. 28.3). A schematic overview of lacunae and vessels is provided on p. 30 (Fig. 32).

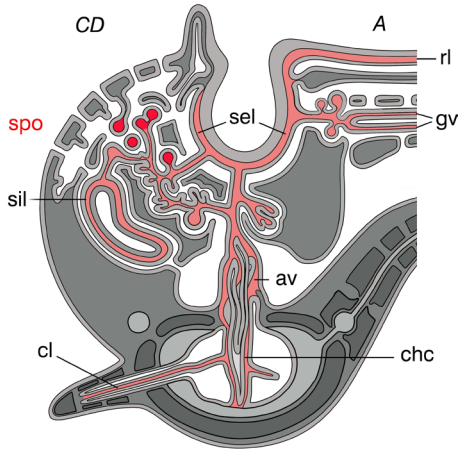

Fig. 27. Locations of major hemal spaces in a schematized feather star with A ray on the right and CD interray on the left. Hemal vessels and lacunae in *pale pink*, vessels of the spongy organ (spo) in *bright red*. Labels: sel=subesophageal lacuna, rl=radial lacuna, gv=genital vessel, sil=subintestinal lacuna, av=axial vessel surrounding the axial tubules, chc=central hemal column, cl=cirral lacuna. (modified from original drawing in Heinzeller & Welsch, 1994, fig. 10B).

LACUNAE

Lacunar Walls

As mentioned earlier, the lacunar space may be in direct contact with the actual connective tissue. Such sites are, for instance, the peripheral margin of lacunae in the septa of the chambered organ (Fig. 29.3, Fig. 29.5b) or both lateral margins of a cirral lacuna (Fig. 24.1).

Typically, however, a lacunar space follows the course of the limiting epi- or coelothelia. Accordingly, there are a variety of lacunar shapes.

TYPES OF LACUNAE

In general, every space naturally extends in three dimensions. However, in simple lacunae, one dimension may predominate, resulting in tubes or ribbons. When two dimensions predominate, laminae result. When all three dimensions are well represented, voluminous spaces result.

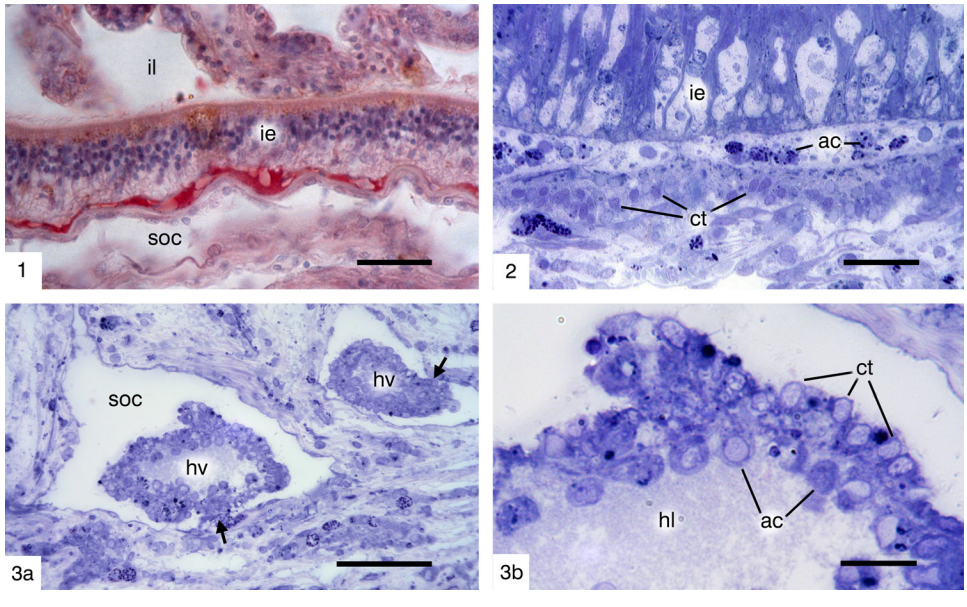

Fig. 28. Lacuna (*1* and *2*) vs. vessel (*3a* and *3b*). *1, Antedon mediterranea* (Lamarck, 1816), lacuna (*red*) between the intestinal epithelium (ie) and the coelothelium bounding the somatocoelomic cavern (soc), il=intestinal lumen, scale bar 50 µm; *2, Himerometra robusstipinna* P. H. Carpenter, 1881a, lacuna between intestinal epithelium (ie) and coelothelium (ct), ac=amebocytes, scale bar 25 µm; *3a, Antedon mediterranea,* large hemal vessels (hv) in somatocoelomic caverns (soc), arrows mark stalk-like contact with cavern wall, scale bar 50 µm; *3*b, detail of the vessel shown in *3a* with the single-layered coelothelium (ct) and what appears to be an inner 'layer' of amebocytes (ac); hl=hemal lumen, scale bar 10 µm. Staining: *1,* VIP antibody, Hemalum, *2–3,* Toluidine blue. Images new, by authors.

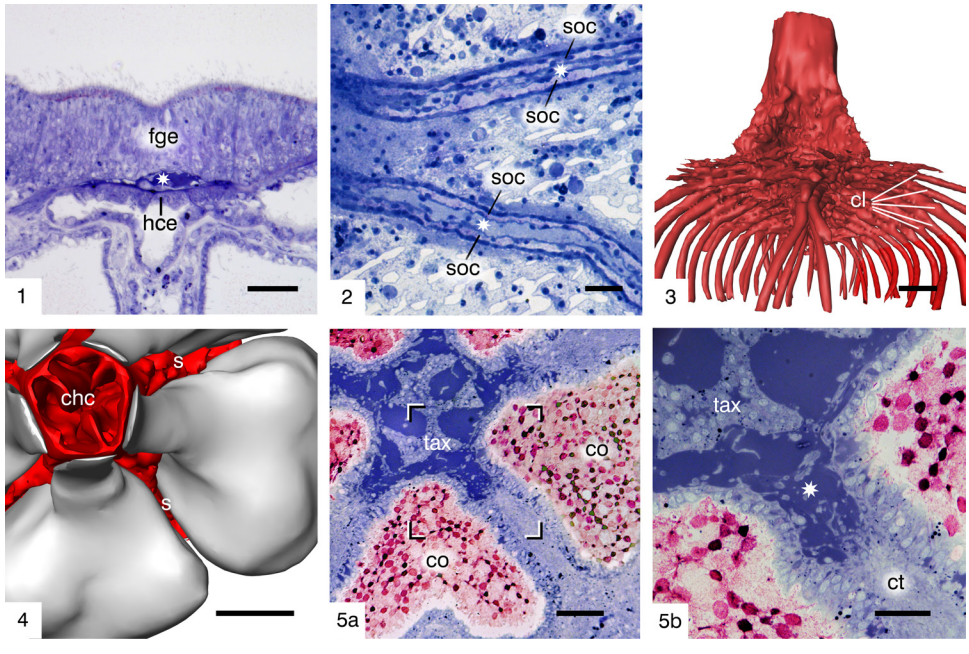

Fig. 29. Lacunae. *1, Antedon mediterranea* (Lamarck, 1816), ribbon-shaped lacuna (asterisk) between food groove epithelium (fge) and hydrocoelomic epithelim (hce), scale bar 25 µm; *2, Himerometra robustipinna* P. H. Carpenter, 1881a, longitudinal section through two tube-shaped lacunae (*asterisks*) connecting cirri with the central hemal column, soc=somatocoel. scale bar 25 µm. *3–5b, Leptometra celtica* M'Andrew & Barrett, 1857, central hemal column. *3,* 3D model of the very voluminous aboral central hemal column with radiating cirral lacunae (cl), scale bar 100 µm. *4*, Oral view of two bulbs of the chambered organ (gray) with the central hemal column (chc) in the middle and septa (s) between the bulbs, scale bar 100 µm. *5a*, Horizontal section of the chambered organ showing two adjacent chambers (co), scale bar 50 µm. *5b*, Magnified area marked by the rectangle in *5a*, the hemal space (*dark blue*) is triple bounded, first by the epithelium of the axial tubules (tax), second by the epithelium of the chambers, and third by the septal connective tissue (ct), scale bar 25 µm. Staining: *1, 2* and *5*: Toluidin blue. Images new, by authors

Unidimensional lacunae

Unidimensional lacunae are present in cirral canals (Fig. 29.2). These lacunae are formed by twins of somatocoelomic tubes enclosing a lacuna that is elliptical to almost circular in cross section (Fig. 24.1). Another approximately unidimensional lacuna is the ribbon-shaped lacuna between the food groove epithelium and the hydrocoelomic epithelium (Fig. 29.1). This lacuna is typically highest in its middle and flattens out on either side. It accompanies the food groove and extends to the finest tips of pinnules and even the tentacles. In the opposite direction, it leads to the mouth region, where it joins the lacunae of the other arms.

Laminar peri-intestinal lacuna

The lacunae below the food grooves merge into the periesophageal and further into the peri-intestinal hemal lacuna (Fig. 28.2). Because the hydrocoelomic epithelium terminates in the periesophageal ring, in the continuing peri-intestinal lacuna the outer boundary is represented by the somatocoelomic epithelium. The resulting lacuna encloses the entire gut except for the anal cone. On one hand, this lacuna envelops the gut as a lamina, but it also follows its spiral course.

Voluminous central hemal column

A very voluminous lacuna is the central hemal column, located within the aboral ganglion of feather stars, aboral to the rosette.

There, the connective tissue surrounds the body axis. It is largely devoid of cells, creating the large central hemal column. Oral of the rosette, within the axial sinus, this hemal column continues as a large vessel containing the axial tubules (Fig. 32.2).

In isocrinids, the equivalent of this lacuna extends deep into the stalk until the most distal cirri-bearing nodal. There the column is narrow and elongate, forming radially arranged quintuple lacunae in each node. In contrast, in comatulids the space within the centrodorsal is narrow, and consequently the central hemal column extends only from the rosette to the base of the aboral ganglion. There, the column forms numerous cirral lacunae, which, because labyrinthically intertwined, contribute to the overall appearance of a rhizome (Fig. 29.3).

Formation of cirral lacunae

Two lacunae of the interradial lacunae (mentioned in Section II), together form a single cirral lacuna in a rather complicated way. After emerging from each of two adjacent septa, each interradial lacuna divides into a left and a right strand. The right strand of the first and the left strand of the second finally meet at the radius (Fig. 30.3–30.4). The actual cirral lacuna rises from this meeting point of the two strands. In conjunction with two somatocoelomic tubes and the cirral nerve, the cirral lacuna extends outward. Along the way, these composite structures bend slightly, alternatively to the left or to the right, resulting in a V-shaped arrangement in a horizontal plane (Fig. 24.4).

The pattern of lacuna development reflects the development of new cirri. For each new cirrus, a lacuna is formed, and the new lacuna always arises orally from the previous one. The new lacunae become larger than the previous ones as the animal grows larger during life. The sets of hemal strands and lacunae are interleaved one above the other. The succession of these generations of cirral lacunae is shown here (Fig. 30.3–30.4). Some of the very early generated cirral lacunae terminate blindly within the centrodorsal, as A. H. Clark stated in 1921, p. 321: "...these are the last traces of cirri which have become obsolete and have been discarded." The combination of the two, aborally the central hemal column and orally the large vessel in the axial sinus, provides a continuous hemal connection along the long axis of the animals. It might be considered a pathway for amebocytes.

VESSEL TYPES

Type 1

Type 1 vessels run freely through wide coelomic caverns (Fig. 28.3, Fig. 31.1). Their wall consists only of the coelothelium. Such vessels contain only hemal matrix and amebocytes, which in certain cases appear to creep along the coelothelial basement membrane, giving the impression of an additional inner layer (Fig. 28.3b). Other amebocytes may be located in the center of the vessel lumen. The diameter of such vessels ranges from 5–50 μm. Type 1 vessels occur in the oral somatocoel and are concentrated in the spongy organ (see below).

Type 2

Type 2 vessels enclose epithelial tubes. This is true in two organ complexes. First, in the genital complex, the vessel encloses the genital tube, either non-gametogenic or gametogenic or differentiated into gonads (see Fig. 57.1–57.4). Second, in the axial complex, a very wide vessel encloses the tree of axial tubes (Fig. 31.2). The diameter of the genital vessels ranges from approximately 30 μm to 1 mm. The axial complex may be even larger, shown by Holland (1970) in *Nemaster rubiginosa* Pourtalès, 1869 to be a giant hemal vessel. In contrast, this large vessel in *Himerometra robustipinna* P. H. Carpenter, 1881a has been interpreted by Ezhova and Malakhov (2020) as a plexus of multiple vessels.

SPONGY ORGAN

The spongy organ (labial plexus, spongy body) represents a particular domain of the somatocoelomic caverns of feather

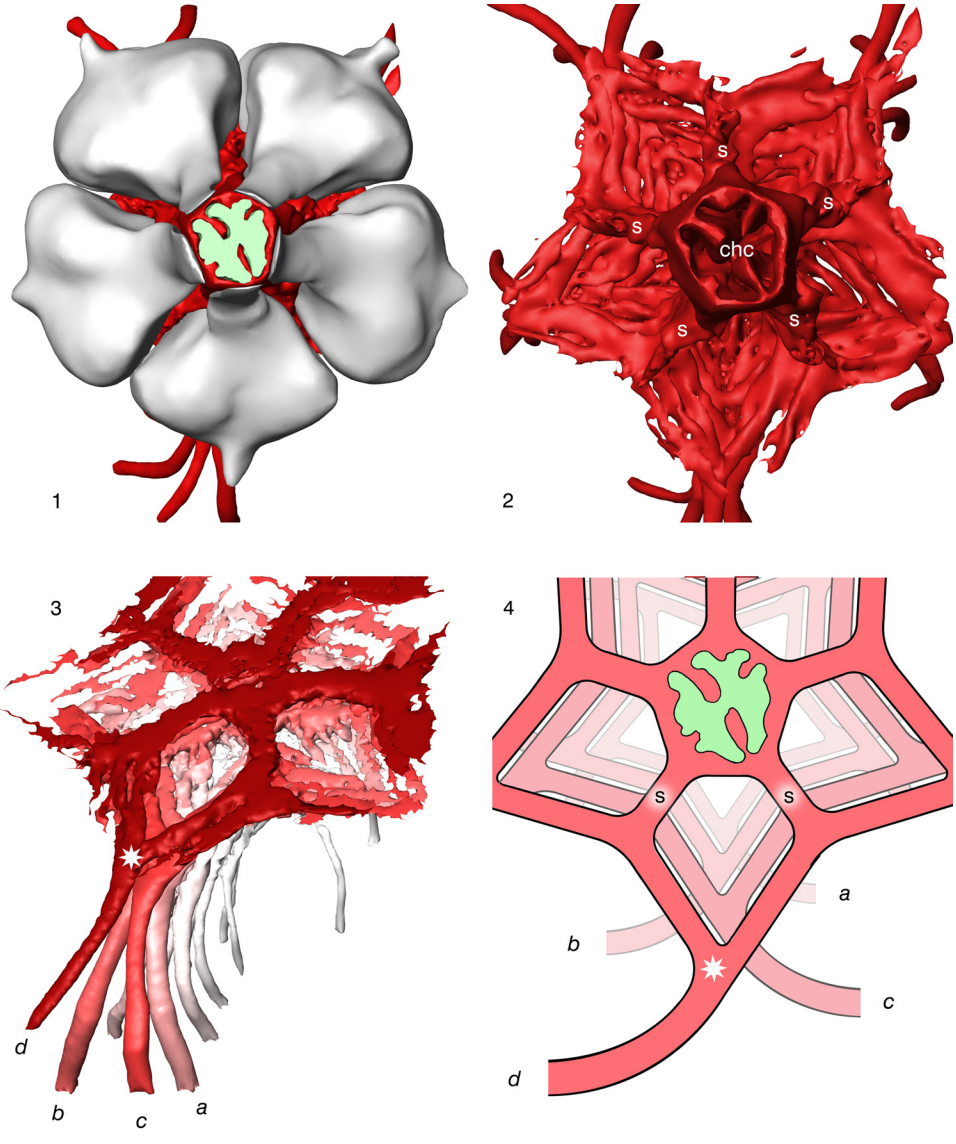

Fig. 30. *Leptometra celtica* M'Andrew & Barrett, 1857, *1–3*, 3D models of the chambered organ and its hemal apparatus. *1,* Oral view of bulbs (*gray*) surrounding the central hemal column (*red*), with the axial tubules enclosed (*green*); *2,* central hemal column (chc), hemal septa (s), and hemal strands arising from the septa; *3,* oblique oral view of the aboral part of the central hemal column from which the youngest four cirral lacunae arise *("d"* marks the current one). Lacunae older than *"d"* have a decreasing *rosy* to *gray* color. *4*, Schematic illustration of the oral view of that aboral part of the central hemal column with hemal strands pattern. The *white asterisk* in *3* and *4* marks the origin of the cirral lacuna "*d*." Images new, by authors.

stars and isocrinid crinoids, rich in hemal vessels. Its main part lies subtegminally in the CD interray in close proximity to the esophagus and may surround it. The structural composition of the spongy organ changes gradually from the oral to the aboral end. The oral part is an accumulation of hemal type 1 vessels (Fig. 33.3–33.4). Such a conspicuous oral part of the spongy organ has been present in adult specimens of all

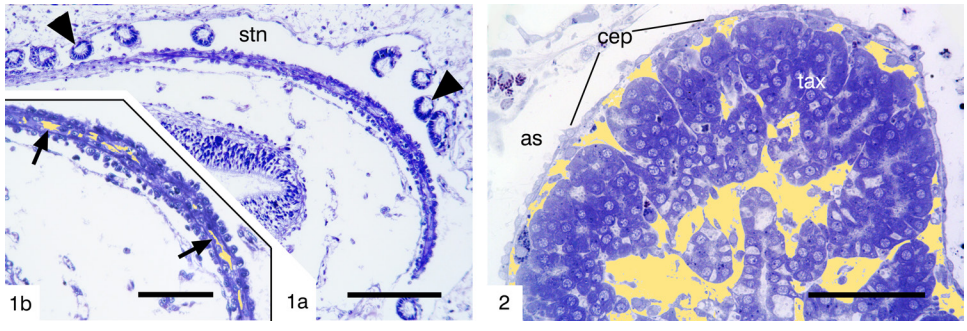

Fig. 31. Type 1 and type 2 hemal vessels. *1a, Metacrinus* sp. juvenile, horizontal section showing a long, curved type 1 vessel in a cavern of the subtegminal net (stn), arrowheads point to stone canals, scale bar 100 µm; *1b,* magnified detail of *1* showing the small lumen of the vessel (arrows, yellow filling), scale bar 50 µm. *2, Caledonicrinus vaubani* Avocat & Roux in Améziane-Cominardi & others, 1990, axial tubules (tax) embedded in a type 2 vessel, most of the hemal lumen filled in *yellow*, cep=coelomic epithelium, as=axial sinus, scale bar 50 µm. Images new, by authors.

feather stars studied so far, as well as in the bathycrinid *Caledonicrinus vaubani* Avocat & Roux in Améziane-Cominardi & others, 1990 (Heinzeller, Welsch, & Améziane, 2010). Vessels of the oral spongy organ open into the subesophageal and initial subintestinal lacunae.

Further aborally, the spongy organ narrows to a kind of peduncle that runs in close contact with the axial tubules. In *Promachocrinus kerguelensis* P. H. Carpenter, 1879, the axial tubules almost enclose the deep spongy organ (Fig. 33.6).

In this part, there are only a few larger hemal vessels, which are mainly located at the edge of the organ that is not covered by axial tubules. The vessels that emerge from the deep spongy organ ascend orally, increase

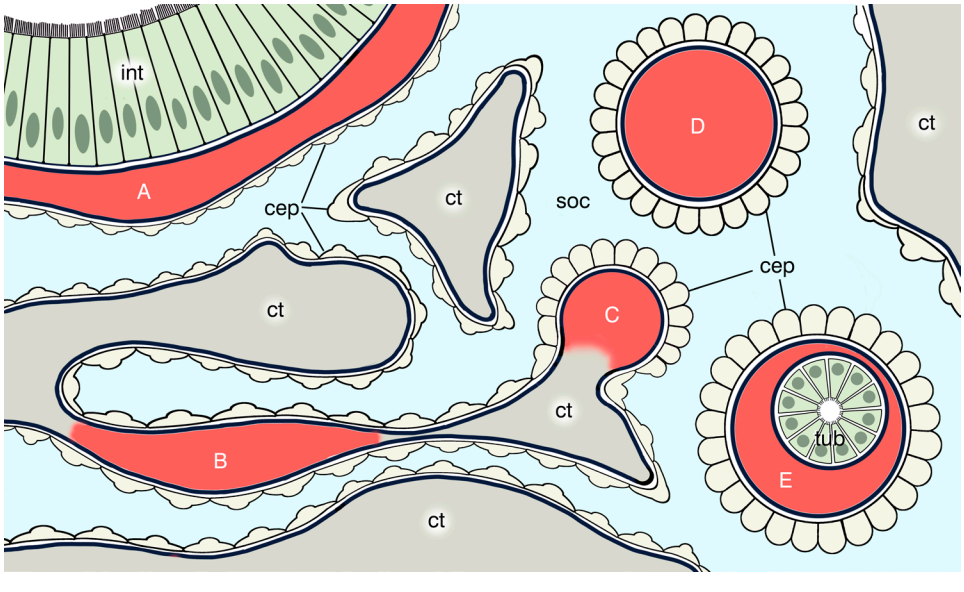

Fig. 32. Schematic illustration of hemal space types. White capitals: A=subintestinal lacuna, B=lacuna in the connective tissue of a trabecula between somatocoelomic clefts, C=vessel in contact with connective tissue; in such locations lacunae and vessels may have open connections. D=type 1 hemal vessel, E=type 2 hemal vessel. ct=connective tissue, soc=somatocoel, cep=coelomic epithelium, int=intestinal epithelium, tub=epithelial tubule. Image new, by authors.

in number, and finally assemble in the oral spongy organ.

REICHENSPERGER'S ORGAN

Reichensperger's organ, originally described by Reichensperger in *Pentacrinus decorus* (currently *Neocrinus decorus* Thomson 1864) in 1905 (Fig. 34.1), apparently replaces the aboral spongy organ of feather stars in isocrinid crinoids (Welsch, Heinzeller, & Holland, 1994). Aspects of location, shape, and size, in particular the relationship to the tubular axial organ, are treated in detail in Section IV (Fig. 42). The main part of this organ consists of a pad of densely packed specific cells (Fig. 34.2, Fig. 34.5). The pad is covered all around by the coelothelium. The coelothelium is deeply ingrown into the organ and preforms hemal lacunae and/or vessels. Oral of the Reichensperger's organ, there are relatively large hemal vessels (Fig. 34.3–34.4) that resemble the accumulated vessels in the spongy organ of feather stars. The cells that are specific to this organ are large and contain spherical nuclei. Based on their electron microscopic pattern, it must be assumed that these cells produce either matrix components or hemal substances (Welsch, Heinzeller, & Holland, 1994). Amebocytes are widely scattered among the specific cells. This is consistent with Cuénot (1948), who also considered the spongy organ of feather stars as the source of amebocytes.

FUNCTION OF THE HEMAL SYSTEM

The function of the entire hemal system, and in particular that of the spongy organ and the Reichensperger's organ, is still under debate. Not even the seemingly self-evident conclusion that these two organs are vasculogenetic has been proven beyond doubt. Vasculogenesis may also occur at other sites, possibly related to functional or developmental requirements. A candidate for this, for example, is the CD int`erray, where primordial germ cells arise early during development (Russo, 1902; Fedotov, 1930). The genital hemal vessels and associated genital strands appear to be required for the translocation of these cells to the peripheral gonads.

However, morphology alone does not seem to be adequate to clarify the question of the function of the hemal system, as various interpretations have been considered on the basis of purely morphological observations. The function was assumed as a site of amebocyte origin (Cuénot, 1948) to provide pathways for amebocytes throughout the animal (Grimmer & Holland, 1979), to be osmoregulatory (Balser & Ruppert, 1993), and to be secretory, possibly for hemal substances (Heinzeller & Welsch, 1994).

Of course, there could be further possibilities of function. For example, it cannot be ruled out that the crinoid hemal system serves to store nutrients, as in other echinoderm classes, e.g., starfish (Chia & Koss, 1994).

IV. AXIAL ORGANS

In most crinoids, an elongated structure has been observed near the central axis of the calyx (Bals & others, 1990; Heinzeller, Welsch, & Améziane, 2010), traditionally called the axial organ or axial gland. This organ extends from the depth of the stalk (or of the centrodorsal ossicle in feather stars) to the subtegminal region of the calyx. It is bounded all around by a coelothelium. Its most striking feature consists of enclosed epithelial tubules. The axial organ is formed early during development; it is already present in the pentacrinoid larva (Grimmer, Holland, & Kubota, 1984).

The tubules inside the organ resemble secretory tubules. For this reason, the organ has been interpreted as a gland (Hamann, 1889: drüsiges Organ; Hyman, 1955: axial gland). Electron microscopic studies have confirmed this interpretation (Holland, 1970). Overall, the tubules form a tree with a slender trunk in the aboral part and the crown in the oral part. Parts of the spongy

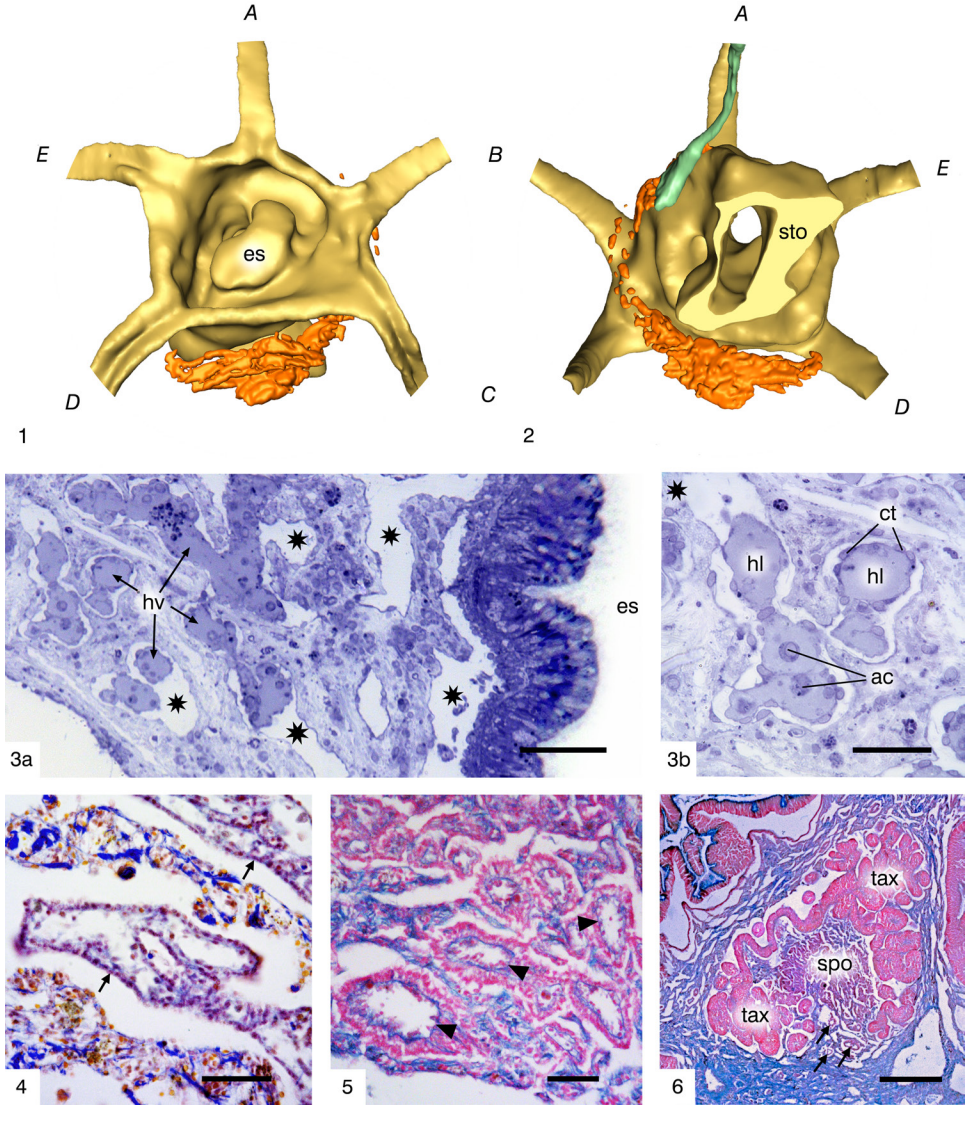

Fig. 33. Spongy organ. *1* and *2, Dorometra nana* (Hartlaub, 1890), 3D model: *1*, oral view, most of the organ (*orange*) lies in the CD interray and surrounds the deep esophagus (es) and upper stomach (sto); *2,* aboral view, in the A ray the spongy organ touches the tubular axial organ (*green*). *3a, Antedon mediterranea* (Lamarck, 1816), radial section through the CD interray; the hemal vessels (hv) are concentrated near the esophagus in the somatocoelomic subtegminal net (*asterisks*), scale bar 50 µm; *3b,* details at higher magnification,hl=hemal lumen, ct=coelothel, ac=amebocytes, scale bar 20 mm. *4–6, Promachocrinus kerguelensis* P. H. Carpenter, 1879; *4,* horizontal section just below the tegmen with wide, branched vessels (*arrows*) of the spongy organ, scale bar 50 µm; *5,* slightly further aborally sectioned, numerous vessels (*arrowheads*) with blue basement membranes clearly visible towards the vessel lumen, scale bar 50 mm; *6,* horizontal section near the aboral end of the spongy organ (spo) where it is almost completely surrounded by the tubular axial organ (tax); hemal vessels (*arrows*) are only at the uncovered edge, scale bar 500 µm. Staining: Toluidine blue in *3*, Azan in *4*, Alcian blue-Azocarmine in *5–6.* Images new, by authors.

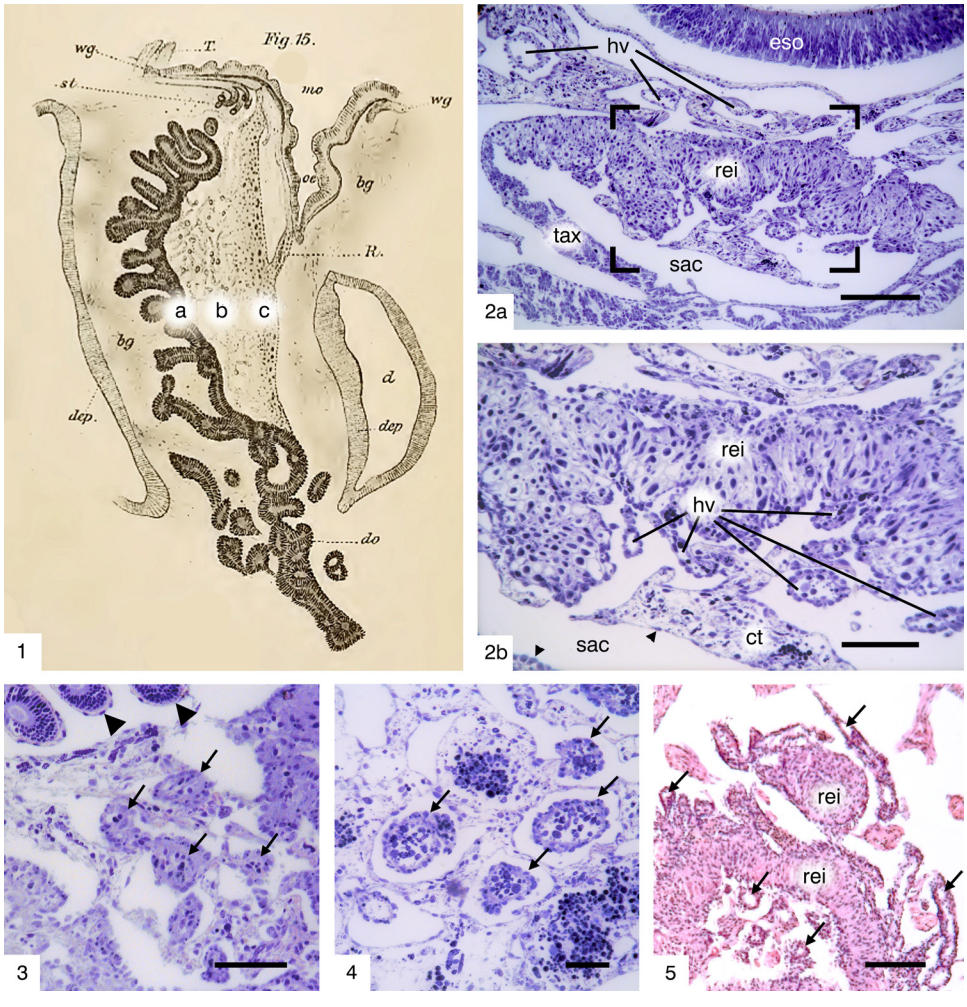

Fig. 34. Reichensperger's organ, histology. *1*, Original drawing by Reichensperger (1905, pl. III, fig. 1), a=glandular organ, b=lumen of the sac containing hemal vessels, c=cell cushion. *2–5*, *Metacrinus levii* (Améziane-Cominardi in Améziane-Cominard & others, 1990), adult specimens, horizontal sections: *2a*, section at about half calyx height, tax=tubular axial organ, sac=coelomic space, rei=Reichensperger's organ, hv=hemal vessels, eso=esophagus, scale bar100 µm. *2b*, higher magnification of area marked in *black* in *2a*, showing deep fissures on the inner surface of Reichensperger's organ and hemal vessels in the lumen of the sac, *arrowheads* point to the coelothelium, ct=connective tissue islet, scale bar 50 µm. *3,* section above the oral end of Reichensperger's organ, *arrowheads* point to stone canals, *arrows* to hemal vessels contributing to the spongy organ and representing oral continuation of those shown in *4*, scale bar 50 µm. *4,* section slightly further aboral than *3,* showing a cluster of large hemal vessels (*arrows*) arising from the Reichensperger' organ, scale bar 25 µm. *5,* deep aboral section of Reichensperger's organ (rei), many hemal vessels (*arrows*) emanate from its edge, scale bar 100 µm. Staining: Toluidine blue in *2–4,* Hemalum-Eosin in *5*. Images *2–5,* new, by authors.

organ and the Reichensperger's organ are attached to the axial organ.

AXIAL ORGAN

Feather stars, oral part, above the rosette. Through the central hole of the rosette, like through a bottleneck, the tubules orally rise (Fig. 35.2). The tubules running through the rosette may be only few in small species as in *Dorometra nana* (Fig. 38.3) or numerous in large species as in *Promachocrinus kerguelensis* (Fig. 37.1–37.2).

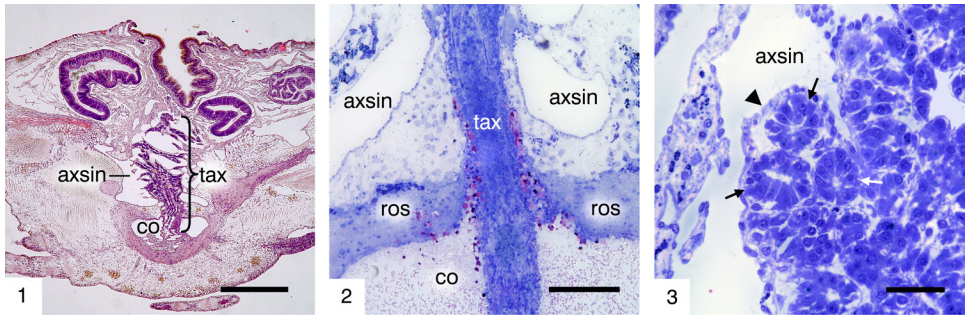

Fig. 35. Axial organ, mediosagittal sections. *1, Antedon mediterranea* (Lamarck, 1816), scale bar 200 µm. *2, Clarkcomanthus albinotus* Rowe, Hoggett, Birtles, & Vail, 1986, axsin=axial sinus, tax=tubular axial organ, co=chambered organ, , scale bar 100 µm. 3, *Comatella nigra* P. H Carpenter 1888, *arrows* point to individual tubules, *arrowhead* points to the coelothelium, scale bar 25 µm. Labels: axsin=axial sinus, tax=tubular axial organ, co=chambered organ, ros=rosette. Staining: PAS in *1,* Toluidin blue in *2* and *3*. Images new, by authors.

Above the rosette, within the axial sinus, the tubule bundle pivots from the axis into the AB interray (Fig. 36.3) and eventually approaches the esophagus (Fig. 36.3–36.4). A 3-D model of the tubular axial organ of feather stars, along with the spongy organ and esophagus is included herein (Fig. 36, Fig. 41).

The ascending tubules lie inside a large type 2 hemal vessel (see Section III, Fig. 32.2), which in turn is surrounded by the axial sinus (Fig. 35.2). The tubular complex progressively branches from aboral to oral: budding, outgrowth, elongation, and branching are observed, and it seems likely that proliferation and differentiation of progenitor cells take place. Toward the oral end, the organ reaches its maximum size and highest differentiation (Fig. 37); at that point the columnar epithelium has grown large and completely fills the lumen of the tubule in many places. Most epithelial cells respond positively to Periodic Acid Schiff stain (PAS), indicating the production of mucopolysaccharides. In addition, ultrastructural data clearly indicate a secretory function, probably of components of the hemal substance (Holland, 1970). However, this so-called gland lacks an excretory duct, and it must be assumed that the product of the cells is discharged directly into the surrounding hemal space or taken over by amebocytes. However, such a function has not yet been demonstrated by physiological examination.

Feather stars, aboral part, below the rosette. In the aboral section of the axial organ, the tubules are embedded in the central hemal column (see Fig. 30.5). The central hemal column and tubules penetrate deeply into the basal plate of the aboral nerve ganglion, where the aboral tips of the axial tubules are present (Fig. 40.1).

A tubular axial organ consisting of both the oral and the aboral parts, as described here, is present in all feather star species studied so far (in adults of the genera *Antedon, Comactinia, Comatella, Comatula, Clarkcomanthus, Davidaster, Himerometra, Oligometra, Promachocrinus*) and in the pentacrinoid larvae of *Leptometra* and *Oxycomanthus* (Heinzeller, Welsch, & Améziane, 2010).

ISOCRINIDS

Within the axial sinus, the tubular axial organ resembles that of feather stars (Fig. 39.1–39.3). Below this, a few or simply one axial tubule descend into the stalk (Fig. 39.4–39.5), accompanied by the tubules of the chambered organ and by the central hemal lacuna, identical to the central hemal column of feather stars.

OTHER STALKED CRINOIDS

The axial organ of most other stalked crinoids seems to differ little from that of isocrinids.

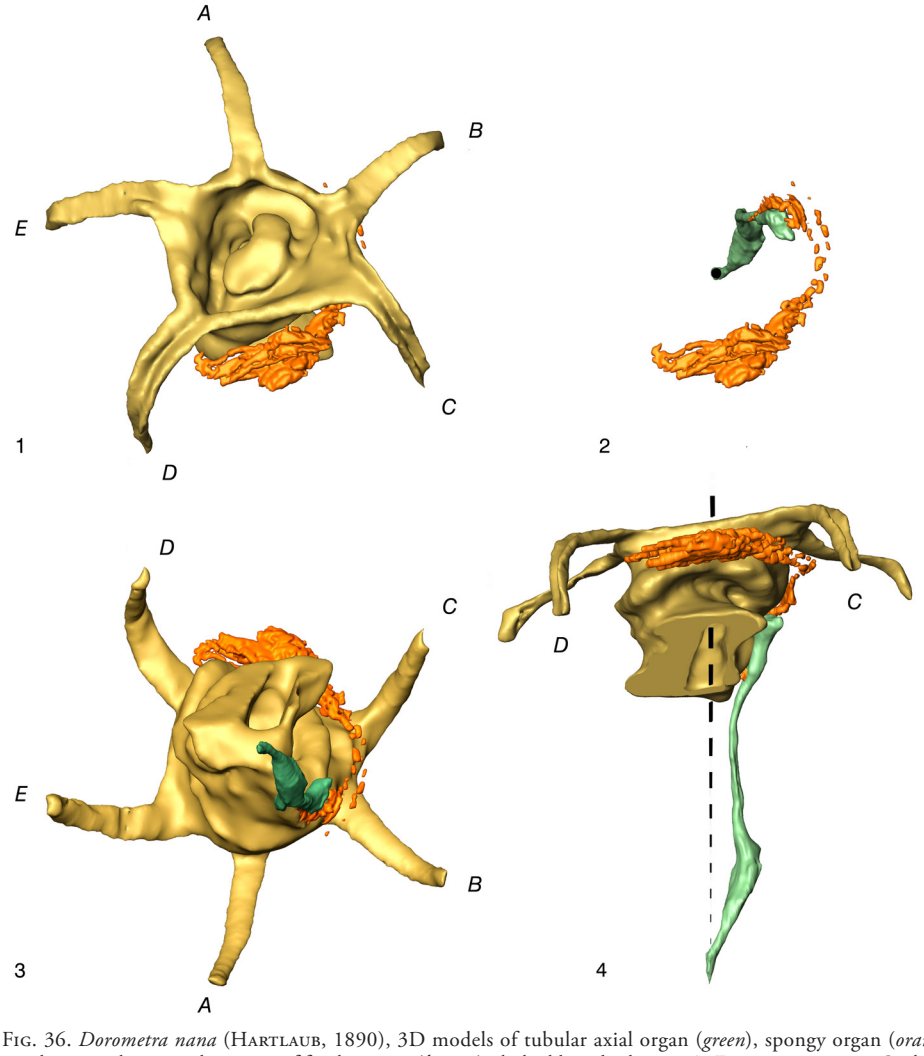

Fig. 36. *Dorometra nana* (Hartlaub, 1890), 3D models of tubular axial organ (*green*), spongy organ (*orange*), esophagus and proximal sections of food grooves (*bronze*), dashed line=body axis, A–E represent rays. *1,* Oral view with spongy organ closely attached to the esophagus. *2,* like *1,* but without esophagus and food grooves, it becomes visible that the most voluminous part of the spongy organ is located in the CD interray. *3,* Aboral view showing the displacement of the axial organ from its aboral beginning exactly in the body axis to the B ray. *4,* Lateral view. Images new, by authors.

Order Comatulida, Suborder Bourgeticrinina. One species from this comatulid suborder (*Caledonicrinus vaubani*) has a voluminous axial organ high in the calyx (Fig. 40.1). In the very slender *Democrinus chuni,* the entire system consists of very few tubules even in its widest part; (Fig. 40.2), in *Democrinus conifer* A. H. Clark,1909b the tubules can be traced far downward into the stalk (Grimmer, Holland, & Messing, 1984).

Order Hyocrinida. Calamocrinus diomedae Agassiz, 1890 has been reported (Holland, Grimmer, & Wiegmann, 1991) to possess both an axial gland of the isocrinid type and a Reichensperger's organ (see p. 40).

Order Cyrtocrinida. In species of the genera *Holopus* and *Cyathidium* (both in the family Holopodidae), the axial gland is completely absent (Grimmer & Holland, 1990; Heinzeller & Fechter, 1995).

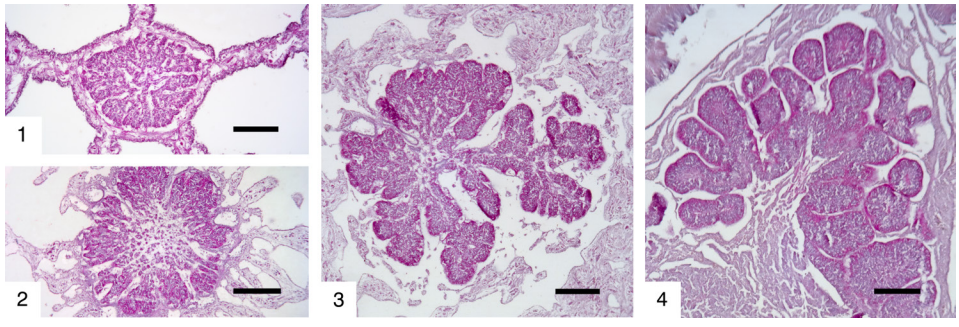

Fig. 37. *Promachocrinus kerguelensis* P. H. Carpenter, 1879, transverse sections, growth and extension of the axial tubular tree: *1,* below the rosette, scale bar 100 µm; *2,* in the deep axial sinus, scale bar 200 µm; *3*, at a slightly higher level than *2,* scale bar 200 µm; *4,* at a high oral level showing the tubules maximally differentiated with a strong PAS reaction of the basal cell compartments, scale bar 200 µm. Staining of 1–4: PAS-Hemalum. Images new, by authors.

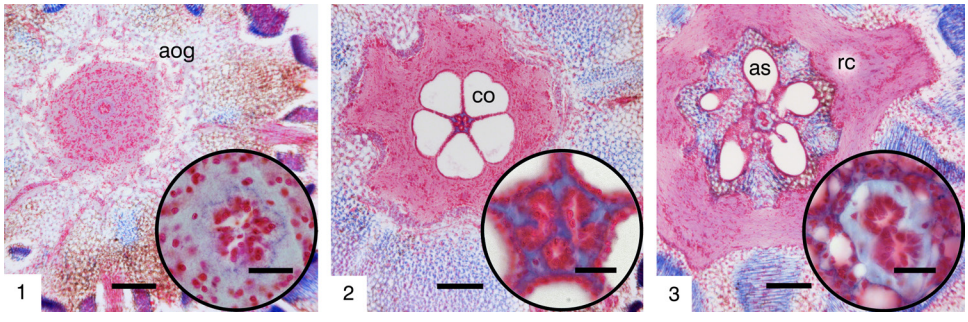

Fig. 38. *Dorometra nana* (Hartlaub, 1890), aboral part of the axial gland, horizontal sections. *1,* Roots of axial tubules in the aboral ganglion (aog), scale bar 100 µm, in inset 20 µm. *2,* Five tubules in the central hemal column (*blue*), co=chambered organ, scale bar 100 µm, in inset 20 µm. *3,* Two tubules passing through the rosette, rc=ring commissure, as=axial sinus, scale bar 100 µm, in inset 20 µm. Staining: Azan. Images new, by authors.

However, in *Neogymnocrinus richeri* (Bourseau, Améziane-Cominardi, & Roux, 1987) (Suborder Cyrtocrinina, Family Sclerocrinidae), the axial sinus contains what can be considered an axial organ based on its position, although the presence of true tubules has not been fully clarified (Fig. 40.3).

RELATIONSHIP AXIAL ORGAN: ATTACHED ORGANS

Although the spongy organ is part of the hemal system (see section III), its oral-aboral differentiation needs to be addressed in more detail in relation to the axial organ, because this relationship is different in feather stars and isocrinids. For this purpose, it is necessary to briefly review the history and definition of the term spongy organ.

Spongy organ, oral part

Perrier (1886) described the assembly of vessels around the esophagus as a labial plexus of a "*spongy* tissue." P. H. Carpenter (1884) removed part of this labial plexus and designated it as the spongy organ. Carpenter's topological description of the spongy organ proves that it is identical to the most voluminous part of the spongy organ in our 3D models in the CD interray. This designation is consistent with that of Holland, Grimmer, & Wiegmann (1991, p. 130), who described it as "a hypertrophied region of the circumesophageal haemal plexus."

Feather stars, aboral part of the spongy organ. As already shown by early authors, the spongy organ belongs to a vascular system that not only spreads around the esophagus

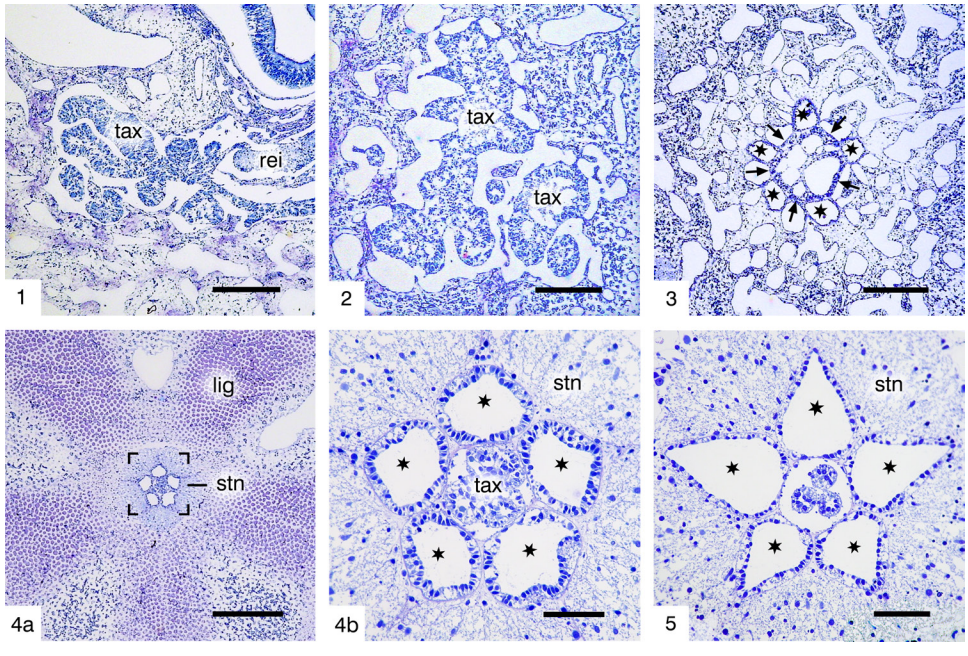

Fig. 39. Axial organ of the isocrinid *Metacrinus levii* (Améziane-Cominardi in Améziane-Cominardi & others, 1990), transverse sections of the body (*1–3*) and the oral most stalk region (*4, 5*). *1,* Lateral part of the organ at its maximum size, tax=tubular axial organ, rei=Reichensperger's organ, scale bar 200 µm. *2,* Section in the plane of the ring commissure, parts of the tubular axial organ (tax) converge to the center, scale bar 200 µm. *3,* Section near the aboral end of the axial sinus, *arrows* point to tubular cells in the periphery of the axial organ enclosed by the chambered organ (*asterisk*), scale bar 200 µm. *4a,* Section aboral of the axial sinus, stn=stalk nerve, lig=ligament, scale bar 200 µm. *4b,* Higher magnification of area marked in black in *4a* with the axial organ (tax) now consisting of only three tubules (*asterisks*), chambered organ reduced to five pipes, stn=stalk nerve, scale bar 20 µm. *5,* Plane of the first cirri, stn=stalk nerve, the elements of the chambered organ (*asterisks*) begin to extend pointedly into the cirri, the tubules of the axial organ have become more slender, scale bar 20 µm. Staining: Toluidine blue. Images new, by authors.

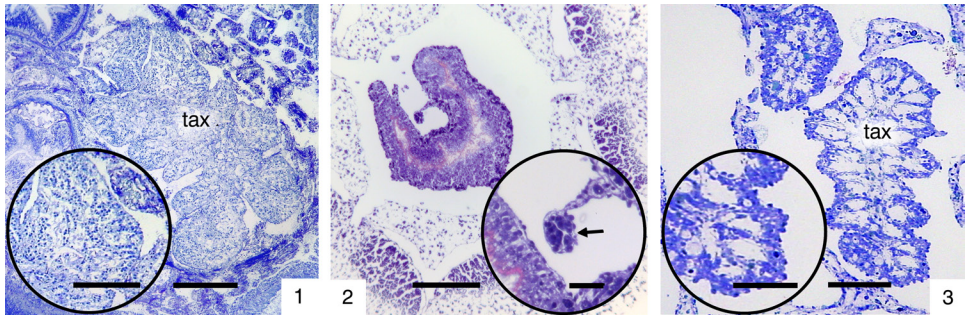

Fig. 40. Axial organ, transverse sections. *1, Caledonicrinus vaubani* Avocat & Roux in Améziane-Cominardi & others, 1990, tax=tubular axial organ, scale bar 100 µm; inset, higher magnification, densely packed tubules, scale bar 50 µm. *2, Democrinus chuni* (Döderlein, 1907) in the center the sickle-shaped rectum with the very small tubular axial organ adhering (*arrow* in magnification), scale bars 50 µm and 10 µm, respectively. *3, Neogymnocrinus richeri* (Bourseau, Améziane-Cominardi, & Roux, 1987), tax=presumed axial organ, scale bar 50 µm, in inset 25 µm. Staining: Toluidine blue. Images new, by authors.

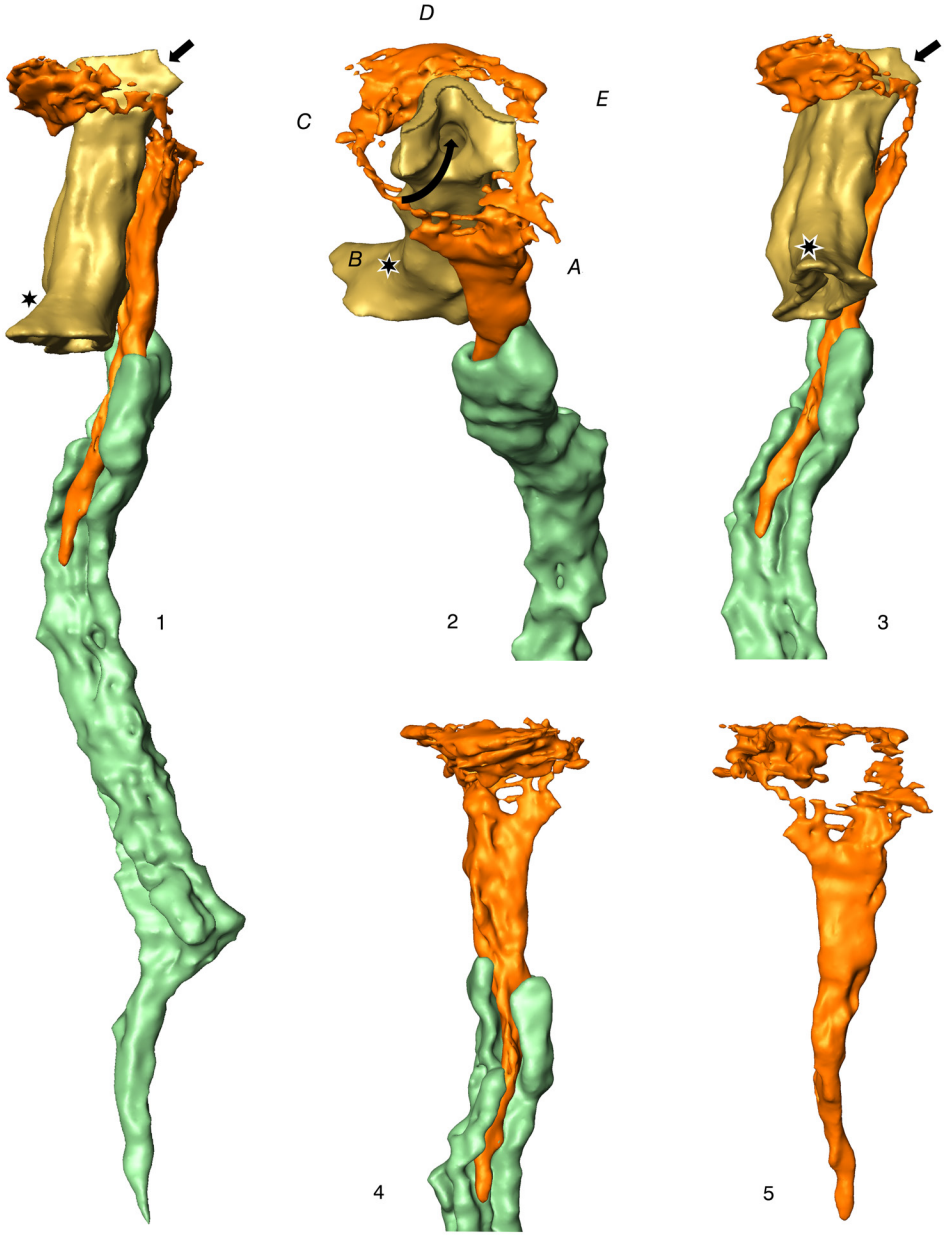

Fig. 41. *Promachocrinus kerguelensis,* large adult specimen, 3D model of tubular complex (*turquois*), spongy organ (*orange*), and esophagus (*bronze*). *1,* C ray view, aborally the tubular complex is anchored in the ventricular organ, ascends orally, turns toward the AB interray and terminates at about the level of the esophageal-midgut boundary (*asterisk*). The thin aboral part of the spongy organ nestles closely to the tubular complex. *2,* Oblique oral view, the oral part of the spongy organ surrounds the esophagus with the main mass in the CD interray. *3,* BC interray view; *4,* D ray view; *5,* AB interray view. *Black arrows* indicate the mouth opening with the direction of the influx of food particles. Image new, by authors.

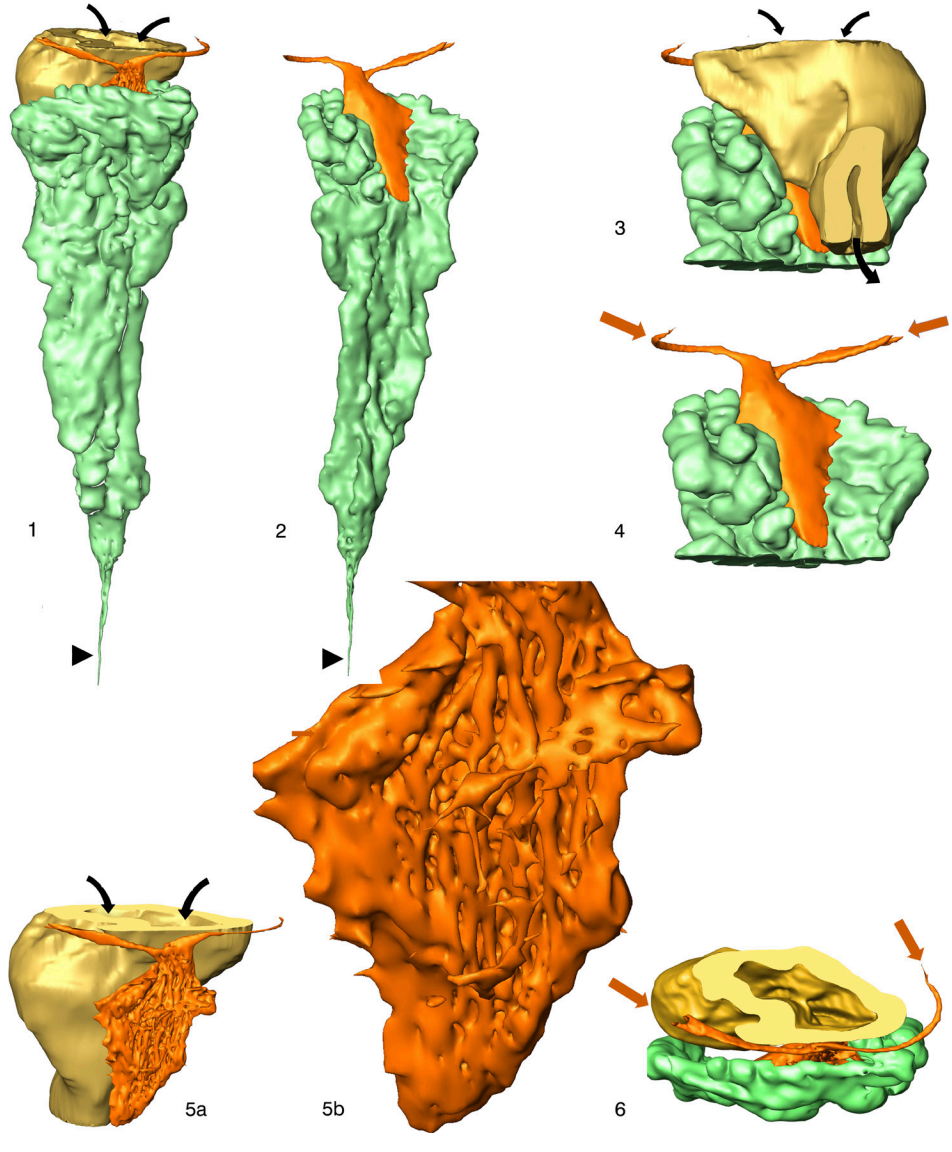

Fig. 42. *Metacrinus* sp., juvenile specimen, 3D model of tubular complex (*turquois*), spongy organ plus Reichensperger's organ (*orange*), esophagus (*bronze*). At this development stage, the oral spongy organ still consists mainly of two large blood vessels (*orange arrows* in *4* and *6*) growing out of the Reichensperger's organ and beginning to surround the esophagus. *1,5a–5b,* A ray views; *2, 3* and *4,* CD interray views; *6,* oral view, model cropped through the esophagus. In *1* and *2, black arrowheads* mark the transition of the delicate tubular complex into the stalk. *2* and *4,* the surface of Reichensperger's organ facing the intestine is quite smooth. Note that in *3* and *6,* Reichensperger's organ is enclosed between the esophagus and the axial organ. *5a* and *5b,* the surface of Reichensperger's organ facing the axial organ is deeply fissured, numerous hemal vessels are attached and appear to be interconnected (also see Fig. 34,*2* and 34,*5*). Images new, by authors.

but also in the aboral direction. Balser and Ruppert (1993) referred to the spongy organ (spongy body in their terminology) as divided into two distinct regions, thereby defining an aboral part that lies lateral to the axial organ. This is true for the different feather stars studied by these authors and can also be observed in the material presented herein (Fig. 41.5–41.6). Like the oral part, the aboral part is also comprised of hemal vessels, which are smaller and denser the more aborally they are located.

Isocrinids, Reichensperger's organ

As for the oral part of the spongy organ, there is little difference between feather stars and isocrinids. However, in isocrinids the aboral part is represented by the Reichensperger's organ. In addition to the mass of hemal vessels, this organ consists of a large cushion of specialized cells (Fig. 34). A corresponding structure does not seem to be present in feather stars. Thus, it seems justified to delineate this cell cushion as a "second kind of axial organ" (Holland, Grimmer, & Wiegmann, 1991, p. 130), rather than a spongy organ (Hyman, 1955).

V. NUTRITION

Crinoids are suspension feeders and collect particles by holding a fan-shaped catching device in the water current (Macurda & Meyer 1974; Meyer 1982). The fan consists of arms and pinnules and arrays of tube feet that border the food grooves. The smallest components of this fan, the tube feet (see below), are covered with a sticky secretion and capture suspended particles according to the aerosol suspension feeding theory (Messing, Ausich, & Meyer, 2021). Simple sieving of particles from the water flow that are larger than the space between the tube feet, thus hardly plays a role. In uniform flow, the fan usually is held in such a way that the aboral arm side faces the flow. During short current reversals, however, when the oral arm side faces the flow, feeding continues, although less effectively (Holland, Leonhard, & Strickler 1987). The food grooves convey food boluses toward the mouth. The total length of the food grooves, estimated from the number and length of the arms and pinnules, is enormous. For example, it measures about 6.5 m in *Antedon bifida* and reaches almost 30 m in *Promachocrinus kerguelensis* and 35 m in *Saracrinus angulatus* P. H. Carpenter, 1884 (see Heinzeller, 1998). With its long food grooves and elaborate detailed organization, the suspension feeding fan of crinoids is highly efficient. All components of the feeding system—the epithelia of the fan, i.e., the tube feet and the food grooves, the mouth field with its tentacles, and finally the upper esophagus are all of ectodermal origin.

Tube feet / tentacles in general

In juvenile free-swimming animals, the food grooves are not yet accompanied by tube-feet arrays, but only by undifferentiated ridges. The only tube feet already developed (following the pentacrinoid stage) are 20 perioral ones, also called mouth tentacles. They are derived from the secondary podia of the embryo and persist throughout the entire lifetime (Fig. 43). The five primary podia of the embryo define the rays and are integrated into the developing arms, where they form the radial canals of the water vascular system. These canals grow and divide in accordance with the arms. At the first point of division, the canals form the first triads of tube feet. Further distally, toward the periphery, the tube feet grow out of the ridges along the food grooves. In adults, the proximal tube feet of the arms are indistinguishable in structure from the neighboring mouth tentacles. Therefore, the number of mouth tentacles often cannot be accurately determined. Determining the number of mouth tentacles is even more difficult when the confluence of food grooves has a somewhat irregular pattern (Fig. 46.1).

The mouth tentacles bend inward, which is probably facilitated by the contraction of strong myoepithelial cells (see Fig. 3.5).

The function of the mouth tentacles is the transport of particles into the esophagus.

Papillae

Both the brachial tube feet and the mouth tentacles are peppered with papillae. These are rod-like cell bundles ~20 µm long and a few µm wide. They have been studied in detail (Holland 1969; McKenzie 1992) and appear to be largely uniform among different taxa. In the center is a slender cell with a characteristic bundle of longitudinal microtubules that can already be resolved at the light microscopic level (Fig. 44.2b). This central cell is surrounded by approximately one dozen of other cells arranged in two circles. All these cells can be characterized as sensory-secretory. However, structures indicative of sensory function, predominate in the cells of the inner circle, whereas signs of secretion predominate in the cells of the outer circle (Fig. 44.3b). Apically, all these cells bear microvilli and a single kinocilium

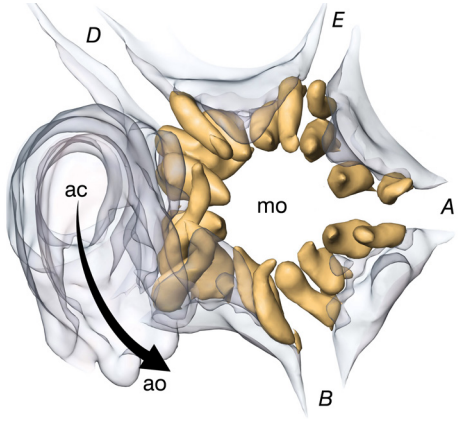

Fig. 43. Juvenile *Leptometra celtica* M'Andrew & Barrett, 1857, 3D model of mouth opening and anal cone. Mouth tentacles are solid and gold colored, other structures are transparent. Oral view of mouth opening (mo), anal cone (ac), and anal opening (ao). The *arrow* follows the axis of the anal cone. Italicized capital letters mark the rays and position of the food grooves, the margins of which are structureless ridges at this stage. Image new, by authors.

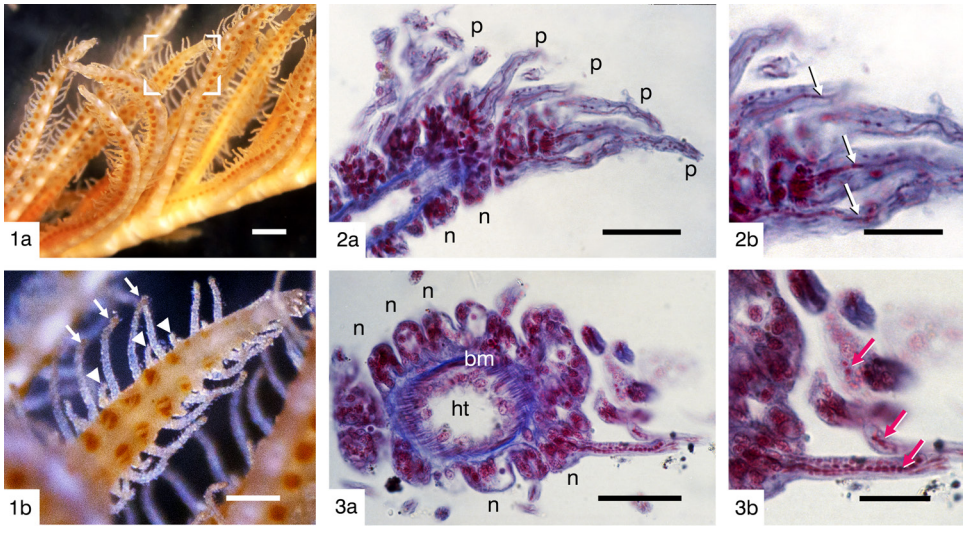

Fig. 44. Tube feet. *1a, Antedon mediterranea* (Lamarck, 1816), arm part with pinnules in back light illumination, scale bar 500 µm; *1b,* higher magnification of area marked in white in *1a*, showing bright large primary tube feet (*arrows*) and short secondary tube feet (*arrowheads*), scale bar 200 µm. *2–3, Cyathidium foresti* Cherbonnier & Guille 1972, primary tube feet; *2a,* longitudinal section of tip, p=papillae, n=nodules, scale bar 20 µm; *2b,* terminal papillae at higher magnification, *arrows* point to the central bundle of microtubules, scale bar 10 µm; *3a,* transverse section near base of tube foot, n=nodules, bm=basement membrane of the hydrocoelomic tube (ht), scale bar 20 µm; *3b,* papillae at higher magnification, *red arrows* indicate secretory granules, scale bar 10 µm. Staining in *2* and *3*: Azan. Images new, by authors.

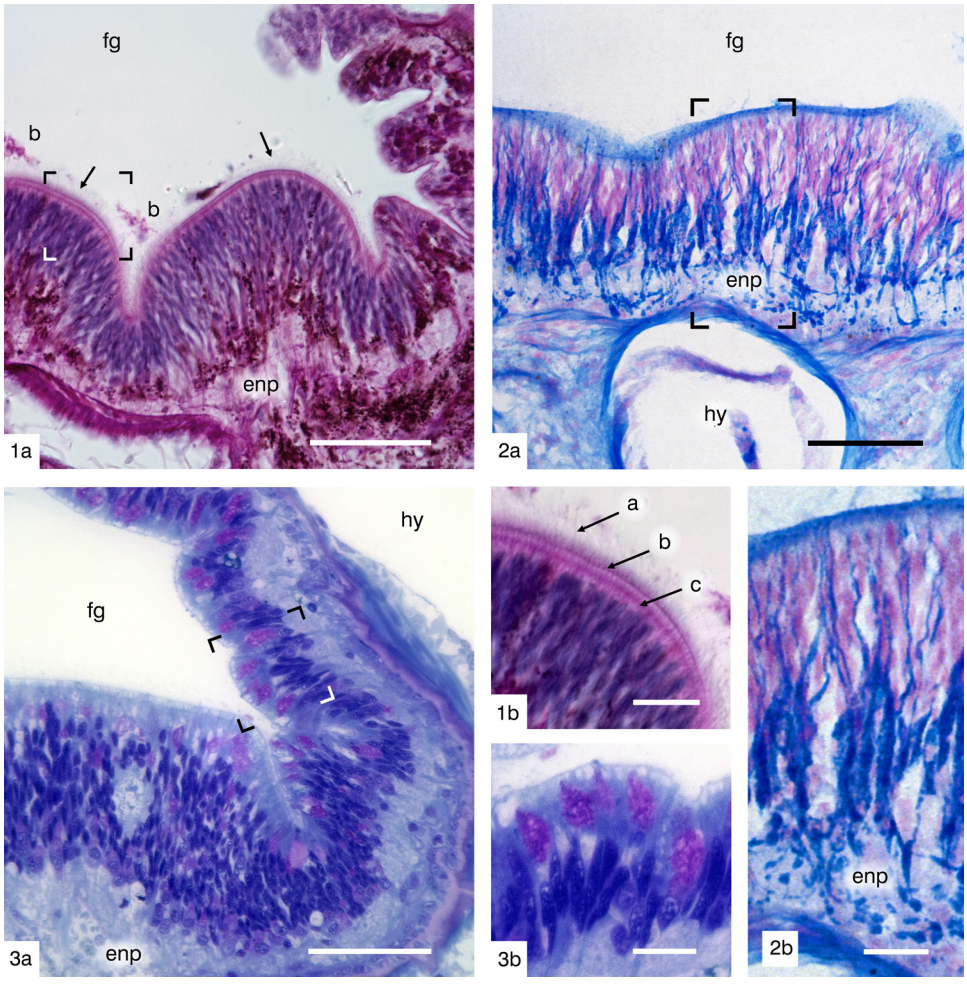

Fig. 45. Epithelium of the food groove. *1a, Comaster schlegelii* P. H. Carpenter, 1881b, fg=food groove, *arrows* point to the fringe of kinocilia, b=food bolus, enp=ectodermal nerve plexus, scale bar 100 µm; *1b,* area marked in *1a,* a=kinocilia, b=cellular junctions, c=basal bodies of kinocilia, scale bar 25 µm. *2a, Comaster schlegelii*, slender blue cells extending from the basal lamina to the apical epithelial margin and presumably secretory, fg=food groove, hy=hydrocoelomic tube, enp=ectodermal nerve plexus, scale bar 100 µm; *2b,* area marked in *2a,* scale bar 25 µm. *3a, Neogymnocrinus richeri* (Bourseau, Améziane-Cominardi, & Roux, 1987), certain segments of the food grooves are encapsulated by the arm skeleton all around; thereby the epithelium is basically of the same type all around, enriched with numerous goblet cells that turn metachromatically pink, scale bar 100 µm; *3b,* area marked in *3a,* scale bar 25 µm. Staining: PAS in *1*, Alcian blue in *2*, Toluidin blue in *3*. Images new, by authors.

each. The nuclei of all papilla cells, except for the central cell, lie basally, causing a nodular thickening at the base of the papilla. Overall, the papillary nodules give the surface of the tube feet a tubercular appearance (Fig. 44.2–44.3). The essential role of papillae in trapping food particles was recognized (Byrne & Fontaine, 1981). However, despite the assumed sensory capacity of the papillae, there is no evidence that the particles are selected according to their nutritional value. Particles sticking to tube feet are wrapped in mucous secretion and delivered to the food groove for transport towards the mouth.

Brachial tube feet

Papillary secretions make the tube feet sticky, allowing them to catch unsorted particles. Tube feet are grouped into triads

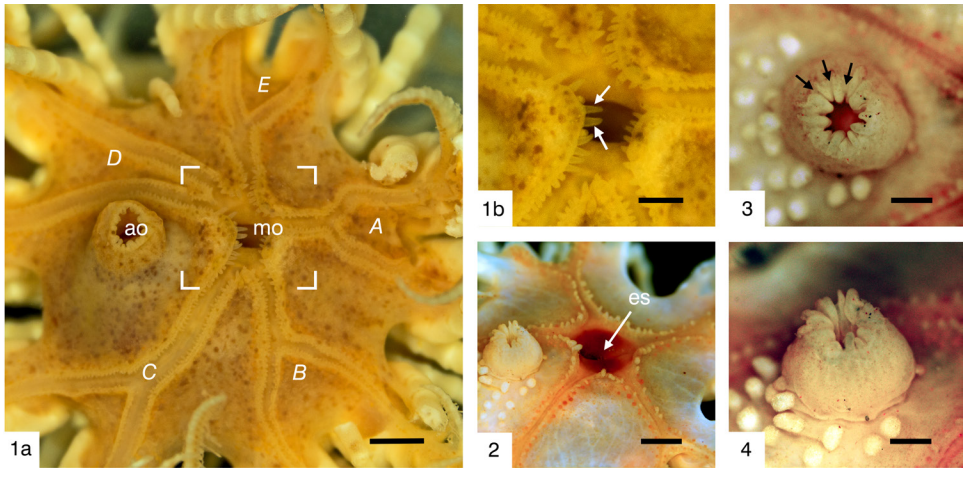

Fig. 46. Mouth field. *Antedon mediterranea* (Lamarck, 1816), two specimens in ethanol. *1a,* Food grooves converging to mouth opening, margins of food grooves and mouth densely armed with tube feet (contraction due to fixation), rays indicated by capital letters. In an unusual way, the food groove of D ray splits already at the edge of the mouth, that of E ray twice, mo=mouth opening, ao=anal opening, scale bar 1 mm. *1b,* Higher magnification of area marked in white in *1a*, *arrows* point to mouth tentacles, scale bar 500 µm. *2,* Mouth with regular estuaries of all food grooves, es=esophagus, scale bar 500 µm; *3–4,* anal cone at higher magnification; *3*, axial aspect, *arrows* point to furrows, scale bar 250 µm; *4,* oblique view, scale bar 250 µm. Images new, by authors.

predetermined by the hydrocoelomic triads. A tube foot triad consists of a large primary, a shorter secondary, and a very short tertiary tube foot (Fig. 44.1b). The primary and the secondary tube foot can be used to collect particles, while the tertiary tube foot mainly scrapes particles from the former two and directs the material into the ciliary tract in the food groove, where it clumps and forms food boluses. Such boluses are kept in the food grooves by the secondary tube feet and by short sections of the food groove rim called lappets. In the rim, the boluses are continuously transported down the food grooves and eventually reach the mouth. Under natural conditions, the mean length of primary brachial tube feet was determined to be 0.75 mm in several comasterid crinoids and 0.65 mm in several non-comasterid feather stars (Meyer, 1979). In fixed material, tube feet are generally shorter because they are contracted. The highly coordinated interaction of tube feet has been studied in detail by Byrne and Fontaine (1983), LaHaye and Jangoux (1985a) and Holland, Strickler, and Leonhard (1986).

Food grooves

The food groove (or ciliary groove or nutritional groove or, compared to other echinoderms, ambulacral groove) is formed by a stripe of specialized epithelium (Fig. 45). It usually rests on a hemal lacuna (see Fig. 29.1), which in turn sits above the radial hydrocoelomic tube. The single-layered epithelium consists of tall, very slender cells, some of which are secretory and others, by far the majority, bear a large kinocilium. By coordinated beating, the dense lawn of kinocilia (Fig. 45.1) transports particles to the mouth. Neurons and fibers of the ectoneural nerve system are interspersed between the slender basal stems of the epithelial cells (Section VII).

Mouth

The confluence of the five main food grooves, which in the periphery assembled all the food grooves of pinnules and arm branches, defines the mouth opening. As mentioned earlier, the rows of brachial tube feet join the ring of commonly taller oral tube feet (mouth tentacles) surrounding the mouth opening (Fig. 46).

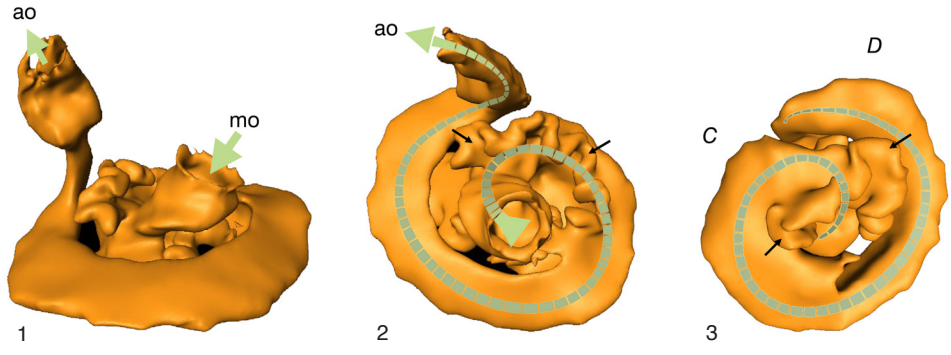

Fig. 47. Single-spiral intestine of an endocyclic crinoid. *Antedon bifida* Pennant 1777, 3D model from serial paraffin sections. *1,* Oblique oral view from BC interray direction; *2,* oral aspect; *3,* aboral aspect, C and D mark rays. The green dashed arrow marks the path of food particles or metabolic end products from the mouth opening (mo) to the anal opening (ao). In *2* and *3* outgrowths and frills of the intestine wall are indicated by *black arrows*. Images new, by authors.

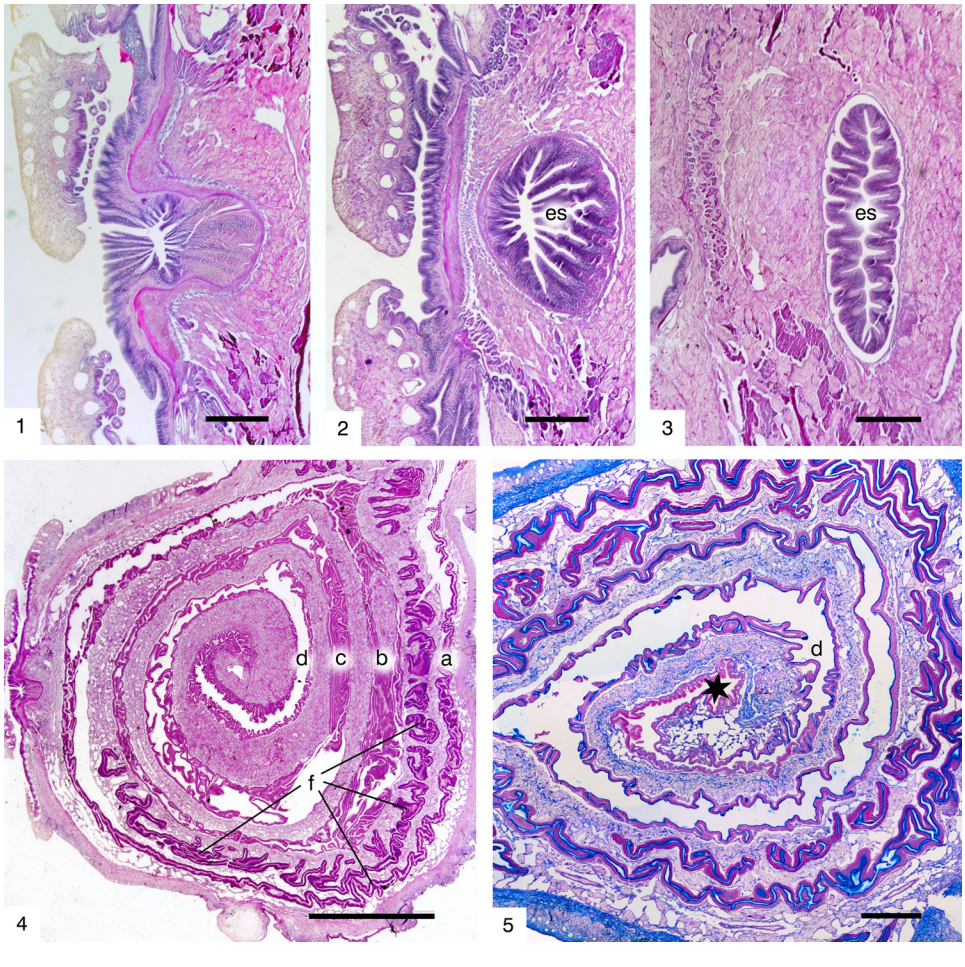

Fig. 48. Exocyclic species (see explanation on next page).

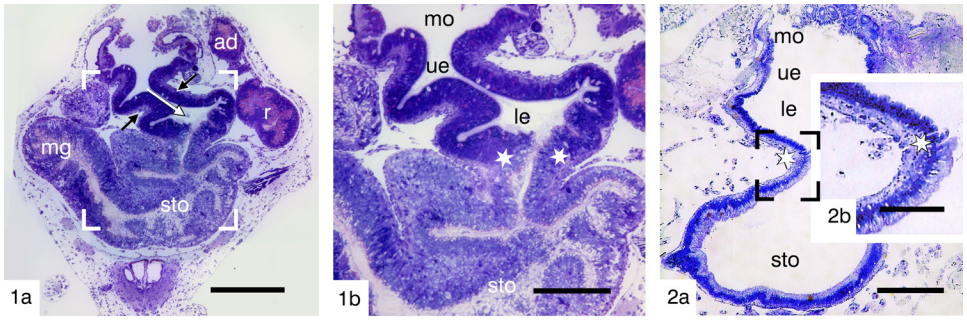

Fig. 49. Epithelial transition between esphagus and stomach. *1, Leptometra celtica* M'Andrew & Barrett, 1857. *1a,* Juvenile animal, sagittal section in plane A to CD; the *white arrow* indicates the obliquely descending esophagus, two lateral folds (*black arrows*) almost close the esophagus, sto=stomach, mg=midgut, r=rectum, ad=anal duct, sto=stomach, scale bar 200 µm. *1b,* Higher magnification of area marked in white in *1a*, *asterisks* indicate the transition of the epithelium from the lower esophagus to the stomach, mo=mouth, ue=upper esophagus, le=lower esophagus, **sto**=stomach, scale bar 100 µm. *2, Cyathidium plantei* Heinzeller & others, 1996, situation similar to *1*, *asterisks* in *2a* and *2b* indicate the the transition of the epithelium from the esophagus to the stomach, mo=mouth, ue=upper esophagus, le=lower esophagus, sto=stomach, scale bars 200 µm in *2a*, 100 µm in *2b*. Staining: Toluidine blue. Images new, by authors.

ENDOCYCLIC AND EXOCYCLIC SPECIES

Regarding the position of the mouth, and in turn the anus, two anatomical arrangement patterns are distinguished in crinoids (P. H. Carpenter 1884): endocyclic with the mouth in the center of the disk and an anal cone in the CD interray and exocyclic with the anus in the center of the disk, while the mouth is peripherally displaced into the AB interray. Stalked crinoids with their elongate bodies belong to the endocyclic type, as do the cyrtocrinids with their stout bodies as well as most feather stars, such as the antedonid family (Fig. 47). Some species of the subfamily Comatulinae, which usually have a broad, somewhat flattened body, are exocyclic (e.g., *Capillaster multiradiatus* or *Comaster schlegelii*) and their intestinal tube is very long with up to four coils (Fig. 48). This type of increase in absorption area by lengthening the tube may be related to the availability and nutritional value of food.

NUTRITIONAL TRACT, SEGMENTS

Esophagus

The funnel-shaped esophagus of crinoids with the endocyclic anatomy descends from the mouth in an aboral direction and opens into the stomach. However, its axis is not perpendicular to the tegminal plane but is slightly declined in an oblique angle (Fig. 49.1), as reported by W. B. Carpenter, 1876, p. 229, "oblique or oesophageal portion." In exocyclics, the esophagus runs nearly horizontal. The axis of endocyclics targets the CD interray and that of exocyclics the D ray. In several specimens, folds are observed to constrict the esophageal lumen (Fig. 49.1). In *Dorometra nana* and *Leptometra celtica,* the esophagus narrows at its aboral end and forms a slit-like connection to the stomach (Fig. 49.1b; Fig. 52).

The esophageal epithelium is the continuation of the food groove epithelium, at least in the endocyclic forms studied. At the transition, both epithelia are very similar (Fig.

Fig. 48. (Fig. on previous page) Exocyclic species *Comaster schlegelii* P. H. Carpenter, 1881b, horizontal sections with the AB interray on the left. *1,* Confluence of food grooves forming a lateral mouth, scale bar 0.5 mm. *2–3,* Further aboral sections showing the narrow esophagus descending within the body wall, es=esophagus, scale bars 0.5 mm each. *4,* Overview of the four clockwise turns (a–d), f=apparently isolated frills of the tube, scale bar 5 mm. *5,* Section further orally than *4*, just below tegmen, the fourth turn (d) merges into the anal duct (*black asterisk*). The epithelium of the anal duct is intensely stained red in this preparation and is clearly different from that of the preceding turn d, scale bar 1 mm. Staining: PAS in *1–4*, Azan in 5. Images new; by authors.

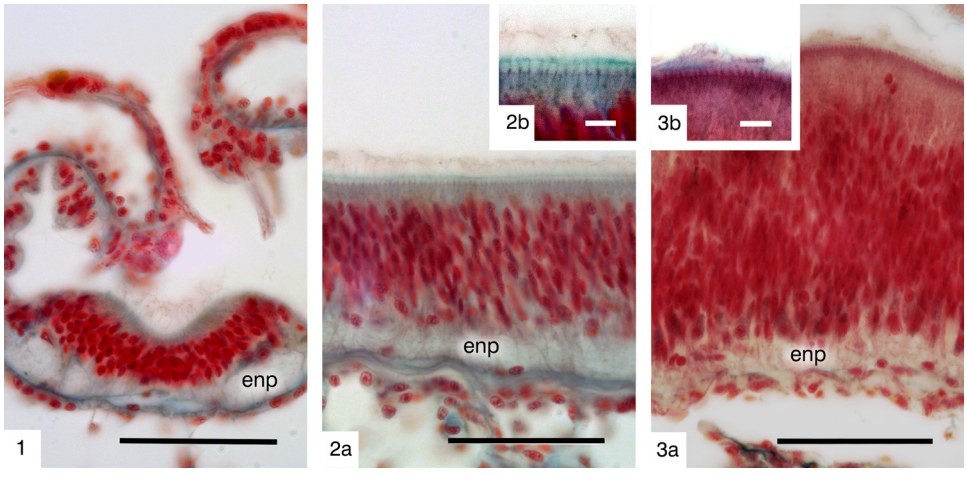

Fig. 50. *Dorometra nana* (Hartlaub, 1890), comparison of epithelia of foot groove (*1*), upper esophagus (*2*) and deep esophagus (*3*), scale bars 50 µm each. The total height of epithelia increases distinctly from *1–3* the esophagus, the layer of nuclei increases in height, and the cell shape becomes even more slender; *2b* and *3b,* margin of the epithelia at higher magnification, *arrows* point to apical cell contacts, its high density is characteristic of very slender cells, enp=ectodermal nerve plexus, scale bars 10 µm each. Azan stain. Images new, by authors.

50.2–50.3), with a rather slender monociliated cell type dominating. However, it should be taken into account that "the esophagus is formed by both the ectoderm and the endoderm" (Engle 2013, p. 83). Roughly speaking, one can distinguish between an upper (ectodermal) and a lower esophagus (entodermal, also called ventriculus) because the boundary is marked by a weak change of the epithelium (Fig. 49.1b). Nevertheless, there is a gradual change in the epithelium from the upper to the lower esophagus, in the form of increasing epithelial height (Fig. 50.2a, 50.3a) and increasing abundance of secretory cells. In the lower esophagus, the epithelium can reach a height of 200 µm, and the thickness of the layer containing the cell nuclei is several times greater than in the upper esophagus. The cell bodies are extremely thin, most clearly seen in the very densely packed cell junctions at the apical edge of the epithelium (Fig. 50.2b, and 50.3b).

As in the food groove, the slender mucous cells are intermingled with the ciliated cells. But the majority of cells can be classified as resorptive, because endocytosis in *Oligometra serripinna* P. H. Carpenter 1881b was experimentally demonstrated by LaHaye and Holland (1984) for each portion of the digestive tract, including the esophagus. This is in agreement with electron microscopic observations (Heinzeller & Welsch 1994).

Ectodermal to entodermal changeover

In addition to the ectodermal unit (food grooves and upper esophagus), most of the nutritional tract is of entodermal origin. This entodermal unit is derived from the larval enteric sac and, besides the lower esophagus, also forms the stomach, midgut, rectum, and, in part, the anal duct. An ectodermal contribution to the anal duct cannot be ruled out. These segments are distinguished by their epithelia, where two types of so-called enterocytes predominate.

Enterocytes

Apart from nerve cells, amebocytes, and rare goblet cells, the epithelium of the stomach, midgut, and rectum consists mainly of two cell types: vesicular enterocytes and granular enterocytes (LaHaye & Holland, 1984), both of which are very slender cells. Both cell types were originally described in

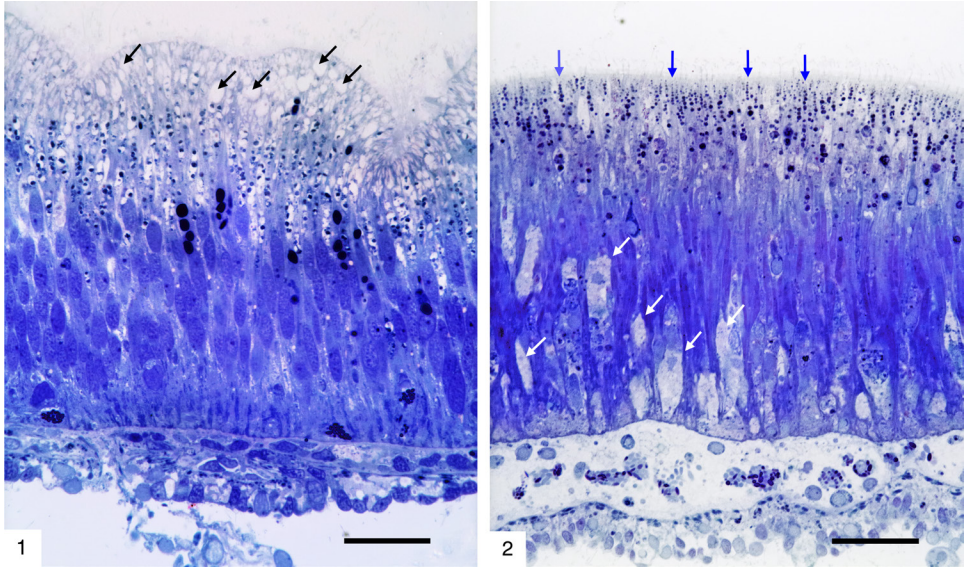

Fig. 51. Enterocytes. *1, Neogymnocrinus richeri* (Bourseau, Améziane-Cominardi, & Roux, 1987), section through the midgut epithelium; the supranuclear part of the epithelium dominated by mucous vacuoles (arrows), typical for vesicular enterocytes, scale bar 50 µm. *2, Himerometra robustipinna* P. H. Carpenter, 1881a, section through the midgut epithelium; granular enterocytes recognizable by the dark granules in the supranuclear part, commonly arranged in vertical rows (*blue vertical arrows*). Large cells with bright cytoplasm (mucus) are interspersed in the infranuclear layer (*white arrows*), scale bar 50 µm. Staining: Toluidin blue. Images new, by authors.

holothuroids (vesicular enterocytes: Feral & Massin 1982; granular enterocytes: Farmanfarian 1969). Vesicular enterocytes (Fig. 51.1) combine, as far as can be concluded from the morphology, their ability to absorb nutritional material and mucus secretion. Apically, each vesicular enterocyte bears a single kinocilium. Below the kinocilia fringe, the apical cell parts contain densely packed mucus droplets leading to the appearance of a mucus layer by superimposition in thick sections (Fig. 53.1–53.3). Granular enterocytes (Fig. 51.2) lack kinocilia. Their apex is smooth, and the abundance of large product-filled organelles suggests secretory activity, potentially consist of the release of digestive enzymes.However, the staining of the vesicular and granular enterocytes indicates that each of these cells do not represent a uniform group, because, for example, they stain differently in the stomach than in the rectum. This could also apply to the granular enterocytes. It seems likely that more detailed studies will provide substantial differences among these cells.

Esophagus to the stomach

In the entire digestive tract, there is a clear demarcation by constriction only between the esophagus and the stomach. In addition, this border is characterized by a distinct change in the epithelium (Fig. 49.1–49.2). The epithelium of the stomach is dominated by vesicular enterocytes, resulting in an apparent mucus layer at the apical margin (Fig. 53.1). In the 3D model of *Dorometra nana* (Fig. 52), the hole connecting the esophagus to the stomach, has a slit-like shape.

Stomach to the midgut

Instead of an abrupt epithelial change between stomach and midgut, a smooth change in epithelial composition is present. Nevertheless, the different epithelial types allow the reliable identification of these different regions. The differences mainly concern the height of the epithelium and

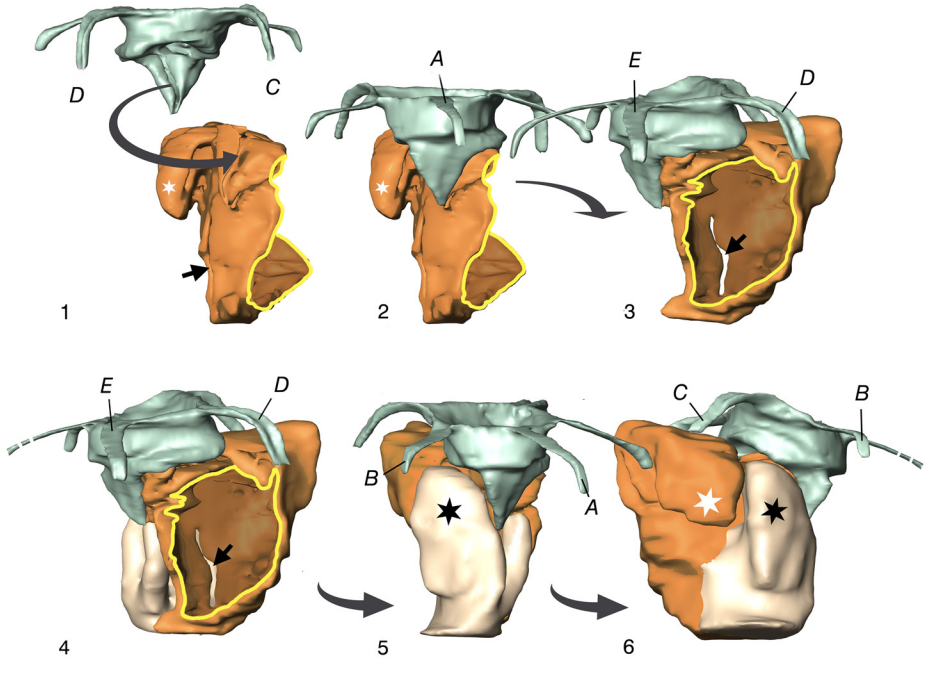

Fig. 52. *Dorometra nana* (Hartlaub, 1890), 3D model of esophagus (*green-grey*) and stomach (*reddisch brown*), letters indicate rays. *1,* Both parts are separated to allow a view on their slit-like openings through which they communicate. Top: esophagus, aspect from CD interray; below: stomach, aspect from A ray. The *curved arrow* symbolizes a 180° rotation of the esophagus to achieve congruence of the two slits. *2–3,* Both parts united in natural position, the *white asterisk* marks a blind protuberance of the stomach projecting aborally from its oral edge. The quarter-turn arrow brings the DE interray forward and shows the wide connection to the midgut (framed by *yellow line*). The *short black arrow* points to the connection with a second blind outgrowth extending from below, which is added in *4*. From there, quarter-turns counter-clockwise lead to *5* and *6*, first outgrowth with *black asterisk*, second outgrowth with *white asterisk*. Images new, by authors.

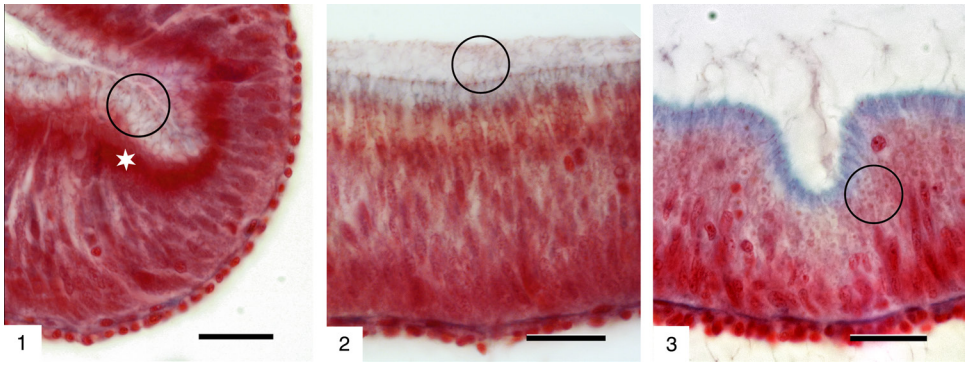

Fig. 53. *Dorometra nana* (Hartlaub, 1890), comparison of epithelia of stomach (*1*), midgut (*2*) and rectum (*3*), In *1,* the circle marks the apical part of the cells, which is filled with mucous secretory granules. Note also the intense staining zone immediately below (*asterisk*), which is characteristic of the epithelium of the stomach. In *2*, a dense fringe of kinocilia (*circle*) is seen. In *3*, the epithelial height gradually decreases and a conspicuous number of granules (*circle*) fill the supranuclear space. The apical mucus-rich zone responds intensely blue to staining (Azan), scale bars 25 µm each. Images new,. by authors.

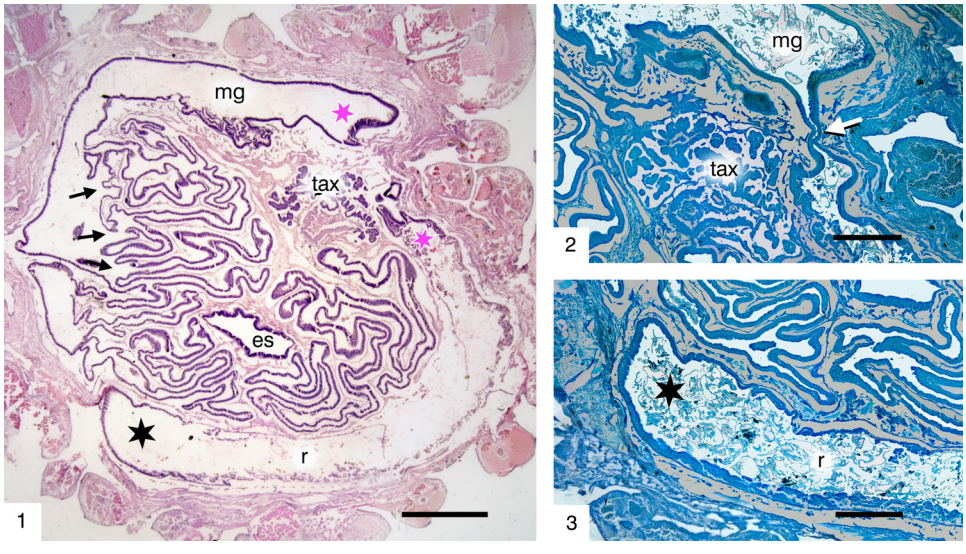

Fig. 54. *Metacrinus levii* (Améziane-Cominardi in Améziane-Cominardi & others, 1990), horizontal sections through the calyx. *1,* Wide, circumferential, intestinal loop (the connection between the *violet asterisks* is out of plane). The left and upper parts clearly represent the midgut, which forms numerous protrusions of its inner wall (*arrows*). The lower part of the loop belongs to the rectum; the *black asterisk* in *1* (and the one in *3*) marks the rising point of the anal duct, es=esophagus, mg=midgut, r=rectum, tax=tubular axial organ, scale bar 500 µm. *2–3,* Details from a section slightly further aboral than *1*; *2,* the *white arrow* points to the connection between the upper and the lower part of the loop, (which is not in the plane in *1*), mg=midgut, tax=tubular axial organ, scale bar 250 µm. *3,* End of the rectum, densely filled with carapaces of eaten crustaceans, r=rectum, scale bar 250 µm. Staining: PAS in *1*, Alcian blue in *2* and *3*. Images new, by authors.

the respective proportions of the cell types. For comparison, the epithelia of these two segments (and of the rectum) are shown (Fig. 53), as observed in *Dorometra nana*.

Stomach. The stomach is a voluminous pouch with a folded wall and, in the case of *Dorometra*, two large outgrowths, one rising from the aboral floor and the other extending downward from the oral wall (Fig. 52). As already shown (Fig. 49), the stomach is separated from the lower esophagus by a constriction. Its other end gradually transmutes into the midgut and can be determined solely by the changing epithelium. In the stomach, the epithelium is about as high as that of the lower esophagus, but it is dominated by vesicular enterocytes with a conspicuous apical band of mucus (Fig. 53.1). Immediately below the mucous band is an optically dense zone of intensely stained cell organelles that presumably represent heterolysosomes.

Midgut. In endocyclic forms, the midgut passes through a four-fifths turn between the D ray and C ray (Fig. 47) or, together with the rectum, almost forms a complete circle (Fig. 54). It gradually emerges from the stomach, then it passes into the rectum. The, presumably resorptive, area of the midgut can be enlarged in two ways: first, by lengthening the midgut with additional coils (exocyclic species, Fig. 48), or second, by folding the wall, creating blind outgrowths, frills, or folds (Fig. 54). In *Dorometra nana* a partitioned blind outbulge extends halfway down from the oral wall (Fig. 56.2, 56.6).

The epithelium of the midgut is largely uniform but decreases in height toward the rectum. The vesicular enterocytes still dominate and bear a fringe of kinocilia, but the mucous band is less pronounced than in the stomach (Fig. 53.2). The proportion of mucus-secreting cells increases at the junction with the rectum. The midgut

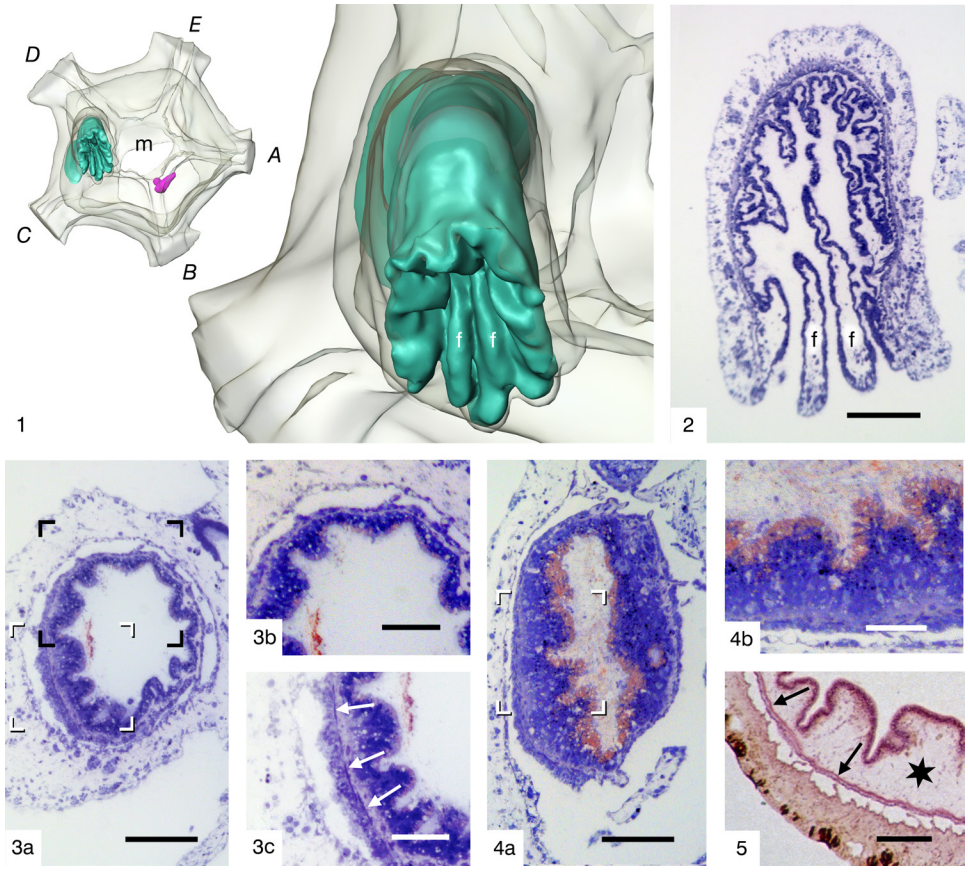

Fig. 55. Anal cone and duct. *1–4, Leptometra celtica* M'Andrew & Barrett, 1857, juvenile specimen. *1,* 3D model with *turquoise* stained anal duct, oral aspect, f=longitudinal folds of anal duct. *2,* Horizontal section, f=folds of anal duct, scale bar 50 µm. *3a,* Cross section at the base of the cone at the tegmen, scale bar 50 µm. *3b,* Area marked within *black brackets* in *3a*, epithelium clearly distinguishable from that in more aboral sections (*4a, 4b*), scale bar 25 µm. *3c,* Area marked in *white brackets* in *3a*, arrows point to sheet of myoepithelial cells, scale bar 25 µm. *4a,* Cross section through the recto-anal junction showing the luminal, mucus-rich zone of the epithelium reacting metachromatically red as a feature of the rectal epithelium, scale bar 50 µm. This feature disappears in the cone (*3b*). *4b,* Area marked in *white brackets* in *4a*, scale bar 25 µm. *5, Comatella nigra* P. H. Carpenter 1888, cross section through the anal cone, arrows point to sheet of myoepithelial cells, scale bar 50 µm. Staining: Toluidine blue in *1–4*, Hemalum-Eosin in *5*. Images new, by authors.

probably contributes the lion's share to food absorption.

Midgut to rectum to anal duct

There is no sharp boundary between midgut, rectum, and anal duct. However, epithelia, like those of the other components before, exhibit specific properties.

Rectum. The final part of the midgut narrows before it merges with the rectum. The midgut and rectum form a common loop in the horizontal plane. In the CD interray, the rectum bends at right angles from this plane (Fig. 54) and ascends orally to about the level of the tegmen. In *Antedon bifida*, the ascending part resembles a long bottleneck (Fig. 47); in *Dorometra nana* it is a flattened tube squeezed by the adjacent stomach (Fig. 56.3; also see Fig. 14.1–14.2). In the tegminal plane, the tract widens and forms the anal duct (Fig. 55.3).The rectal epithelium consists only of vesicular entero-

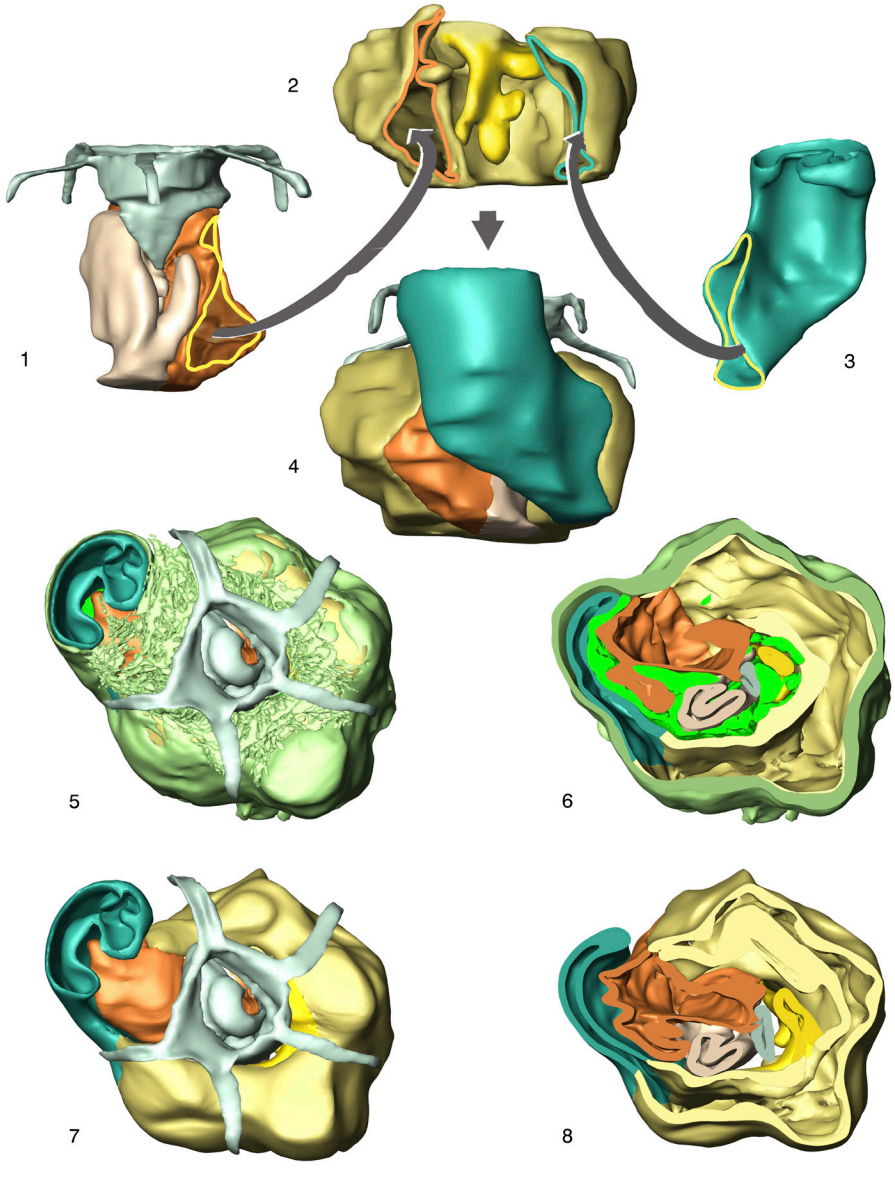

Fig. 56. *Dorometra nana* (Hartlaub, 1890), 3D model of the complete nutritional complex (see also Fig. 52.1–52.3); *1–4* shows the integration of the midgut (*light gold*) between the stomach (*copper*) and rectum (*turquoise*, without anal cone). Sites of contact are mutually colored like the associated organs. In *2,* a palmate outgrowth (*yellow*) of the midgut extends aborally from the oral edge of the intestine. *4,* The entire complex, view from the CD interray. *5,* Oral aspect of the complete model. *6,* Oral aspect with oral half cropped; near the center, the stomach (*copper*) and the deepest end of the esophagus (*gray*) can be seen, as well as the blind sacs of the stomach (*dark pink*) and midgut (*yellow*). *7,* Same aspect as *5* with periintestinal girdle and subtegminal net added (both *light olive green*). *8,* Similar crop as in *6* (slightly more aboral), the periintestinal girdle surrounds midgut and rectum; in addition, the mesenteric components of the somatocoel are shown in *light green* (compare with Fig. 12 and 13). Images new, by authors.

cytes (*Oligometra serripinna;* see LaHaye & Holland, 1984). This was also observed in *Dorometra nana* (Fig. 53.3), where additionally crowded granules in the supranuclear cytoplasm are a conspicuous epithelial feature. These granules might represent heterolysosomes; they suggest exocytosis in addition to resorption.

In addition, some mucus-forming cells are interspersed basally, in particular, at the site where the rectum merges with the anal duct. At this location intense mucus secretion is evidenced by the metachromatic histochemical reaction in some species (Fig. 55.4).

Anal cone and duct. Already in the pentacrinoid larva, an anal cone extends above the tegmen. It raises the anal opening above the level of the mouth throughout the life cycle. Typically, the anal cone has several outer longitudinal furrows toward the tip, with corresponding furrows on the inside (Fig. 55.1–55.2). Toward the tip, the furrows break through to form a short tuft of separate processes of the anal cone wall (Fig. 46.4).

The epithelium of the anal duct inside the cone is the extension of the rectal epithelium. Deep in the calyx, where the tube rises vertically from the horizontal rectum, its epithelium initially corresponds to that of the rectum (Fig. 53.3). In *Leptometra celtica*, the anal duct has particularly high mucus secretion at this site (Fig. 55.4). In the oral direction, the epithelial height steadily decreases and the vesicular enterocytes become increasingly rare; finally, the epitelium merges into the epidermal layer.

The end of the rectal epithelium may mark the end of the entodermal parts of the digestive system or, conversely, the beginning of the ectodermal part of the anal duct. The hemal lacuna, which lies immediately underneath the epithelium in the stomach, midgut, and rectum (Fig. 35.1), is replaced in the anal cone by a special connective tissue layer where sclerotization may occur. Externally this layer is covered by a muscular sheet (Fig. 55.3, 55.5), which is capable of constricting and probably completely closing the anal duct.

CONCLUSION

Based on epithelial features, a number of intestinal segments can be distinguished in *Dorometra nana*. Figure 56 shows the arrangement of these segments. This 3D model might be taken as a generalization for crinoids, at least for endocyclic species. When attempting this, it should be considered:

- There are differences among taxa.
- For many organs, the shape depends on the physiological state, which is especially true for the digestive system, where the filling state strongly modifies lumina and folds.
- Conventional morphological data alone cannot clarify whether certain outgrowths must be regarded simply as enlargements of the intestinal surface or as glandular components.

VI. REPRODUCTION

Unlike other echinoderms, asexual reproduction does not occur in crinoids. Crinoid species are generally bisexual, with only a few species exhibiting hermaphroditism (Dan & Dan 1941; Mladenow 1986; Vail 1987). Externally, the sexes cannot be discerned, except for females of some brooding species (Mortensen 1920; Haig & Rouse 2008).

Both sexes have an identical leading structure that forms either ovaries or testes. This structure is a narrow epithelial tube within a hemal vessel, which in turn lies in a compartment of the brachial somatocoel (Fig. 57). During the breeding season, the gonocoel completely encases the full-grown ovaries or testes (Fig. 60, Fig. 61). Because of its narrow, almost invisible lumen, the tube was originally called genital strand or rachis (herein, called genital tube). The corresponding component in the brachial somatocoel is the gonocoel between the oral and the aboral somatocoelomic canals (see Section II). Certain parts of the genital tube in arms or pinnules transform into gonads. Primordial germ cells are thought to originate either subtegminally in the CD interray (Fig. 58.1). or locally by a *de novo* generation. At certain times of the year, gametogenesis takes place in the gonads.

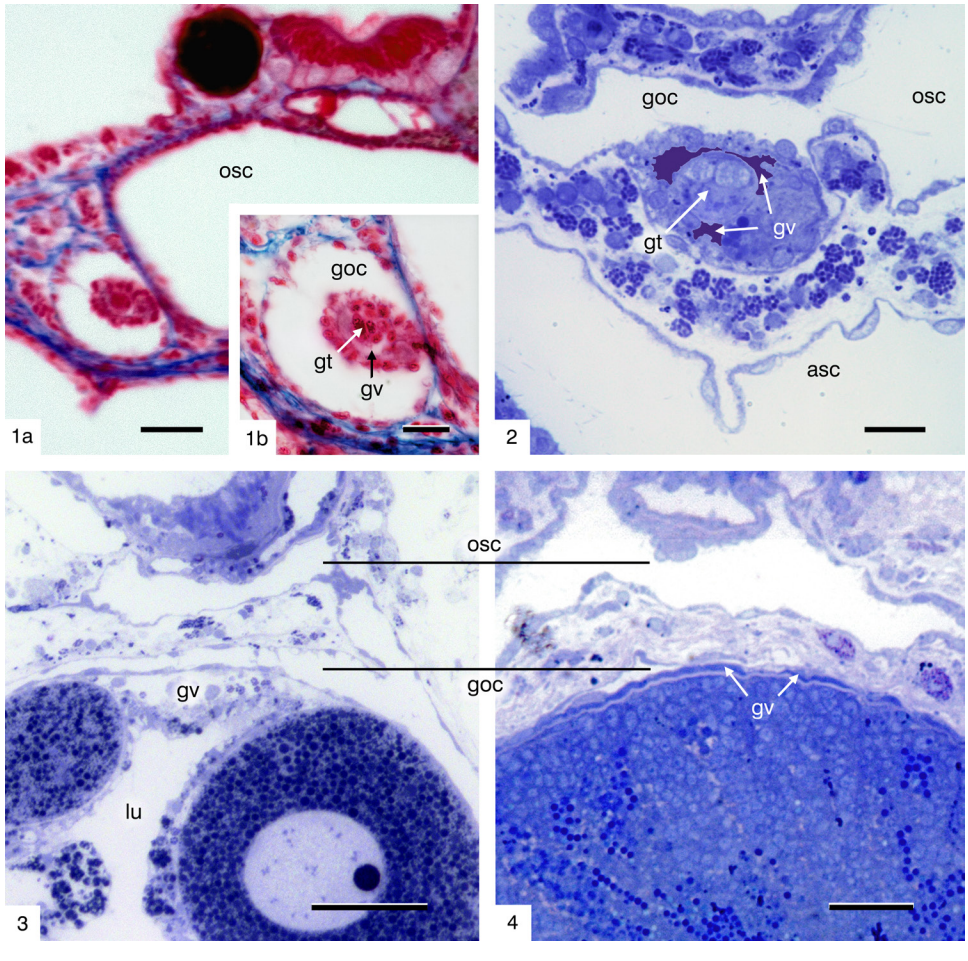

Fig. 57. Gonocoel, genital tube, and genital vessel. *1a* and inset *1b, Dorometra nana* (Hartlaub, 1890), female, transverse section of an arm near the calyx, osc=oral somatocoelomic canal, goc=gonocoel, gv=genital vessel, gt=non-gametogenic genital tube, scale bar 20 µm in *1a*, and 10 µm in *1b*. *2. Antedon mediterranea* (Lamarck, 1816), pinnules in cross section, asc=aboral somatocoelomic canal, other abbreviations as in *1*, scale bar 10 µm. *3, Endoxocrinus parrae* (Gervais in Guérin, 1835), gametogenic tube differentiated to an ovary, lu=lumen of the ovary, other abbreviations as in *1*, scale bar 50 µm. *4, Antedon mediterranea*, gametogenic tube differentiated to a testis, abbreviations as in *1*, scale bar 20 µm. Note that the hemal lumen of the genital vessel (gv) in 3 is wide and houses oocytes, whereas in 4 it is compressed. Staining: Azan in *1*, Toluidine blue in *2–4*.
Images new; by authors.

In most cases gametes enter the open water by rupturing of the pinnular wall; such simultaneous spawning results in external fertilization and development.

GONADAL STRUCTURES AND STEM CELLS

Genital tube and gonocoel

In adult animals, the portions of the genital tube that are not prospective or active gonads are called non-gametogenic and consist mostly of inconspicuous, slender, ciliated cells, which are presumably sterile. Mixed with these cells in gametogenic portions of the tube, depending on the season, primordial germ cells and different developmental stages up to mature gametes occur. Even in silent gonads, the tubular epithelium contains germ cells with an ovoid shape and a spherical nucleus. These may represent

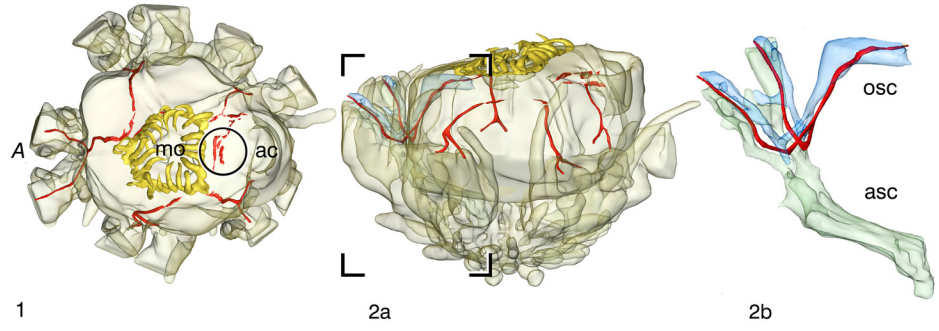

Fig. 58. Genital vessels. *Dorometra nana* (Hartlaub, 1890), 3D model showing the course of the genital vessels (*red*) in calyx and proximal arm portions. *1,* Oral aspect, circle marks (hypothetical) location of primary gonad in larvae between mouth (mo) and anal cone (ac). *2a,* Lateral view with A ray on left side and CD interray on right side. In *1* and *2*, calyx and arm portions are *transparent*, the crown of mouth tentacles is *golden*; *2b,* part of the model as marked by brackets in *2a*, genital vessel in *red*, osc=oral somatocoelomic canal, asc=boral somatocoelomic canal. Images new, by authors.

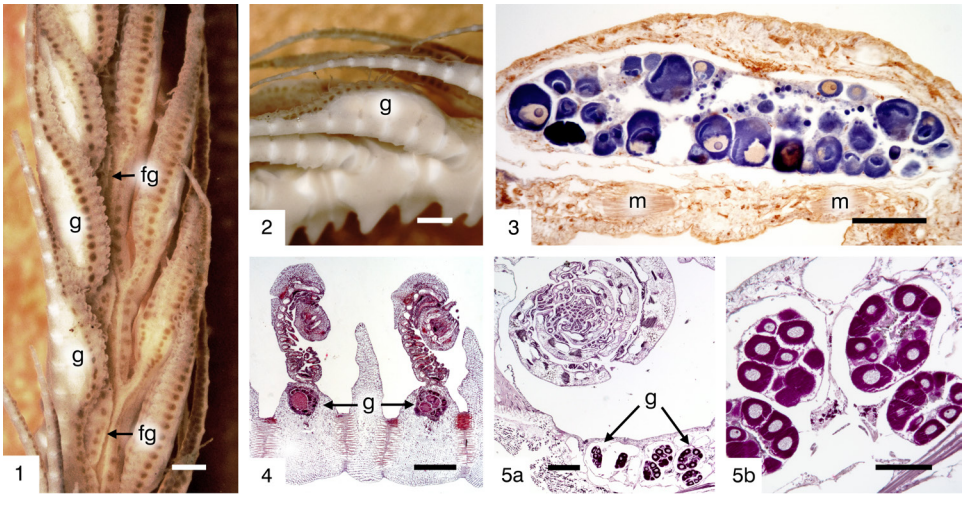

Fig. 59. Location of gonads. *1–2, Anthometrina adriani* Bell, 1908 in ethanol, gametogenic pinnules, oral (*1*) and lateral (*2*) aspects, g=gonad, fg=food groove, both scale bars 1 mm. *3*, *Antedon bifida* Pennant 1777, longitudinal section of a pinnule with an ovary extending over at least three pinnular segments as indicated by the interossicular muscles (m), scale bar 100 µm. *4, Neogymnocrinus richeri* (Bourseau, Améziane-Cominardi, & Roux, 1987), longitudinal section of an arm piece with globular gonads (g) in the pinnular bases, scale bar 0.5 cm. *5a, Cyathidium foresti* Cherbonnier & Guille 1972, longitudinal section of curled arm, g=small globular or ovoid ovaries in the arm at pinnular bases, scale bar 0.5 mm; *5b,* ovaries of *5a* at higher magnification, scale bar 200 µm. Staining: Hemalum in *3*, Azan in *4*, and PAS in *5*. Images new, by authors.

primordial germ cells. In mature gonads, the mass of sex products causes the organs to swell and push aside the somatocoelomic canals, including the gonocoel, which can be compressed to a narrow slit (Fig. 57.3–57.4).

Primordial germ cells

In larval stages the presence of a special cluster of large cells with prominent nuclei was already observed in quite early studies (Seeliger 1893, Russo 1902) and confirmed by several authors in the twentieth century (e.g. Mortensen, 1920). These cells occur in cystidean or pentacrinoid stages in the CD interray, near the primary stone canal and the early axocoel (see Fig. 6). The cell cluster has been interpreted as part of a

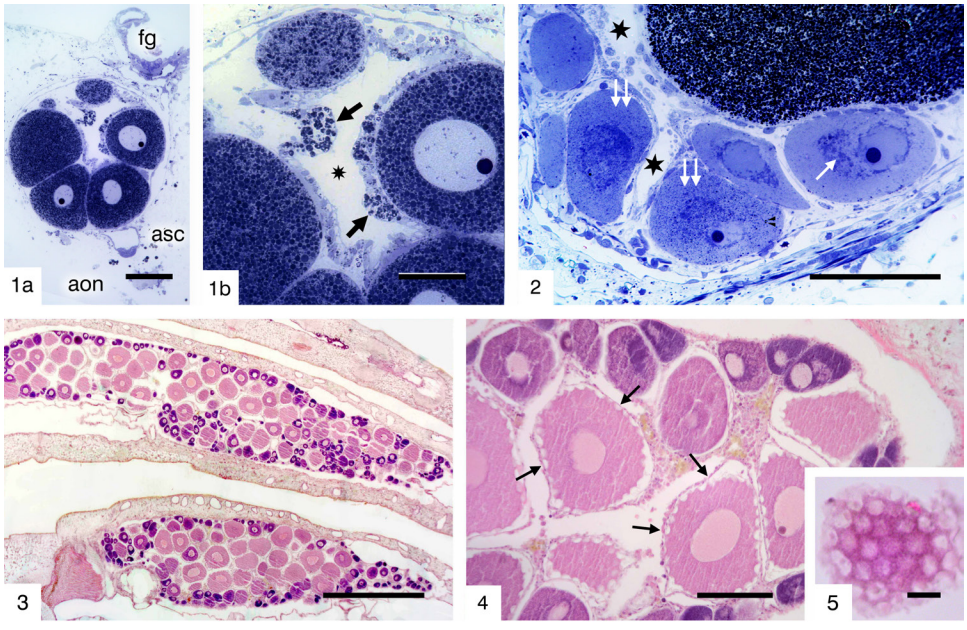

Fig. 60. Ovary. *1a, Endoxocrinus parrae* (Gervais in Guérin, 1835), pinnule with ovary in transverse section (see Fig. 57.3), fg=food groove, asc=aboral somatocoelomic canal, aon=aboral arm nerve, scale bar 100 µm; *1b,* detail of *1a* showing the genital tube with a wide lumen (*asterisk*), free of oocytes; in contrast, large egg cells (large primary oocytes with nuclei in the first meiotic division and densely packed yolk droplets in the cytoplasm) are apparently located "outside" the tubular epithelium in the hemal space. *Arrows* point to presumably phagocytotic epithelial cells, scale bar 50 µm. *2, Neogymnocrinus richeri* (Bourseau, Améziane-Cominardi, & Roux, 1987), ovary with primary oocytes (nuclei with prominent nucleoli); accumulated yolk droplets appear as basophilic granules near the nucleus (*arrows*), and they distribute evenly in the cytoplasm during the transition to the ovulating or mature cell (*double arrows*), scale bar 100 µm. *3–5, Tropiometra afra* (Hartlaub, 1890); *3,* ovaries with a many large mature ova in the center (*), and oocytes of various sizes and developmental stages in the periphery, scale bar 400 µm; *4,* at higher magnification, the spiny surface (*arrows*) of mature ova can be seen, scale bar 100 µm; *5,* tangential section, the apparent "spines" result from hexagonally arranged ridges, scale bar 10 µm. This surface pattern is typical for many but not all species. Staining: Toluidin blue in *1–2,* Hemalum-Eosin in *3–5*. Images new; by authors.

primary gonadal anlage that soon disappears and cannot be detected in adults (confirmed by Engle 2013). However, most authors agree that this cluster is a source of primordial germ cells. Nevertheless, it remains unclear whether they migrate (ameboid as Hamann speculated in 1889) to the gonads. In this case, they may be guided by the genital tube or, more precisely, the hemal vessel with the genital tube inside. This hemal vessel can be clearly traced from the pinnules and proximal arm portions (site of gonads) to the subtegminal hemal complex (Fig. 58). The other possibility is that primordial germ cells develop locally from undifferentiated rachis cells, a theory that cannot be excluded with certainty even today. In any case, cells like those of the embryonic cluster occur as oogonia in the ovaries or as spermatogonia in the testes.

GONADS

Location and shape of the gonads

As far as known, all crinoids have their gonads in the proximal portions of arms and pinnules (Holland 1991), whereas the non-gametogenic tube also extends peripherally to the tips of arms and pinnules. However, there are group-specific differences. The vast majority of feather stars develop elongated gonads in pinnules near the body, except for the very first one. Such gonads cause the pinnules to swell on the oral side (Fig. 57.1–57.2). This is the same in isocrinids

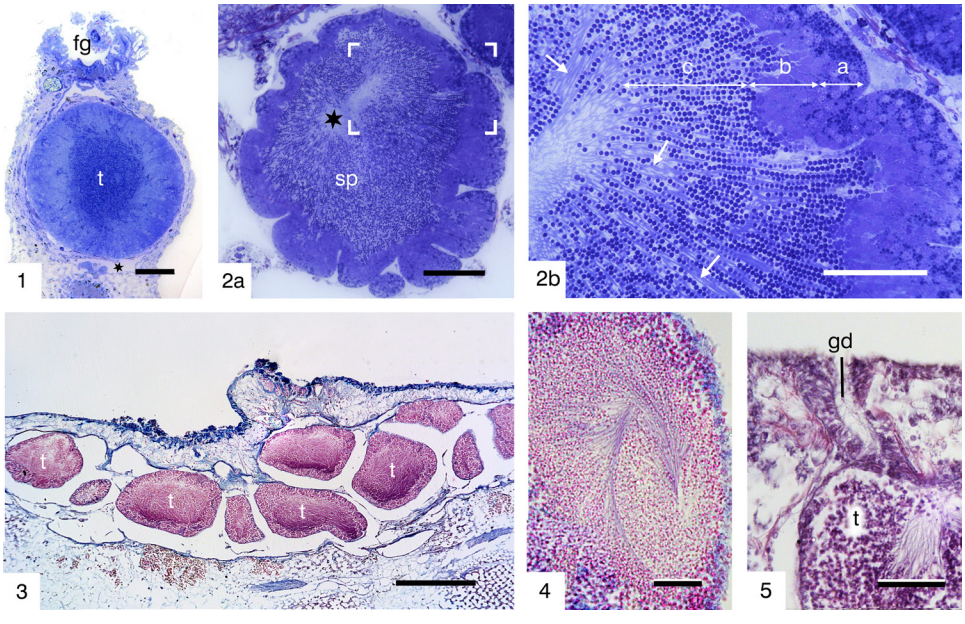

Fig. 61. *1, Antedon mediterranea* (Lamarck, 1816), cross sectioned pinnule showing a testis (t) that has replaced most of the somatocoelomic space by functional swelling (see Fig. 57.4), fg=food groove, asterisk=aboral somatocoelomic canal, scale bar 100 µm. *2a, Cyathidium plantei* Heinzeller & others, 1996, testis with lumen (*) of former genital tube full of spermatids (sp), scale bar 100 µm; *2b,* detail of *2a* (marked with angles), a=zone of spermatogonia and bodies of Sertoli-cells, b=zone of differentiating spermatocytes, c=zone of spermatids, lined up linearly along the tails (*arrows*) of Sertoli-cells, scale bar 50 µm. *3–5, Cyathidium foresti* Cherbonnier & Guille 1972, horizontal sections through the base of an arm; *3,* multiple mature testes (t), each loaded with sperm, scale bar 500 µm; *4,* bundled flagella forming whorls, scale bar 200 µm; *5,* gonoduct (gd), comparable to a madreporic canal (see Fig. 9, 2–9.3), scale bar 50 µm. Staining: Toluidin blue in *1–2;* Azan in *3–4;* PAS in *5*. Images new, by authors.

and all other stalked crinoids, except for the very first pinnules, which in these crinoids contain gonads. In addition to elongated gonads extending over several pinnular segments (Fig. 59.3), globular gonads are present in the pinnules of certain feather star species. In cyrtocrinids (Fig. 59.4–59.5) the globular gonads are located in the arms at the pinnular bases. There is one large gonad in *Neogymnocrinus* and several smaller gonads in *Cyathidium*.

Production of gametes

Females. In females, the primordial germ cells grow within the tubular epithelium to large spherical oogonia with round cell nuclei that typically have one prominent nucleolus (for electron microscopic details see Holland [1988] or Heinzeller & Welsch [1994]). Further growth of the oogonia into primary oocytes results in a conspicuous bulge of the tubular epithelium toward the hemal space. In the light microscope, these oocytes seemingly lie in the hemal space. However, electron microscopy studies show that these cells sit on the epithelial basement membrane, which they share with the rest of the epithelium, indicating that these primary oocytes stay aligned with adjacent epithelial cells. Finally, the oocytes hatch from the epithelial collective (ovulation, according to Holland & Dan, 1975) and come to lie in the ovarian lumen, where they complete the first and undergo the second meiotic division (Holland 1991). After a species-specific, mostly short interval, the resulting mature ova are spawned.

Males. In the gametogenic tube of males, a specific type of nongerminal cells plays a

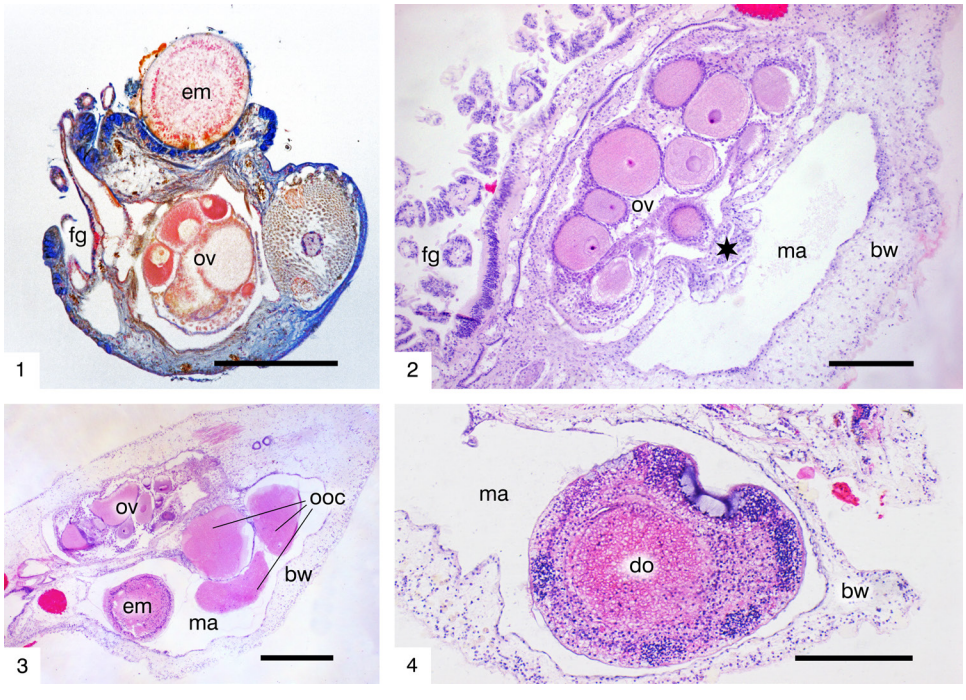

Fig. 62. *1, Antedon mediterranea* Lamarck, 1816, pinnule in cross section with the pinnular ossicle on the right side, the food groove with some tentacles on the left side; on top, an embryo (em) cemented to the pinnular flank, ov=ovary, fg=food grove, scale bar 100 µm. *2–4, Isometra vivipara* Mortensen, 1917. *2.* Similar orientation to *1,* but the body wall (bw) arches over the site where the egg cells leave the ovary (*asterisk*), forming thereby a marsupium (ma), fg=food grove, scale bar 100 µm. *3,* Longitudinal section through a pinnule with a marsupium (ma) containing three oocytes (ooc) and one embryo (em), ov=ovary, bw=body wall, scale bar 100 µm. *4,* Doliolaria larva (do) in marsupium (ma), bw=body wall, scale bar 100 µm. Image *1,* new, by authors, *2–4* courtesy of R. M. Pertossi.

crucial role. Its shape is described as approximately stellate (Holland, 1991). It rests with most of the cytoplasm and the cell nucleus on the basement membrane and sends out branches in various directions. In particular, a slender tail grows apically very long and reaches the lumen. Along such slender tails the spermatids are lined up in strikingly long rows, close together like swallows on a telegraph line (Fig. 61.2a). Because of their intimate contacts with spermatocytes and spermatids, these stellate cells are compared to and named after the Sertoli cells in vertebrate testes.

In the testis, the primordial germ cells grow as in the ovaries and become spermatogonia within the tubular epithelium, still sitting on the basement membrane. The spermatocytes resulting from the two cell divisions of spermatogonia, or more precisely their nuclei, are hardly discernable in the light microscope (compare zone b in Fig. 61.2b). In contrast, the small dense globules of the spermatid nuclei of zone c are clearly visible. During their final transformation into mature sperm, the spermatids develop a species-specific nuclear shape, a long flagellum and further ultrastructural peculiarities, as described by several authors, for example by Bickell, Chia, and Crawford (1980); (reviewed by Holland 1991).

SPAWNING, FERTILIZATION AND DEVELOPMENT

Non-brooding species

In the majority of crinoid species, both sexes spawn simultaneously or shortly after each other, with females possibly stimu-

lated by pheromones from spawning males (Holland, 1991). Eggs and sperm become discharged through a rupture in the pinnular wall. In cyrtocrinids, however, which carry the gonads at the base of the arm and thus close to the tegmen with its madrepores, the gametes use these pores to exit. Eggs are inseminated in open water, fertilized eggs typically sink to the bottom. Exceptionally, the eggs of *Promachocrinus kerguelensis* remain floating (McClintock & Pearse, 1987). Whether on the bottom or in open water, the eggs develop into a lecidotrophic larva (in most cases a doliolaria) that lives pelagic (Holland, 1991; Barbaglio & others, 2012).

Brooding species

Maternal care requires that the mature eggs remain on or in the maternal body. Although the number of such species is low, they can be categorized by their mode of brooding.

The first mode is realized by only few species, for example, *Antedon bifida* or *A. mediterranea*. The mature eggs break through the pinnular wall and are immediately externally fixed to this wall by the secretion of cement glands (Reichensperger, 1908) (Fig.79.7; Fig. 62.1). Dozens of eggs can be attached to a single pinnula in this way. There they become fertilized, and they develop within the fertilization envelopes until they hatch as doliolaria larvae. After spawning, *Antedon bifida* females exhibit a characteristic behaviour of maternal care by wrapping their arms closer together over the brood (Lahaye & Jangoux, 1985b).

In the second mode, females provide a brooding pouch, called marsupium, at the gonadal pinnules. This is true for species of the genera *Isometra, Notocrinus*, and *Aporometra*. The first to describe a brooding crinoid (*Isometra vivipara* Mortensen 1917) was K. A. Andersson in 1904. His material has been analysed in detail by Mortensen (1920) who in turn added *Notocrinus virilis* to the brooding crinoid group. A marsupium represents an overarching of the egg exit site by the body wall but retaining an opening to the outside. There are no signs of any feeding capacity (Fig. 62.2). A marsupium has no open connection to the lumen of the ovary. The question of how sperm can meet ova is still under debate (Pertossi & others, 2019). The larvae feed on their yolk; the assumption of Mortensen 1920 that the giant larvae of *Notocrinus* nourish on additional sterile ova was rejected by Haig and Rouse (2008).

Generally, brooded larvae leave the maternal nest as doliolariae, but in two species, development continues until the pentacrinoid stage: *Kempometra grisea* (John, 1939) and *Aporometra wilsoni* (Haig & Rouse, 2008).

A third, special (and possibly unique) mode of brooding takes place in *Comatilia iridometriformis* (see Messing 1984), in which the larvae develop within the ovary. This lead to the assumption that fertilization also takes place in the ovary. However, the question remains as to which route the sperm use to reach the eggs. The larvae hatch at an early cystidean stage.

VII. NERVOUS SYSTEM

Traditional tripartite division

In his fundamental study on the histology of crinoids (1889), Hamann classified the nervous sytem into three subsystems. The first is located basally in the food groove epithelia (Ambulacralnerven), the second in the oral connective tissue (ventrales Nervensystem), and the third in the aboral connective tissue (dorsales Nervensystem). With explicit reference to Hamann's work, Hyman (1955) again distinguished three subsystems corresponding to those of Hamann; she called them ectoneural, hyponeural, and aboral. These terms, which have since been widely accepted, are also used in the present description, but the general categorization is replaced by a bipartite one (Fig. 63) based on fine histological criteria.

Reasons for bipartion rather than tripartion.

After Hyman (1955), additional nerve cell groups and fiber plexus have been reported. These have been identified by higher reso-

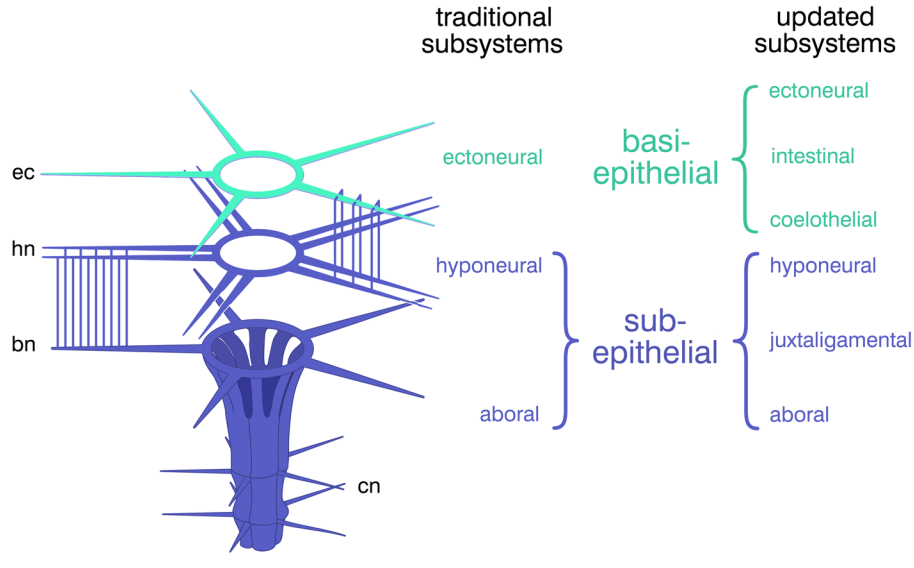

Fig. 63. Schematic representation of the nervous system of an isocrinid crinoid, showing the traditional categorization into three subsystems (Hyman, 1955) and the grouping of six subsystems into the two categories basiepithelial and subepithelial, ec=ectoneural cord, hn=hyponeural nerves, bn=brachial nerve, cn=cirral nerves (modified from Heinzeller, 1998, fig 1 and 2).

lution techniques (electron microscopy uncovered ubiquitous plexus in coelothelia) and with an improved understanding of the role of juxtaligamental cells as neurosecretory cells. These new neurons and the plexus were not captured by the traditional three subsystems and can be considered as three additional subsystems (Fig. 63). Moreover, the tripartite categorization of the nervous system has been related to the concept of three germ layers (ectoderm, endoderm, and mesoderm). However, in most cases, an origin of neurons from specific germ layers has not been adequately demonstrated, with the exception of the ectoneural subsystem, which is clearly derived from the ectoderm. If the subsystems are categorized according to the location of their associated basal lamina as the only criterion, two categories (superorders) emerge under the terms basiepithelial and subepithelial (Fig. 63).

Basiepithelial nervous tissue is located in the ectodermal and entodermal epithelia, as well as in the coelothelia; neurons and fiber plexus are normally located near the basal lamina between the feet of the epithelial cells. In addition to the ectoneural strands in the food groove epithelium with a circumoral nerve ring, the basiepithelial nervous plexus is present in the intestinal epithelium and in the coelothelia of the somato-, hydro-, and the axocoelium.

Subepithelial nervous tissue is located in the extracellular matrix below the basal lamina. This is the case with the hyponeural subsystem with its paired para-radial nerve cords in the arms that communicate centrally via a nerve ring, further the juxtaligamental cells, and finally the aboral subsystem. The latter is unique among echinoderms; radial nerves extend from a very voluminous aboral ganglion into the arms and pinnules and also into the cirri.

BASIEPITHELIAL SUBSYSTEMS

Ectoneural subsystem

In simplified terms, the ectoneural subsystem consists of as many radial strands as the animal has arms, a circumoral ring commissure, and the intraepithelial plexus of the (presumably ectodermal) upper esophagus. The ectoneural tissue is integrated into the food groove

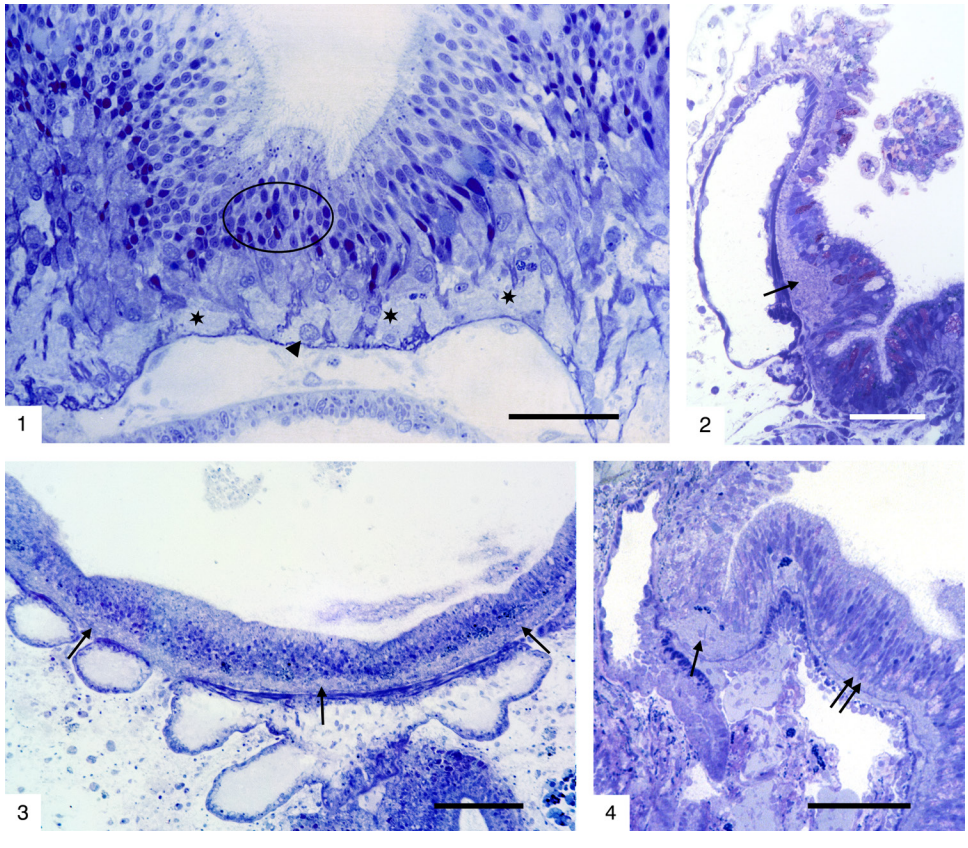

Fig. 64. Ectoneural subsystem. *1, Capillaster multiradiatus* (Linnaeus, 1758), transverse section through the food groove epithelium; nerve fiber plexus lies basally (*asterisks*), *arrowhead* points toward a putative neuron (large, spherical, bright nucleus); nuclei of primary food groove cells encircled, scale bar 50 µm. *2–4,* Circumoral ring commissure (*arrows*); *2, Leptometra celtica* M'Andrew & Barrett, 1857, longitudinal section through a mouth tentacle, scale bar 50 µm; *3, Antedon bifida* Pennant 1777, horizontal section, scale bar 100 µm; *4, Saracrinus nobilis* P. H. Carpenter, 1884, radial section through the edge of the mouth, basally on a tentacle root, the circumoral ring (*single arrow*) is significantly thicker than the uppermost esophageal nerve plexus (*double arrow*), scale bar 100 µm. Staining: Toluidine blue. Images new, by authors.

epithelium (Fig. 64), which merges into the esophageal epithelium. The fusion zone is also where the neural components of the epithelia fuse. We commonly refer to this zone as the circumoral ring commissure (Fig. 64.3), which is noticeable as a particular thickening in some preparations (Fig. 64.2, Fig. 64.4). However, this may be partially explained by contraction of the perioral musculature.

In the periphery, the radial strands extend into the tentacles toward the inner side of the tentacles—the outer side of the tentacle is supplied by a branch of the hyponeural subsystem. This location suggests a role in coordinating the movements of the tube feet, especially in their well-graded interaction (see Section V on Nutrition).

Intestinal subsystem

Structurally quite similar to the ectoneural subsystem, the neurons and numerous small projections of the intestinal subsystem lie between the basal extensions of the primary cells of the intestinal epithelium The ectoneural/intestinal boundary is likely to be that between the upper and lower esophagus (see Fig. 50.2–50.3). The nerve plexus is also well developed in the lower esophagus but

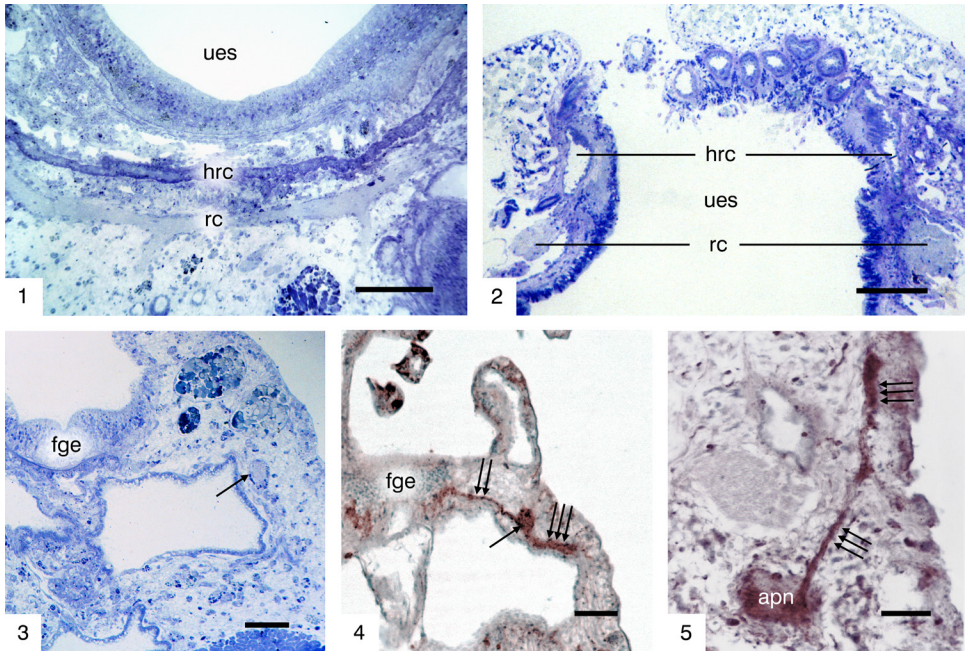

Fig. 65. Hyponeural subsystem. *1, Antedon bifida* Pennant 1777, horizontal section, *rc*=perioral ring commissure, hrc=hydrocoelomic ring canal, ues=upper esophagus, scale bar 100 µm. *2, Cyathidium plantei* Heinzeller & others, 1996, coaxial section through the perioral region showing the hyponeural ring commissure (**rc**) aborally of the hydrocoelomic ring canal (hrc), ues=upper esophagus, scale bar 50 µm. *3–5, Antedon bifida*, transverse sections through pinnules, *single arrows* point to the hyponeural nerve, *double arrows* point to the connection with the ectoneural plexus in the food groove epithelium (fge), *triple arrow* marks the connection with the aboral pinnular nerve (apn), scale bars 25 µm. Staining: Toluidine blue (*1–3*), anti-NGF serum, Hemalum (*4, 5*). Image new, by authors.

decreases in thickness in the deeper parts of the intestine and even disappears as a distinct layer. Specific functional data are not at hand.

Coelothelial subsystem

As noted by Engle (2013), even the cystidean larva of *Antedon bifida* has numerous neurites located basally in each epithelium, particularly in the coelothelia of the extension tubes of the chambered organ projecting into the stalk. In some isocrinid species, these nerve fiber bundles are also observed in adults, e.g., in *Neocrinus decorus*. However, most of them are too fine to be resolved by light microscopy.

SUBEPITHELIAL SUBSYSTEMS

Hyponeural subsystem

The central structure of the hyponeural subsystem is a circumoral ring commissure (without aboral continuation and thus a true ring compared to the ectoneural ring commissure). The hyponeural ring is located peripherally adjacent to the water vessel ring canal (Fig. 65.1). Pairs of para-radial nerves branch off from the ring commissure and accompany the oral somatocoelomic canal with some spacing on either side through arms and pinnules (Fig. 65.3). Bundles of nerve fibers regularly connect the hyponeural nerves to both the ectoneural plexus in the food groove epithelium and the brachial nerves of the aboral subsystem (Fig. 65.4–65.5).

Juxtaligamental cells

Juxtaligamental cells are neuroendocrine cells that play a crucial role in controlling the consistency of collagenous structures, particularly of the so-called mutable connective tissue (Fig. 66). In all echinoderm taxa, the

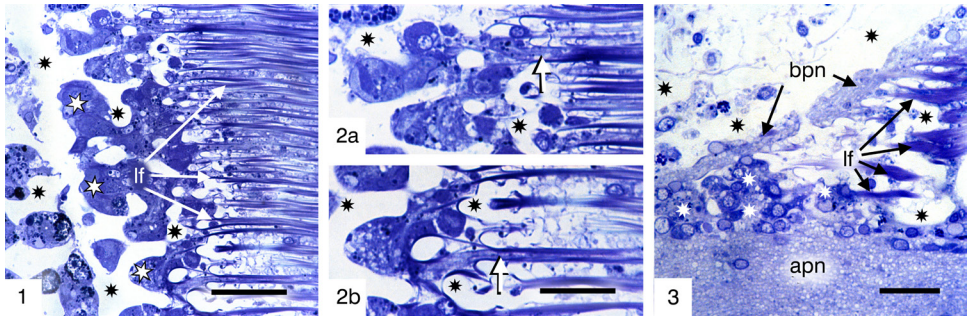

Fig. 66. Juxtaligamental cells, *Antedon bifida* Pennant 1777, longitudinal sections of arm ligament (*1, 2a, 2b*) or pinnular ligament (*3*). *1,* On the right, ligament with thin, dark blue ligament fibers (lf); on the left, ossicular stereom (*black asterisks*) and groups of juxtaligamental cells in its cavities (*white asterisks*), scale bar 50 µm. *2a–2b,* Details of *1*, *arrows* point to the juxtaligamental cell outgrowths between ligament fibers, scale bars 25 µm for both. *3,* Group of juxtaligamental cells in the axilla between the aboral pinnular nerve (apn) and a branch ascending obliquely from it (bpn), scale bar 25 µm. Staining: Toluidine blue. Image new, by authors.

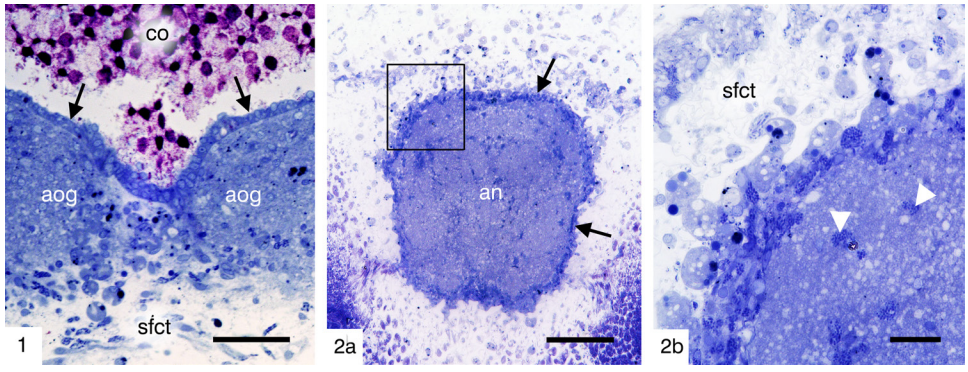

Fig. 67. Mesodermal boundary of the aboral subsystem. 1, *Leptometra celtica* M'Andrew & Barrett, 1857, horizontal section, on the inner side of the aboral ganglion (aog), nervous tissue borders the coelothelium (*black arrows*) of the chambered organ (co), on the opposite side it borders sclerite-forming connective tissue (sfct), scale bar 20 µm. *2a–2b, Antedon petasus* Düben & Koren,1846, transverse section through the arm nerve (an) embedded all around in sclerite-forming connective tissue, amebocytes on the surface are marked by *black arrows*; *2b,* higher magnification of rectangle marked in *2a*, showing many granulated amebocytes in the sclerite-forming connective tissue (sfct) on the nerve surface and amebocytes migrating into the nervous tissue (*white arrow heads*), scale bars 100 µm in *2a*, 50 µm in *2b*. Staining: Toluidine blue. Image new, by authors.

mutable connective tissue is a special feature that allows the ligaments to stiffen and, conversely, to relax. Stiffening is necessary to maintain a certain posture for a long period of time without expending much energy, whereas relaxation facilitates autotomy and evisceration. Different types of juxtaligament cells have been distinguished on the basis of size and vesicle type (Welsch, Heinzeller, & Cobb, 1990; Welsch & others, 1995). Juxtaligamental cells are in contact with the hyponeural and aboral subsystems (Mashanov & others, 2016).

Pioneering studies on the regulation of mutable connective tissue have been performed mainly on the body wall connective tissue of holothurians (Motokawa, 2019). Several proteinaceous factors have been shown to be responsible for the connective tissue stiffness (e.g., Trotter & others, 1996). Moreover, these factors have been demonstrated in granules of juxtaligamental cells of *Cucumaria frondosa* (Keene & Trotter, unpublished, cited in Wilkie, Candia Cardenali, & Trotter, 2004, p. 375). Juxtaligamental cells were originally

described in brittle stars and named by Wilkie (1979) based on their location adjacent to ligaments.

In crinoids, clusters of juxtaligamental cells are in arms, pinnules, and cirri within gaps in the stereom along the attachment zone of the ligaments (Fig. 70). The cell bodies and nuclei are relatively large. Long thin cell processes penetrate the ligaments parallel to the collagenous fibers (Fig. 70.2a–70.2b). In combination with their neural contacts, these juxtaligamental cells can enable the above-mentioned, long-lasting postures as well as autotomy of the arms. Wilkie and others (2010) demonstrated for *Antedon mediterranea* (Lamarck, 1816) that autotomy at the syzygies occurs under glutamatergic control of cellular elements close to the syzygial ligaments.

A different type of juxtaligamental cells has been described in the feather star *Himerometra robustipinna by* Kalachewa and others (2017) in the connective tissue of the intercoelomic septa that hold the intestine. These juxtaligamental cells are thought to be responsible for destabilization of the holding collagenous structures and, after evisceration, for gut regeneration by transdifferentiation.

Aboral (apical) subsystem

The name of the aboral subsystem derives from the aboral location of its ganglion; (entoneural as a synonym, the "aboral or entoneural system" of Hyman, 1955, p. 62) is misleading because it evokes the association of an entodermal origin. The prominent aboral ganglion of feather stars has attracted the interest of scientists in the past because of its conspicuous size. The ganglion, the stalk nerves, and their cirral extensions border the coelothelium of the chambered organ and its tubular processes into the stalk on one—the inner—side. Their outer side is covered by mesodermal tissues, either connective tissue or sclerites (Fig. 71.1). The arm nerves and their pinnular offshoots are completely embedded in mesodermal tissues (Fig. 67.2). In the marginal area of the nerves, various types of amebocytes commonly accumulate, in some cases forming an envelope-like layer (Fig. 67.2a and 67.2b).

In terms of total volume, the aboral subsystem by far exceeds all other subsystems. It consists of prominent brachial nerves (radial) and stalk nerves (interradial) that meet in the radial ossicles and form a ring commissure. Of all the parts of the aboral system, this aboral nerve ring is the only one that is consistent in all crinoids studied to date, whereas the configuration of the aboral ganglion varies in shape and extent.

Central parts of the aboral subsystem

Bourgeticrinina. In several stalked species of the genera *Bathycrinus, Rhizocrinus*, and *Democrinus*, the organization of the aboral subsystem represents what appears to be fundamental to crinoids (Bohn & Heinzeller, 1999) (Fig. 68). These species clearly reveal that a junction of radial arm and interradial stalk nerves inevitably lead to a ring-shaped, commissural structure. The oral processes of the stalk nerves widen to a certain degree—varying among species—during their ascent from the basal ossicle into the radial ossicle. In *Bathycrinus gracilis* Thomson, 1872, the oral processes of the stalk nerves (primary interradial strands) form a triangular plate (Fig. 68.5). In *Bathycrinus aldrichianus* Thomson, 1876, the equivalent strands do not form such a triangle but split into pairs of secondary interradial strands (P. H. Carpenter, 1884). This observation may be valuable for comparison with the condition in isocrinids. However, no such splitting was observed in the material examined for this article.

The question of the presence of an aboral ganglion in bathycrinid crinoids remains open. In *Democrinus chuni,* the interradial strands could presumably be traced aborally until the chambered organ (see Fig. 22.6–22.7). This is the site where an aboral ganglion would be expected. However, no ganglionic swelling could be found there.

Isocrinida. In isocrinid crinoids, the stalk nerves run parallel close together, so that in cross section through the upper stalk they

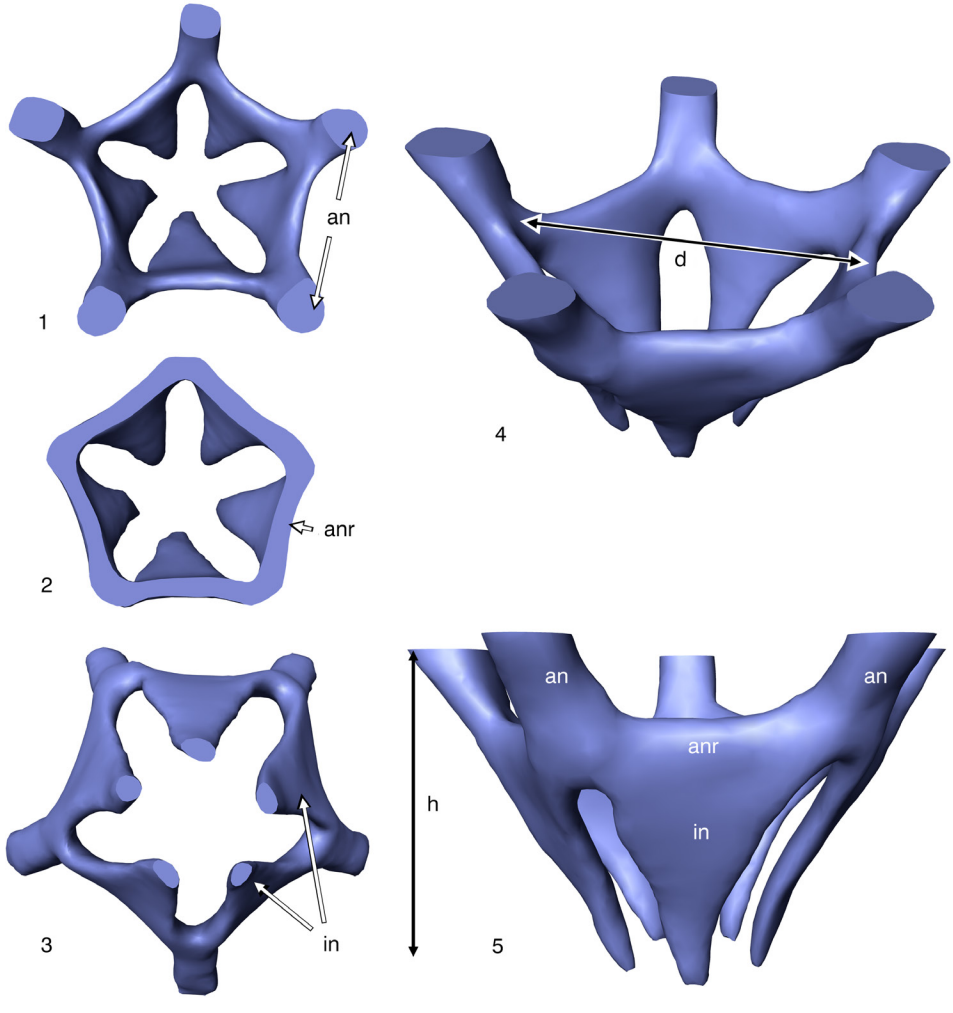

Fig. 68. *Bathycrinus gracilis* Thomson, 1872, 3D model of the aboral nervous subsystem. *1,* Oral view with cropped arm nerves (an). *2,* Oral view with cropped aboral nerve ring (anr), *3,* Aboral view with cropped interradial nerves (in). *4,* Oblique lateral view, d=diameter of the aboral nerve ring, approximately 0.4 mm. *5,* Lateral view, h=height of the model, approximately 0.3 mm, other labels as in *1–3.* Image new, by authors.

have the appearance of a homogeneous nerve cylinder (Fig. 75.3) The most oral part of the stalk nerves and their direct oral extensions, the primary interradials (Fig. 69), might be considered equivalent to what appears in feather stars as a voluminous aboral ganglion (Fig. 71). There may be some exchange of fibers between the oral parts of stalk nerves. Furthermore, cross-connections, albeit minute, between primary interradial strands as well as between secondary interradial strands have been described (Reichensperger, 1905).

The condition in adult isocrinids (Fig. 69) reflects that of a very early stage of the free-swimming feather star *Antedon bifida* (Fig. 70) and is strikingly similar to what P. H. Carpenter (1884) reported in *Bathycrinus aldrichianus*.

Anatomically, an aboral ganglion as a distinct swelling is not seen in bathycrinid and isocrinid crinoids. Nevertheless, it must

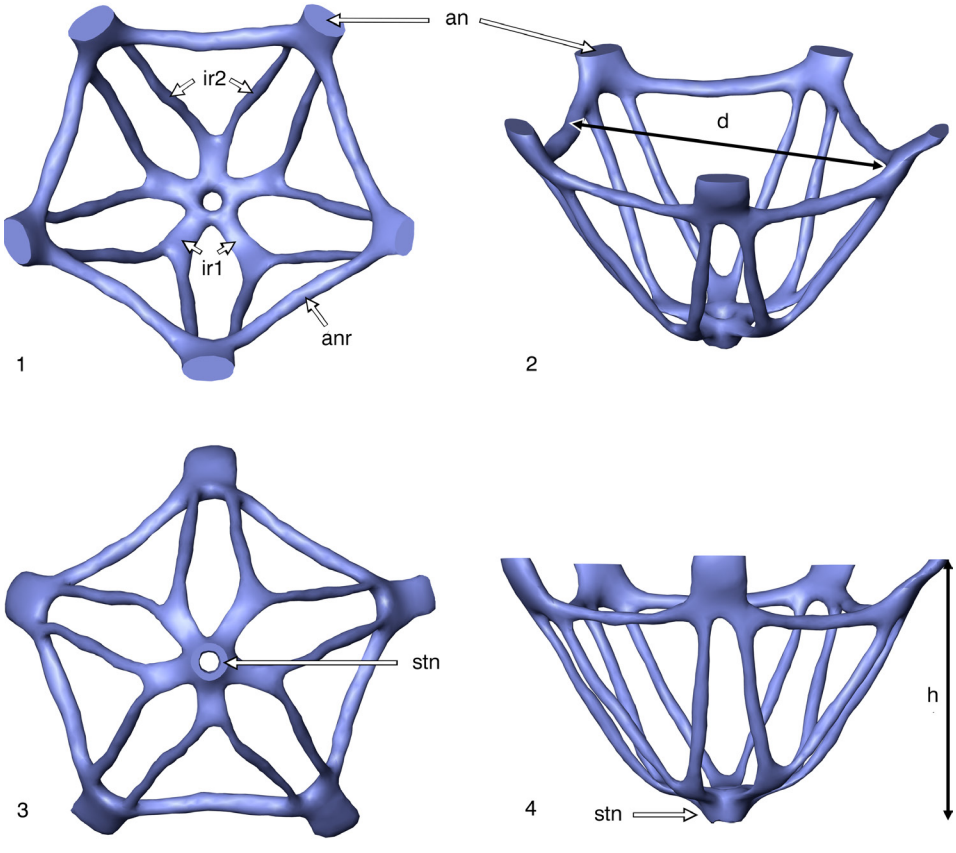

Fig. 69. *Metacrinus levii*, (Améziane-Cominardi in Améziane-Cominardi & others,1990), 3D model of the aboral nervous subsystem. *1,* Oral view with cropped arm nerves (an). The connections of the arm nerve roots represent the pentagonal aboral nerve ring (anr). Each arm nerve root receives two slender strands (ir2) from two different secondary interradial strands (ir1). *2,* Oblique lateral view, d=diameter of the aboral nerve ring, approximately 3.5 mm. *3,* Aboral view with central cropped cylinder of stalk nerves (stn). *4,* Lateral view, h=height of the model, approximately 2.75 mm. New, by authors.

be assumed that this region is essential for the exchange of fibers between the stalk, calyx, and arms in these crinoids as well.

Feather stars. The voluminous aboral ganglion of feather stars represents the most significant difference between their aboral subsystem and the one of other crinoids (Fig. 71). In all feather stars studied so far, this ganglion can be compared to two bowls on top of each other, with the upper bowl inverted. The wall of the lower bowl is very thick, and the upper bowl has a large hole in the bottom (Fig. 72, Fig. 73, Fig. 74).

In the comparison between feather stars and isocrinids, the aboral bowl (eather stars) corresponds to stalk nerves (isocrinids) (Fig. 71, Fig. 73.6). Cirral nerves arise from the surface of this bowl. In older animals, the central aboral surface is smooth because no cirral nerves arise there (Fig. 72.3). During the early stages of growth, the first cirri developed here, which were reduced and lost in later stages.

The oral bowl of feather stars corresponds to the primary interradial strands of isocrinids. Here, the equivalents of the primary interradial strands are fused (Fig. 75, Fig. 74.4–74.5), forming an abundance of commissural fiber bundles within the homogeneous-looking wall of the ganglion.

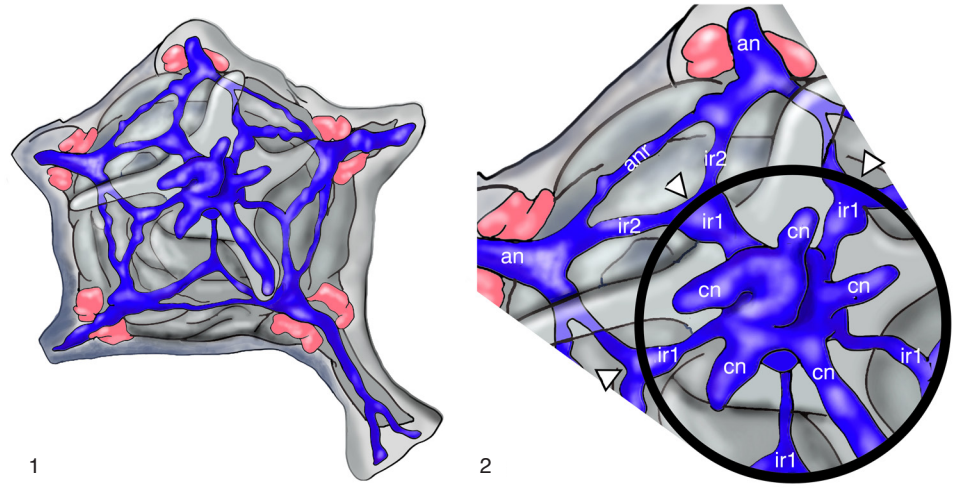

Fig. 70. Aboral view (*1*) of a juvenile specimen of *Antedon bifida* Pennant 1777 (calyx diameter 0.6 mm). The aboral nervous subsystem is shown in *blue*, the anlagen of muscles in *red*. Detail (*2*) at higher magnification, anr=aboral nerve ring, ir1 and ir2 = primary and secondary interradial strands, arrowheads=bifurcation, an=radial arm nerve, cn=cirral nerve. The *black circle* outlines the area between the primary interradial cords that fills with nerve tissue as growth progresses, forming the ganglion. New drawings, based on Engle, 2013, fig 20A.

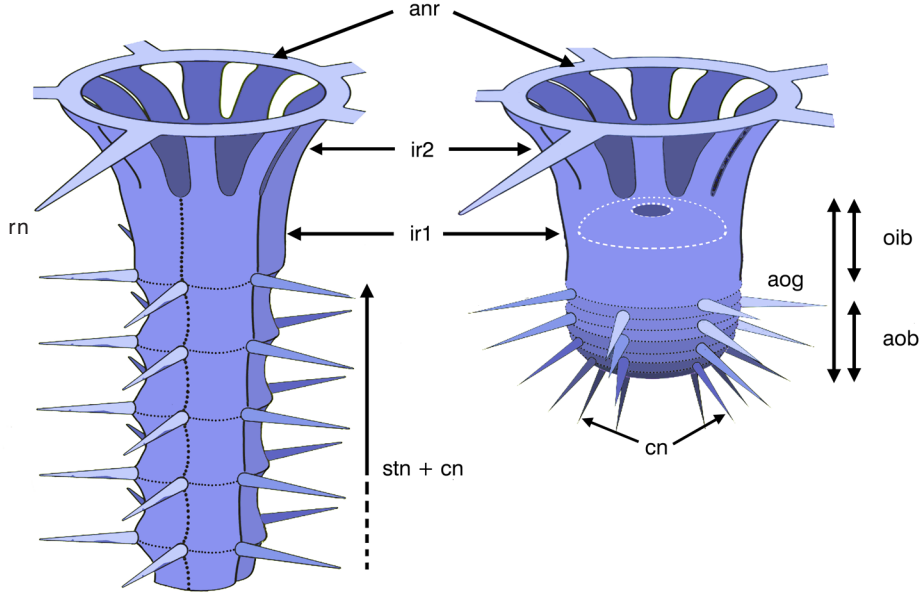

Fig. 71. Schematic representation of components of the aboral nervous system of an isocrinid (left) and a feather star (right) for comparison. Labels: anr=boral nerve ring, rn=radial nerve (the other four cropped), ir2=secondary interradial strands, ir1=primary interradial strands, stn=stalk nerves, cn=cirral nerves, aog=aboral ganglion, oib=oral inverted bowl, aob=aboral bowl, *dashed white line* in the feather star scheme indicates the roof (invisible from externally) above the chambered organ (modified from Heinzeller, 1998).

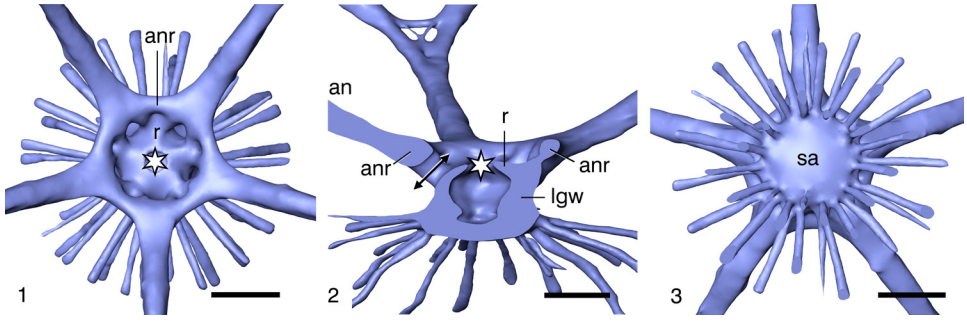

Fig. 72. *Antedon bifida* Pennant 1777, 3D model of the aboral nervous subsystem. *1,* Oral view, aboral nerve ring (anr) surrounds the roof (r) over the chambered organ and its central hole (*white asterisk*). *2,* Vertical crop, radial structures on the left (an=arm nerve) and interradial structures on the right, lgw=lateral ganglion wall. The bidirectional *arrow* marks a hole between secondary interradial strands. *3,* Aboral view, cirral nerves (truncated) radiating in all directions, central smooth area (sa) without cirral nerves. All scale bars 0.5 mm. New, by authors.

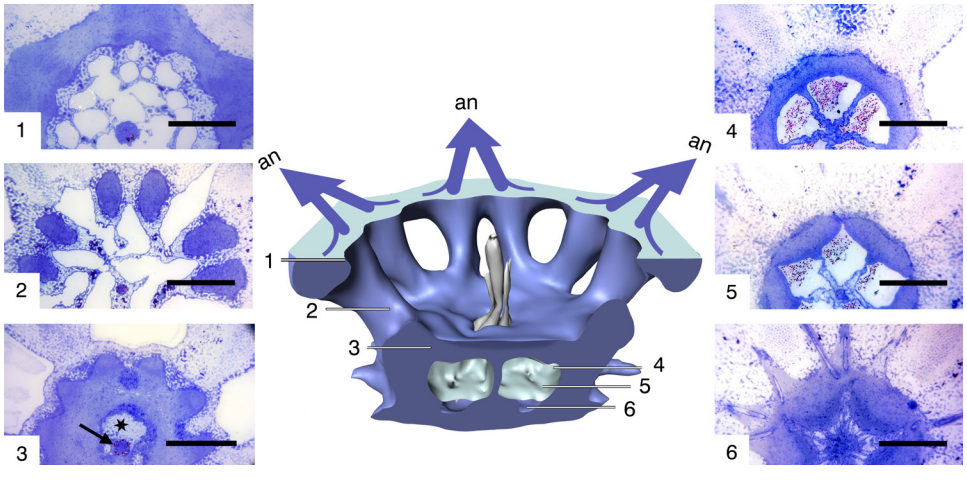

Fig. 73. *Comatella nigra* P. H. Carpenter 1888, aboral nervous subsystem. *1–6,* horizontal sections at the planes labeled in the 3D model. The model is cropped horizontally through the aboral nerve ring, and frontally to show the large chambers of the chambered organ. Planes: *1,* aboral nerve ring surrounding multiple coelomic cavities of the axial sinus; *2,* secondary interradial strands; *3,* oral "bowl" of the aboral ganglion, roof with the oral processes of the chambered organ (*arrow*) ascending through the hole (*asterisk*); *4,* oral bowl of the aboral ganglion; *5,* aboral most part of the oral bowl showing separate stalk nerves; *6,* aboral bowl of the aboral ganglion, smaller cavities under the large chambers of the chambered organ contain the labyrinth (omitted in the model). Label: an=arm nerve. Scale bars in *1–6* each 0.4 mm. Staining: Toluidine blue. New, by authors.

The most oral part of the oral bowl covers the chambered organ, and in the middle, it holds open the aperture through which the oral tubular processes of the chambered organ enter the axial sinus (Fig. 72.1–Fig. 72.2, Fig. 73.3). Further orally, there is no fundamental difference between feather stars and isocrinids; in both groups, the secondary interradial strands remain separate, unlike the primary interradial strands, which are fused in feather stars, and connect the ganglion orally to the aboral nerve ring (Fig. 73).

Relation to the chambered organ. There is a small space between the chambers of the chambered organ and the bottom of the aboral ganglion (Fig. 73.6). This space contains the cirrus-related labyrinthic part of the chambered organ (see Fig. 23). At the same level, on the outside of the ganglion, the cirrus nerves arise (Fig. 73.6).

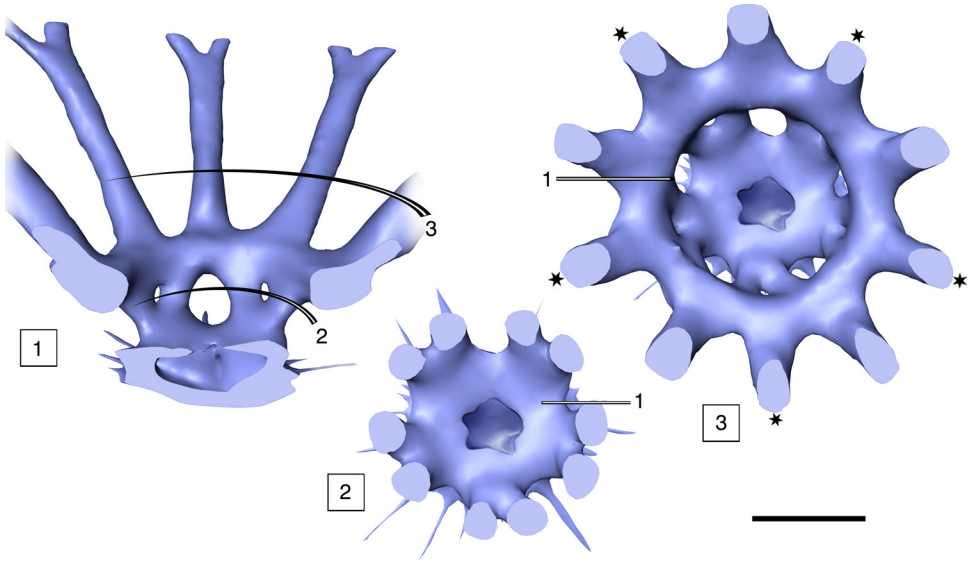

Fig. 74. *Promachocrinus kerguelensis* P. H. Carpenter, 1879, 3D model of the main components of the aboral nervous subsystem. *1,* Vertical crop at the plane labeled "1" in *2* and *3*, unobstructed view of two pairs of secondary interradial strands. *2,* Horizontal crop just below the aboral nerve ring (plane labeled "2" in *1*) showing five pairs of secondary interradial strands. *3,* Horizontal crop just orally from the nerve ring (plane labeled "3" in *1*). Five arm nerves (*asterisks*) run continuously with the five pairs of secondary interradial cords as in the five-armed species; five additional arm nerves are intercalated. Scale bar 1.8 mm for all. New, by authors.

The pattern described above is also present in the ten-armed comatulid *Promachocrinus kerguelensis* (Fig. 74), but the dimensions seem to be particular. The ganglion as such is relatively small, as is the space for the chambered organ. In contrast, the volumes of nerve ring and arm nerves are relatively large. This could be due to the ability of this species to swim by arm strokes and also to cling to the substrate with the aid of the arms (see below).

Cyrtocrinida. No evidence of an aboral nervous system below the aboral nerve ring was detected in either *Holopus rangii* (Grimmer & Holland, 1990) or two species of *Cyathidium* (Heinzeller, 1998). Obviously, not only the stalk proper is missing in these species, but also all organs that are associated with a stalk in other species. This concerns, for example, cirri or the chambered organ and its aboral extensions (see Section III) or the axial organ (see Section IV). Overall, these crinoids lack an aboral ganglion along with stalk nerves and all other structures assiociated with a stalk in other species.

Nerves of the aboral subsystem

Typically, amoebocytes are ubiquitous on the surface of these nerves. They may occur singly, in groups, or even in the form of sheath-like aggregates (as evident in Fig. 67) or as reported in *Gymnocrinus richeri* (Heinzeller, Améziane-Cominardi, & Welsch, 1994). Internally, densely packed, mostly longitudinal fibers of quite variable thickness and/or vesicle content dominate the appearance of the strands. The putative neurons, more precisely their nuclei, are commonly located in rows in the middle or at the surface. Their electron microscopic appearance is that of bipolar cells emitting long fibers; synapses are rarely present (Heinzeller & Welsch, 1994).

Roughly speaking, the brachial, pinnular, and cirral nerves can be assigned to the locomotor system and the hyponeural nerves to surface sensibility. Nevertheless, it must

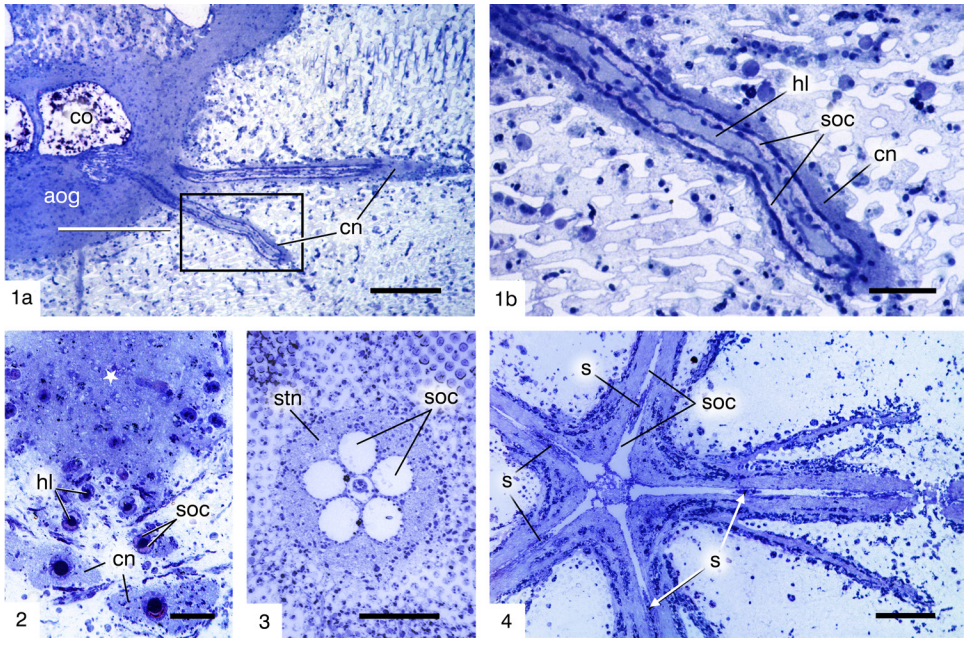

Fig. 75. Cirral nerves (compare to Fig. 30 and Fig. 25). *1a–1b, Himerometra robustipinna* P. H. Carpenter, 1881a, vertical section, in *1a* two cirral nerves (cn) arise from aboral "bowl" of the aboral ganglion (aog), co=chambered organ; *white bar* marks the approximate sectional plane of *2,* scale bar 200 µm. *1b,* Higher magnification of the rectangle in *1a*; the cirral nerve containing the innermost hemal lacuna (hl) and the associated pair of somatocoelomic canals (soc), scale bar 50 µm. *2, Leptometra celtica* M'Andrew & Barrett, 1857, horizontal section through the aboral tip of the aboral ganglion showing transversely sectioned cirral nerves, the hemal substance is (unusually dark) blue. The *white asterisk* marks the oral-aboral body axis, scale bar 50 µm. *3, Metacrinus* sp. (young specimen), internodal transverse section of the stalk showing the stalk nerves (stn) forming a sheath around the quintuplets of somatocoelomic tubes (soc), scale bar 100 µm. *4, Endoxocrinus sibogae* (Döderlein, 1907), horizontal section through a node with five radiating cirral nerves, the right of which has two small branches. The septum (s) separating the two somatocoelomic canals in each nerve contains the hemal lacuna, scale bar 200 µm. Staining: Toluidine blue. Images new, by authors.

be assumed that all strands—with varying proportions—contain both motor and sensory fibers. Most authors agree "that in echinoderms there is no 'real'coordination center, and that NS (nervous system) functions and control are more widely dispersed throughout the body than in most other animals" (Díaz-Balzac & García-Arrarás, 2018, p. 8 of pdf print). Therefore, a high-level coordinative capacity of local circuits appears likely. However, these should be complemented by far-reaching linkages to cope with complex behavior such as swimming, light-dependent walking, or escape from predators. The extensive fiber exchanges (Fig. 76) at branching sites and at the contact between arm nerves and the aboral nerve ring potentially indicate such long-distance connections.

Stalk- and cirral nerves in isocrinids. As mentioned above, the stalk nerves of isocrinids run from the level of the radial ossicles through the stalk to almost the holdfast or to the free end of a broken stalk. In *Metacrinus rotundus* the stalk nerves can regrow as long as the aboral ganglion is present (Nakano & others, 2004).

This ganglion appears to correspond to what Nakano, Nakajima, & Amemiya (2009) refer to as the nerve center in the basal plates in their developmental studies. According to this description, the nerve

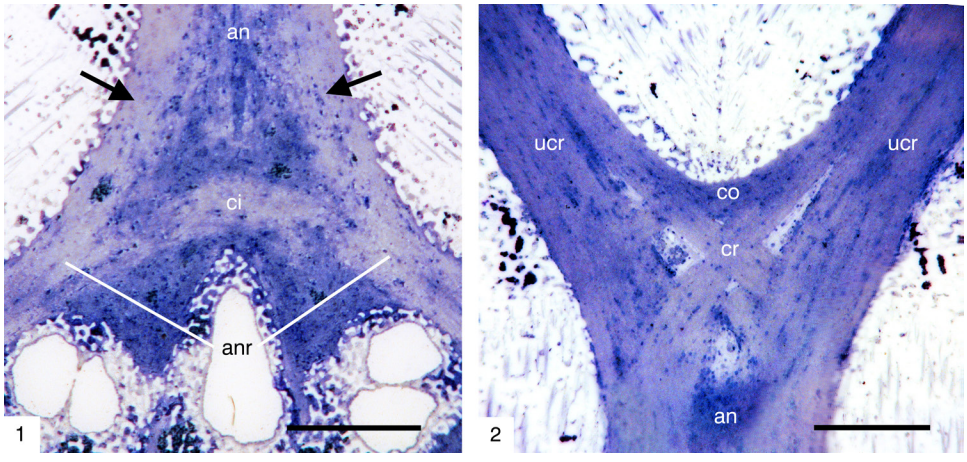

Fig. 76. Aboral arm nerves. *1, Clarkcomanthus albinotus* Rowe, Hoggett, Birtles, & Vail, 1986, horizontal section through the aboral nerve ring (anr) showing the base of an arm nerve (an), *arrows* point to nerve fiber bundles ascending into arm nerve; ci=circular bundle, scale bar 2 mm. *2, Comatella nigra* P. H. Carpenter 1888, bifurcation of an arm nerve with regular exchange pattern of fiber bundles, either commissural (co) or crossing to the other side (cr); other bundles run uncrossed (ucr), scale bar 2 mm. Staining: Toluidine blue. Images new, by authors.

center, which is indispensable for stalk nerve regrowth, must be the transition from the stalk nerves to the primary interradial strands. Aboral of the basal plates, the nerves run shoulder to shoulder and form a cylindrical sheath around the five coelomic tubes (Fig. 75.3). In each nodal, five branches of the stalk nerves extend to two coelomic tubes each and form the cirral nerves (Fig. 75.4, also see Fig. 25–Fig. 26).

The main function of cirri—i.e. to cling to the ground or even to locomote, including crawling (Birenheide, Yokoyama, & Motokawa, 2000)—may be controlled by these cirral nerves or, rather, by juxtaligamental cells associated with them.

"Stalk" and cirral nerves in feather stars. Comatulid crinoids (except Bourgeticrinina) are free-living and have no obvious stalk as an adult. Their equivalents to stalk nerves, characterized by the formation of cirral nerves, are regarded as an integral part of the aboral ganglion (Fig. 71).

The cirri articulate in sockets with which the centrodorsal is paved. Because cirri, which develop earliest, are reduced later, the apex of the centrodorsal is smoothed. As a result, the centrodorsal is typically occupied only by peripheral circles of larger cirri (Fig. 72.3). Like isocrinids, most comatulids can cling to the substrate with the terminal claws of the cirri. Species such as *Promachocrinus kerguelensis*, which bear few or no cirri, do so only with the aid of a few arms (Macurda & Meyer, 1983). At each branching, the fiber bundles are mutually exchanged and recombined in the branches.

Arm nerves and pinnular nerves. Typically, arm nerves arise as quintuplets from the aboral nerve ring in the radial ossicles and bifurcate in the succeeding axial ossicles. The stem ascending from the nerve ring clearly integrates fiber contingents originating from both sides of the ring (Fig. 76.1) but also allows commissural fibers to pass at its base. At each branching, the fiber bundles are mutually exchanged and recombined in the branches. Branching in daughter nerves apparently follows a strict scheme of combination and mutual exchange of fiber bundles. Although this crosswise exchange of fibers is obvious (Fig. 76.2), the detailed internal organization and functional significance are still enigmatic.

Between two brachials, the course of the nerves is slightly curved (Fig. 77.1) and of a constant thickness. In histological longitudinal sections, the curved course may

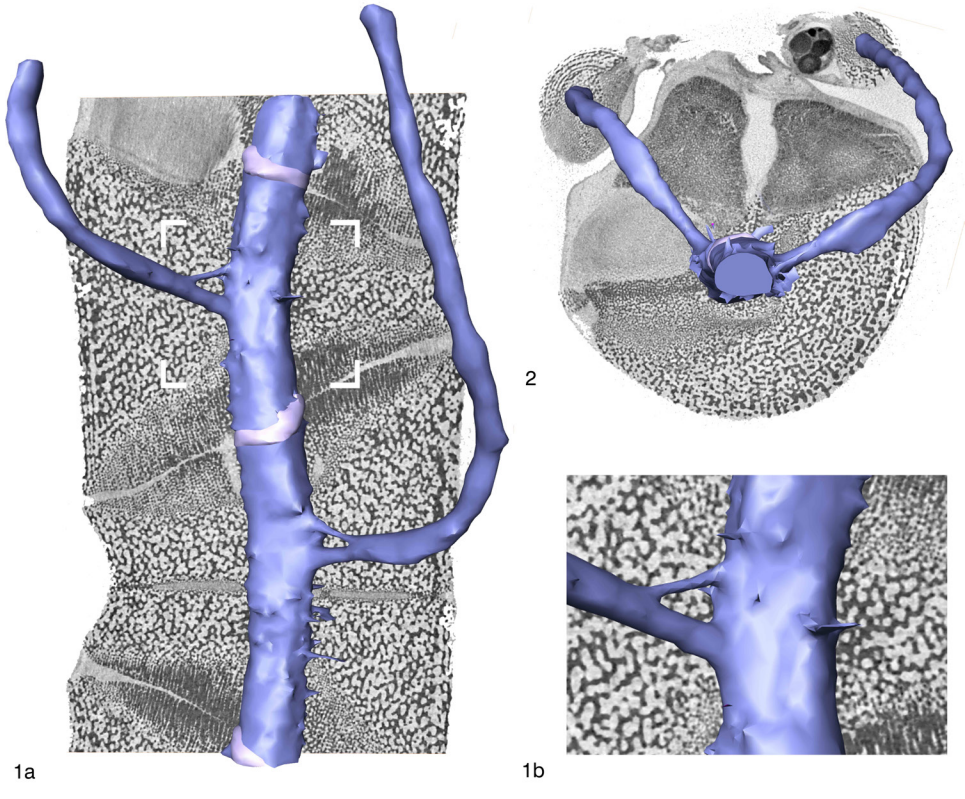

Fig. 77. *Antedon mediterranea* (Lamarck, 1816), 3D model and ortho slices of an arm nerve and two pinnular nerves from µCT data. *1a,* Oral view, ortho slice slightly aboral to the nerve, upward = distal; nerves in blue, inter-ossicular rings in pale pink show the sites where the nerve is not enclosed by ossicles. *1b,* Detail from *1a* showing a double origin of the pinnular nerve. 2, Distal view along arm axis, the most distal ortho slice showing the two target pinnules of the two pinnular nerves. The right pinnule contains an ovary with large dark eggs. Images new, by authors.

give the false impression of an interjoint swelling. The nerve is almost completely embedded in the brachials. Only in the space between brachials, a narrow, annular part of the nerve surface makes contact with the interosseous connective tissue (Fig. 77.1) and its ligamentous fibers. The arm nerves send branches in all directions, some of them probably terminating in the flexor muscles, others ascending to the hyponeural cords (Fig. 65.5); the thickest one (one per brachial) supplies the pinnules (Fig. 77.2). The organization of the pinnular nerves resembles that of the arm nerves.

VIII. INTEGUMENT

The filigree crinoid body is covered by an extensive integument consisting of a single-layered epithelium, the epidermis, and subepidermal connective tissue. The latter may be locally loose or dense, or even replenished with sclerites. There is no clear boundary between the integument and the general connective tissue of the body. Therefore, the integument is not comparable to the skin of vertebrates. Accordingly, it should not be called dermis (Holland, 1984).

In detail, the structure of the epithelium depends on the particular site, but it is generally comprised of three groups of cell types: squamous superficial and supporting cells, cilated cells, and secretory cells.

CELL TYPES

Squamous superficial and supporting cells

Most parts of the epidermis are comprised of these two cell types, both of which can

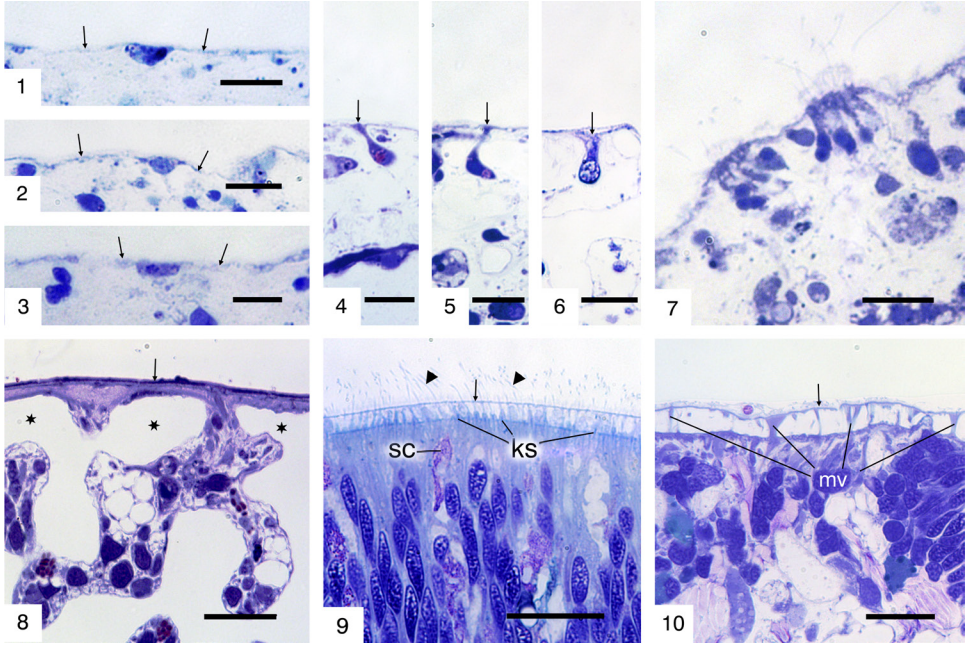

Fig. 78. Surface cells and cuticle. *1–7, Leptometra celtica* M'Andrew & Barrett, 1857; *1–3,* flat superficial cells, mainly the nucleus is visible with a prominent nucleolus, *arrows* point to the thin lateral extensions; *4–6,* supporting cells with stalk below the surface but still in contact (*arrows*) with the covering layer, *7,* Group of ciliated cells in the integument of the anal cone; scale bars *1–7,* 10 µm. *8–10, Neogymnocrinus richeri* (Bourseau, Améziane-Cominardi, & Roux, 1987). *8,* cuticle (*arrow*) covering the sclerites (*), with neither cells nor a space underneath the cuticle; *9,* cuticle (*arrow*) held up by the kinocilia (*arrowheads*) of a food groove epithelium, ks=kinetosomes, sc=secretory cell; *10,* cuticle (*arrow*) held up by large microvilli (mv) on the tegmen; Scale bars *8–10,* 20 µm. Staining: Toluidine blue. Image new, by authors.

be very small. It is known from electron microscopic studies (Holland, 1984; Heinzeller & Welsch, 1994) that intercellular contacts between these cells make the surface layer dense, thus providing a tight barrier between inside and outside.

The squamous superficial cells can be thought of as fried eggs, with the perinuclear compartment with its lenticular nucleus representing the yolk, and the peripheral, very flat extensions with unidentifiable cell boundaries represent the albumen (Fig. 78.1–78.3). The cell shape can change to cuboidal, for example, in the armpit between the arm and pinnule. By elongation or, conversely, compression, the superficial cells of mouth tentacles can achieve any shape between aquamous (squamous superficial cells), cuboidal, and cylindrical. Cells of such a shape resemble—or are identical to—typical supporting cells.

Typical supporting cells (Fig. 78.4–78.6) are iterspersed among the flat superficial cells and contribute to the covering layer by a compartment that can be compared to the flat umbrella of a mushroom. The stalk of the mushroom extends deeply into the connective tissue, where its deepest part broadens into a tuberous foot containing a round nucleus.

The epidermis is covered by a cell-free cuticle, presumably produced by all epithelial cells. This consists of a fine filamentous felt; its thickness and presumably also chemical composition may vary among species. In some places, the cuticle appears to lie immediately above the connective tissue or sclerites, with no epithelial layer visible (Fig. 78.8). Elsewhere, the cuticle appears to hover several micrometers above the epithelium, and the space beneath the cuticle is stabilized by kinocilia and/or unusually large microvilli (Fig. 78.9–78.10).

Ciliated cells

The majority of the cells of the food groove epithelium are ciliated (see Section V) (Fig. 45; Fig. 78.9). The same is true for the cells in the outer part of the madreporic canals (Fig. 8.3–8.4). Elsewhere, ciliated cells are present on all parts of the body, either individually or in groups. Groups may simply consist of loose aggregations of a few cells, as in the numerous clusters in the integument of the anal cone of a young *Leptometra celtica* (Fig. 78.7). Other groups of ciliated cells are firmly integrated into the special organization of sensory papillae that decorate the tentacles (see Section V). In these papillae, the cells of the inner and outer circles are ciliated.Each ciliated cell bears a single, long kinocilium that extends well beyond the cuticle. Of course, the cilia in the feeding groove and madreporic canals serve for transport. For the other ciliated cells, a sensory function is most likely, but it is still not known whether a particular cell responds to either mechanical or chemical stimuli, to both types of stimuli, or even to completely different ones. Thus, from a morphological point of view, the non-transporting ciliated cells appear to be a unitary group; from a physiological point of view, they probably are not.

Secretory cells

The crinoid mode of feeding requires the secretion of mucus in and lateral to the food groove. Corresponding mucous cells are present in the food groove epithelium among the ciliated transporting cells (Fig. 79.1). Additional mucous cells are accumulated in epithelial depressions at the edge of the food groove (Fig. 79.2b). At the tip of the sensory papillae, the cells of the outer circle release a secretion that is thought to be adhesive (Flammang & Jangoux, 1992) (Fig. 79.3c).

During development, the first secretory structure formed by the doliolaria larva for attachment to the substrate is the adhesive pit and then its transformed structure, the attachment disk. Both structures have been studied in detail by Jangoux and Lahaye (1990). In addition to the pure sensory cells, there are mucous cells, predominantly located in the adhesive pit, and cells that produce a proteinaceous product, predominantly located in the attachment disk. The product of the latter cements the larva to the substrate, even after the glandular cells themselves have disappeared (Chia & others, 1986). In mature female individuals of some species, glands with an adhesive secretion attach spawned ova to the mother's surface for early larval life (Fig. 79.7, Fig. 62).

In adults, a variety of secretory cells are present in the integument (Fig. 79.4, Fig. 79.8). Mucus cells can be identified—to some degree—by the size/shape of the granules or by staining reactions (PAS, Alcian blue, metachromasia with Toluidine blue). Unfortunately, in histological preparations, the characteristic water binding capacity of mucus causes the granules to swell and lighten—depending on the fixation method, causing morphological artifacts.

An overwhelming number of substances of importance and use as pigments or for cytotoxicity and antifish activity (Feng, Khokhar, & Davis, 2017) have been isolated from complete crinoids. It is likely, but not yet proven, that some of these substances are released by secretory cells of the integument, such as the black mucus spread on the surface of *Comatella nigra* P. H. Carpenter 1888 (Fig. 79.6). With some certainty, some secretory products can be described as mucous based on their histological properties; all non-mucous products are tentatively summarized as proteinaceous. This is most likely incorrect in a chemical sense and requires further investigations with more specific techniques.

SACCULI

Sacculi were discovered by W. B. Carpenter (1876) in *Antedon rosaceus* (now A. *bifida bifida*) and studied in detail by Reichensperger (1912). Despite a number of subsequent studies by several authors, they still remain enigmatic structures. Sacculi are conspicuous, spherical structures of most feather stars and some isocrinids, whereas they are completely absent in cyrtocrinids.

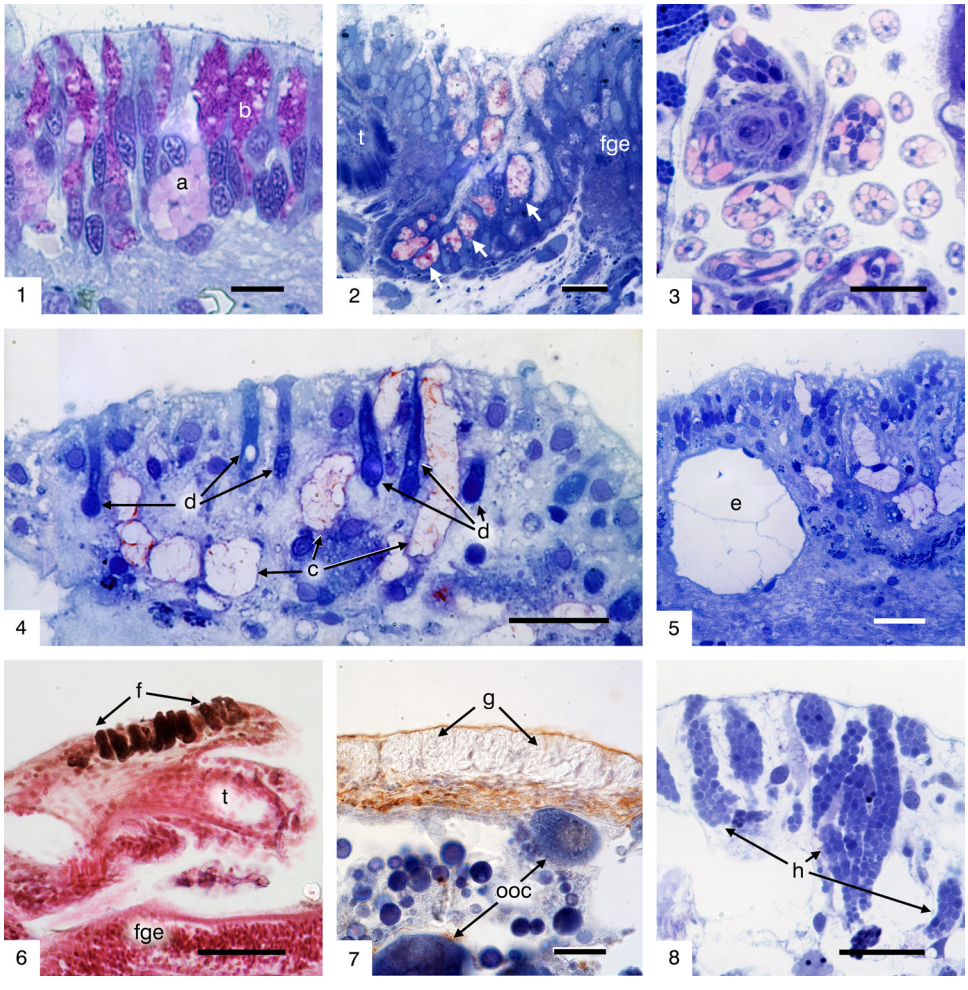

Fig. 79. Secretory cells. *1, Neogymnocrinus richeri* (Bourseau, Améziane-Cominardi, & Roux, 1987), solitary mucus secreting cells at the edge of the food groove, two types (a, b) differing in granule size and metachromatic behavior, scale bar 10 µm. *2, Leptometra celtica* M'Andrew & Barrett, 1857, aggregation of mucous cells (arrows) in a pit at the base of a tentacle (t); fge=food groove epithelium, scale bar 10 µm. *3, Neogymnocrinus richeri,* papillae in cross section with pink staining secretion in cells of the outer circle, scale bar 10 µm. *4, Comatella nigra* P. H. Carpenter, 1888, tall tegmenal epithelium with different types of secretory cells, one of which (c) releases a mucoid product and another (d) a possibly proteinaceous product, scale bar 20 µm. *5, Comatella nigra*, large gland-like cell aggregate (e), here addressed as atypical sacculus, scale bar 20 µm. *6–8,* Secretory cells in the integument of pinnules. *6, Comatella nigra*, cells with a black pigmented secretion (f), t=tentacle, fge=food groove epithelium, scale bar 50 µm. *7, Antedon mediterranea* (Lamarck, 1816), cells of the cement gland (g), oral/lateral of an ovary, ooc=oocytes, scale bar 20 µm. *8, Cyathidium plantei* Heinzeller & others, 1996, cells with conspicuous spherical granules of unknown significance (h), scale bar 20 µm. Staining: Azocarmin in *6*, Hemalum in *7*, and Toluidin blue in all others. Images new, by authors.

Sacculi are positioned in rows on both sides of pinnules and arms (Fig. 80.1) and also on the tegmen.

Typical structure

The composition of sacculi resembles that of a holocrine gland, although they are thought to arise from mesodermal or even coelothelial cells rather than epithelial cells (Nocart, 1993). As far as can be deduced from the various histological appearances, the formation, maturation, and disintegration of sacculi in *Antedon* may proceed as follows.

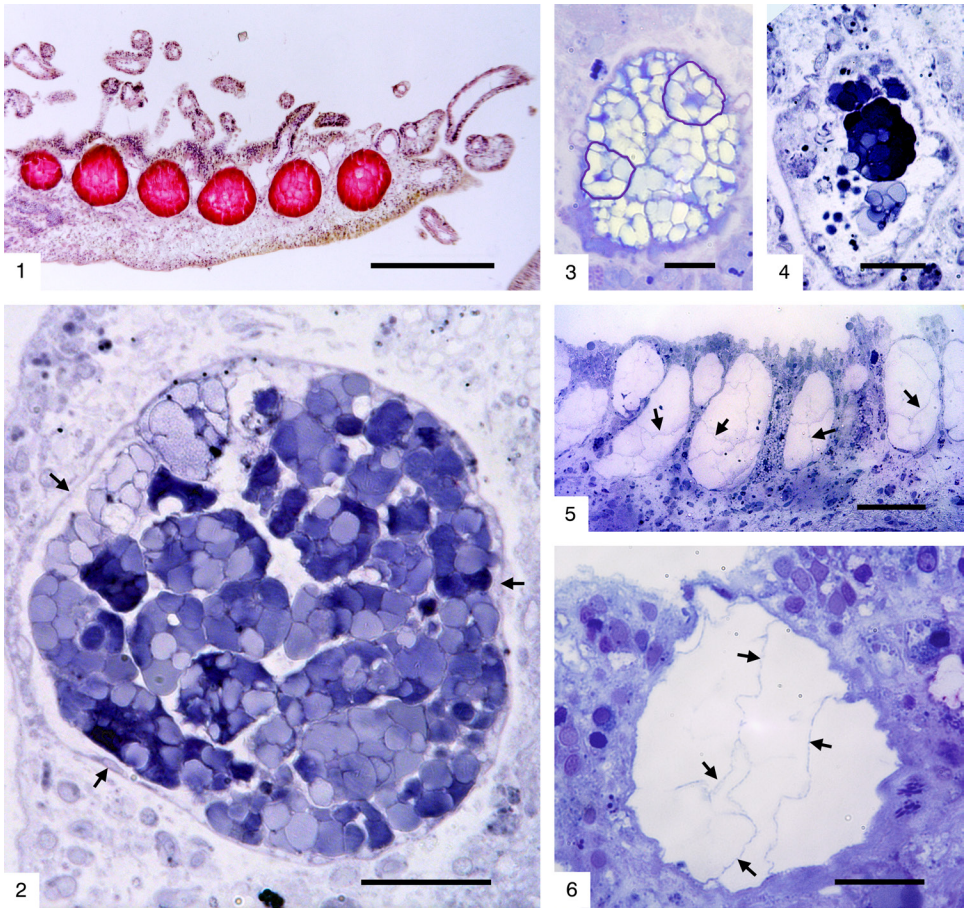

Fig. 80. Sacculi. *1, Tropiometra afra* (Hartlaub, 1890), longitudinal section, of a pinnule, slightly lateral, showing the dense row of sacculi (stained *red*), scale bar 200 µm. *2, Antedon petasus* (Düben & Koren, 1846), sacculus showing cells in different stages of transformation, reflected in the different intensity of staining. *Arrows* point to the thin epitheloid cover, scale bar 200 µm. *3, Antedon petasus*, sacculus with about ten cells enlarged but still visibly separable, two of them artificially framed, scale bar 10 µm. *4, Antedon petasus,* sacculus after incomplete depletion, scale bar 20 µm. *5, Clarkcomanthus luteofuscum* H. L. Clark, 1915, row of atypical sacculi in the tegmen, scale bar 50 µm. *6, Comatella nigra* P. H. Carpenter, 1888, atypical sacculus, probably ready for depletion. The atypical sacculi in *5* and *6* appear to be filled with a translucent material, except for some very fine membranes (*arrows*) that can be interpreted as remnants of the former cell boundaries or intercellular material, scale bar 20 µm. Staining: *1,* Hemalum-Eosin; *2–6*, Toluidin blue. Images new, by authors.

Sacculi arise in the form of spherical cell clusters in the connective tissue (Fig. 80.3) that initially grow by proliferation. Subsequently, cell differentiation proceeds in two ways. The principal cells swell by accumulating a proteinaceous material in inclusion bodies. These grow to several µm in diameter, and some acquire prismatic outlines.

The accumulating material apparently undergoes a maturation process that alters its staining capacities (Fig. 80.2). The final granular inclusions exhibit high light refraction (Holland, 1967). The cell organelles, including the nucleus, are degraded in parallel with the maturation of the globules. The second cell type encases the cluster of granulated cells with an epitheloid envelope (Fig. 80.2) resembling a very flat coelothelium. Sacculi can break through the overlying tissue and empty their package

of granulated cells (Fig. 80.4); however, the initiating stimulus is still unknown.

Atypical sacculi

Several feather stars have structures that are very similar to, but not identical to, sacculi. In *Clarkcomanthus luteofuscum* H. L. Clark, 1915, for example, such atypical sacculi are in aggregations in the tegmen epithelium (Fig. 80.5*)*. The tegmen of *Comatella nigra* is also rich in similar sacculus-like structures (Fig. 79.5–79.6.), which apparently open at the body surface to release their contents (Fig. 80.6). Whereas in a typical sacculus the original composition of individual cells or inclusion bodies can be recognized even in the extrusion-ready state, this is hardly possible in atypical sacculi (Fig. 80.5–80.6). The material of the granules has a finely punctate texture in both typical and atypical sacculi, but this texture is much more pronounced in typical sacculi.

Function

The fact that there are several groups of crinoids without any sacculi complicates the formulation of a general function hypothesis. It is obviously not vital to have sacculi. But it seems too costly to have sacculi if they are not functional. The most popular interpretation, among many others, is an excretory function, as suggested by the earliest researchers (e.g., Ludwig, 1877). Because there are no physiological results available as yet, the statement of Hyman (1955, p. 50) is still valid: "The function of these sacculi is obscure." One might add "and probably manifold." A recent observation expands the range of possible functions. Bioluminescence has been noted in some abyssal crinoid species. In one species of the family *Thalassometridae*, this ability was attributed to sacculi. These observations suggest that sacculi might represent the luminescent organ "in at least some crinoids" (Martinez Soares, 2020, personal communication from Jerome Mallefet).

REFERENCES

Agassiz, Alexander. 1890. Notice of Calamocrinus diomedae, a new stalked crinoid from the Galapagos, dredged by the U.S. Fish Commission Steamer "Albatross." Bulletin of the Museum of Comparative Zoology, Harvard 20(6):165–167.

Améziane-Cominardi, Nadia, J-P. Bourseau, Renaud Avocat, & Michel Roux. 1990. Les Crinoïdes pedonculés de Nouvelle-Calédonie: inventaire et réflexions sur les taxons archaïques. *In* C. de Ridder, P. Dubois, M-C. Lahaye, Michel Jangoux, eds., Echinoderm Research, Proceedings of the Second European Conference on Echinoderms, Brussels, Belgium, September 1989. Balkema. Rotterdam. p. 117–124, 1 pl.

Andersson, K. A. 1904. Brutpflege bei *Antedon hirsuta* Carpenter. Wissenschaftliche Ergebnisse der schwedischen Südpolar Expedition Südpolar-Expedition 1901–1903 1:1–7.

Bals, Robert, Thomas Heinzeller, Ulrich Welsch, Gerd Rehkämper, & J. L. S. Cobb. 1990. Morphological observations on the axial organ of *Antedon bifida*. *In* C. de Ridder, P. Dubois, M-C. Lahaye, Michel Jangoux, eds., Echinoderm Research, Balkema. Rotterdam. p. 197–202.

Balser, E. J., & E. E. Ruppert. 1993. Ultrastructure of Axial Vascular and Coelomic Organs in Comasterid Featherstars (Echinodermata: Crinoidea), Acta Zoologica 74(2):87–101.

Barbaglio, Alice, Claudia Turchi, Giulio Melone, C. Di Benedetto, Tiziana Martinello, Maira Patruno, Marco Biggiogero, I. C. Wilkie, & M. D. Candia Carnevali. 2012. Larval development in the feather star *Antedon mediterranea*. Invertebrate Reproduction & Development 56(2):124–137.

Baumiller, T. K., & G. A. Janevski. 2011. On the swimming function of crinoid cirri. Swiss Journal of Palaeontoloy 130:19–24.

Bell, F. J. 1908. National Antarctic Expedition 1901-04. Echinoderma. Natural History, Zoology 4:1–16, 5 pl.

Bickell, L. R., F.-S. Chia, & B. J. Crawford. 1980. A fine structural study of the testicular wall and spermatogenesis in the crinoid *Florometra serratissima* (Echinodermata). Journal of Morphology166:109–126.

Birenheide, Rüdiger, & Tatsuo Motokawa.1995. Motility and stiffness of cirri of the stalked crinoid *Metacrinus rotundus*. *In* Emson, Smith, & Campbell, eds., Echinoderm research 1995. Balkema. Rotterdam. p. 91–94.

Birenheide, Rüdiger, Koji Yokoyama, & Tatsuo Motokawa 2000. Cirri of the stalked crinoid *Metacrinus rotundus:* neural elements and the effect of cholinergic agonists on mechanical properties. Proceedings of the Royal Society of London B 267:7–16.

Bohn, J. M., & Thomas Heinzeller. 1999. Morphology of the bourgeticrinid and isocrinid aboral nervous system and its possible phylogenetic implications (Echinodermata, Crinoidea) Acta Zoologica 80:241–249.

Bourseau, J-P., Nadia Améziane-Cominardi, & Michel Roux. 1987. Un crinoïde pédonculé nouveau (Echinodermes), représentant actuel de la famille jurassique des Hemicrinidae: Gymnocrinus richeri

nov. sp. des fonds bathyaux de Nouvelle-Calédonie (S.W. Pacifique). Comptes Rendus de l' Académie des Sciences Paris (série 3) 305:595–599, 1 pl.

Breimer, Albert. 1978. Recent crinoids. *In* R. C. Moore & Curt Teichert, eds., Treatise on Invertebrate Paleontology, Part 1, Echinodermata 2, volume 1. The Geological Society of America, Inc. & The University of Kansas Press. Boulder & Lawrence. p. 9–58.

Bury, H. 1888. The early stages in the development of *Antedon rosacea*. Philosophical Transactions of the Royal Society B 179:257–301.

Byrne, Maria, & A. R. Fontaine 1981. The feeding behavior of *Florometra serratissima* (Echinodermata: Crinoidea). Canadian Journal of Zoology 59(1):11–18.

Byrne, Maria, & A. R. Fontaine 1983. Morphology and function of the tube feet of *Florometra serratissima* (Echinodermata: Crinoidea). Zoomorphology 102(3):175–187.

Carpenter, P. H. 1879. Preliminary report upon the Comatulae of the Challenger Expedition. Proceedings of the Royal Society of London 28:383–395.

Carpenter, P. H. 1881a. On the genus Solanocrinus, Goldfuss, and its relations to recent Comatulae. Journal of the Linnean Society of London (Zoology) 15:187–217, pl. 9–12.

Carpenter, P. H. 1881b. Note 35. The Comatulae of the Leyden Museum. Notes from the Leyden Museum 3:173–217.

Carpenter, P. H. 1884. Report on the Crinoidea collected during the voyage of H.M.S. Challenger, during the years 1873–1876. Part I. The Stalked Crinoids. Report on the Scientific Results of the Voyage of H.M.S. Challenger during the years 1873–76. Zoology. 11 (part 32):i–xii, 1–442, pl. 1–62.

Carpenter, P. H. 1888. Report on the Crinoidea collected during the voyage of H.M.S. Challenger, during the years 1873-76. Part II. The Comatulae. Reports of the Scientific Results of the Voyage of H.M.S. Challenger, Zoology. 26 (part 60):i–x, 1–402, pl. 1–70.

Carpenter, P. H., & L. Von Graff. 1885. XVII. On three new Species of Metacrinus. Transactions of the Linnean Society of London (Series 2) Zoology 2(14):435–446

Carpenter, W. B. 1876. On the structure, physiology, and development of *Antedon* (Comatula, Lamk.) *rosaceus*. Proceedings of the Royal Society of London B 24:211–231 +plates viii–ix.

Cherbonnier, Gustave, & Alain Guille. 1972. Sur une nouvelle espèce de Crinoïde Crétacique de la famille Holopodidae: *Cyathidium foresti* nov. sp. Comptes rendus de l'Academie de Sciences, Paris C 274:2193–2196.

Chadwick, H. C. 1907. Antedon. Proceedings and Transactions of the Liverpool Biological Society 21:371–417.

Chia, F. S., R. D. Burke, Ron Koss, P. V. Mladenov, & S. S. Rumrill. 1986. Fine structure of the doliolaria larva of the feather star *Florometra serratissima* (Echinodermata: Crinoidea), with special emphasis on the nervous system. Journal of Morphology 189:99–120.

Chia, F.-S., & Ron Koss. 1994. Asteroidea. *In* Microscopic Anatomy of Invertebrates, F. W. Harrison, ed., Wiley-Liss. New York 14:169–245.

Clark, A. H. 1907. New genera of recent free crinoids. Smithsonian Miscellaneous Collection 50(29):343–364.

Clark, A. H. 1908a. Preliminary notice of a collection of recent crinoids from the Philippine Islands. Smithsonian Miscellaneous Collection, Quarterly Issue 52(2):199–234.

Clark, A. H. 1908b. New genera of unstalked crinoids. Proceedings of the Biological Society of Washington 21:125–136.

Clark, A. H. 1909a. The type of the genus Comaster. Proceedings of the Biological Society of Washington 22:87–90.

Clark, A. H. 1909b. Revision of the crinoid family Comasteridae, with descriptions of new genera and species. Proceedings of the U.S. National Museum 36(1685):493–507.

Clark, A. H. 1909c. Four new species of the crinoid genus Rhizocrinus. Proceedings of the U.S. National Museum 36(1693):673–676.

Clark, A. H. 1917. A revision of the crinoid family Antedonidae, with the diagnoses of nine new genera. Journal of the Washington Academy of Science 7(5):127–131.

Clark, A. H. 1921. A monograph of the existing crinoids, Vol. 1. The comatulids, Part 2. Bulletin of the United States Natural Museum 82:1–771.

Clark, A. H. 1923. A revision of the recent representatives of the crinoid family Pentacrinidae, with the diagnoses of two new genera. Journal of the Washington Academy of Sciences 13:8–12.

Clark, H. L. 1915. The comatulids of Torres Strait: with special reference to their habits and reactions. Papers from the Department of Marine Biology, Carnegie Institue of Washington 8:67–125.

Cuénot, Lucien. 1948. Anatomie, ethology et systeématique des Échinodermes. *In* P. P. Grassé, ed., Traité de Zoologie, 11. Masson. Paris. p. 3–363.

Dan, Katsuma, & J. C. Dan. 1941. Spawning habit of the crinoid, *Comanthus japonicus*. Japanese Journal of Zoology 9:565–574.

Díaz-Balzac, C. A., & J. E. García-Arrarás. 2018. Echinoderm Nervous System [doi.org/10.1093/acrefore/9780190264086.013.205].

Döderlein, Ludwig. 1907. Die gestielten Crinoiden der Siboga-Expedition. Siboga Expeditie: Uitkomsten op zoologisch, botanisch, oceanographisch en geologisch Gebied, verzameld in Nederlandsch Oost-lndie 1899–1900, vol. 42a. Brill. Leiden. p. 1–54, fig. 1–12, pl. 1–23.

Düben, von, M. W., & J. Koren. 1846. Ichthyologiska Bidrage. Kongliga Svenska Vetenskaps-Akademiens Handlingar for 1844. p. 27–120, pl. 2–3.

Eléaume, Marc, Hans Hess, & C. G. Messing 2011. Nomenclatorial Note (concerning *Anthometrina,* new name for the genus *Anthometra*). *In* Paul Selden, ed., Treatise on Invertebrate Paleontology, Part T, Echinodermata 2 Revised, Crinoidea, vol 3. University of Kansas Press. Lawrence. p. 224.

Engle, Sabine. 2013. Ultrastructure and development of the body cavities in *Antedon bifida* (Pennant, 1777)

(Comatulida, Crinoida). Dissertation, Freie Universität Berlin. 174 p. [https://refubium.fu-berlin.de/handle/fub188/4024?locale-attribute=en].

Ezhova, O. V., & V. V. Malakhov. 2020. Axial complex of Crinoidea: Comparison with other Ambulacraria. Journal of Morphology 281:1456–1475.

Farmanfarmaian, A. V. 1969. Intestinal absorption and transport in Thyone. 1. Biological aspects. Biology Bulletin137(1):118–131.

Fedotov, D. 1930. Über die vergleichende Morphologie der Crinoiden. Zoologischer Anzeiger 89:303–309.

Feng, Y., S. Khokhar, & R.-A. Davis. 2017. Crinoids: ancient organisms, modern chemistry. Natural Product Reports 2017 34:571–584.

Feral, J. P., & C. Massin. 1982. Digestive systems: Holothuroidea. *In* Michel Jangoux & J. M. Lawrence, eds., Echinoderm Nutrition. Balkema. Rotterdam. p. 191–212.

Flammang, Partrick, & Michel Jangoux. 1992. The sensory-secretory structures of the podia of the comatulid *Antedon bifida* (Echinodermata). *In* L. Scalera-Liaci & C. Canicatti, eds., Echinoderm Research 1991. Balkema. Rotterdam. p. 59–65.

Fréminville (de la Poix de Fréminville), C. P. 1811. Mémoire sur un nouveau genre de Zoophytes de l'ordre des Radiaires. Nouveau Bulletin des Sciences / par la Société Philomathique Paris 2:349–350.

Gervais, F. L. P. 1835. Encrine. *In* M. F.-E. Guérin, Dictionnaire pittoresque d'histoire naturelle et des phénomènes de la nature. Paris, Au Bureau de Souscription 3:49–50, pl. 147.

Goyette, D. E. 1967. Light and electron microscope study of the aboral nervous system and neurosecretion in the crinoid *Florometra serratissima*. Master's Thesis, University of Alberta, Edmonton, Canada. 89 p., 31 pl. Database: University of Alberta Library.

Grimmer, J. C., & N. D. Holland. 1979. Haemal and coelomic circulatory systems in the arms and pinnules of (Echinodermata: Crinoidea). Zoomorphology 94(1):93-109.

Grimmer, J. C., & N. D. Holland. 1990. The Structure of a Sessile, Stalkless Crinoid (*Holopus rangii*). Acta Zoologica 71(2):61–67.

Grimmer, J. C., N. D. Holland, & I. Hayami. 1985. Fine structure of the stalk of an isocrinid sea lily (*Metacrinus rotundus*) (Echinodermata, Crinoidea). Zoomorphology 105:39–50.

Grimmer, J. C., N. D. Holland, & H. Kubota. 1984. The fine structure of the stalk of the pentacrinoid larva of a feather star *Comanthus japonica* (Echinodermata: Crinoidea). Acta Zoologica 65:41–58.

Grimmer, J. C., N. D. Holland, & C. G. Messing. 1984. Fine structure of the stalk of the bourgueticrinid sea lily *Democrinus conifer* (Echinodermata: Crinoidea). Marine Biology 81:163–176.

Haig, J. A., & G. W. Rouse 2008. Larval development of the feather star *Aporometra wilsoni* (Echinodermata: Crinoidea). Invertebrate Biology 127(4):460–469.

Hamann, Otto. 1889. Anatomie der Ophiuren und Crinoiden. Verlag von Gustav Fischer. Jena. p. 61–132, 12 pl.

Hartlaub, Clemens. 1890. Beitrag zur Kenntnis der Comatuliden-Fauna des indischen Archipels. Nachrichten von der Königlichen Gesellschaft der Wissenschaften und der Georgs-August-Universität zu Göttingen 5:168–187.

Heinzeller, Thomas. 1998. The nervous system of crinoids: survey and taxonomic implications. *In* R. Mooi & M. Telford, eds., Echinoderms. Balkema. Rotterdam/Brookfield. p. 169–174.

Heinzeller, Thomas, Nadia Ameziane-Cominardi, & Ulrich Welsch. 1994. Light and electron microscopic studies on arms and pinnules of the cyrtocrinid *Gymnocrinus richeri*. *In* B. David & others, eds., Echinoderms through Time. Balkema. Rotterdam. p. 211–216.

Heinzeller, Thomas, & Hubert Fechter. 1995. Microscopical anatomy of the cyrtocrinid *Cyathidium meteorensis* (sive foresti) (Echinodermata, Crinoidea). Acta Zoologica 76.1:25–34.

Heinzeller, Thomas, Hans Fricke, J.-P. Bourseau, Nadia Améziane-Cominardi, & Ulrich Welsch. 1996. *Cyathidium plantei* sp. n., an extant Cyrtocrinid (Echinodermata, Crinoidea): Morphologically identical to the fossil *Cyathidium depressum* (Cretaceous, Cenomanian). Zoologica Scripta 25:77–84.

Heinzeller, Thomas, & Ulrich Welsch. 1994. Crinoidea. *In* F. W. Harrison, ed., Microscopic Anatomy of Invertebrates. Wiley-Liss. New York 14:9–148.

Heinzeller, Thomas, Ulrich Welsch, & Nadia Améziane .2010. Organs of the axial complex in crinoids: Structure and occurrence. Proceedings of the 12th International Echinoderm Conference. Francis & Taylor (Balkema). Leiden. p.199–206.

Hess, Hans. 2006. Crinoids from the Lower Jurassic (Pliensbachian) of Arzo, southern Switzerland. Schweizerische paläontologische Abhandlungen 126:143 p., 29 fig., 29 pl.

Hess, Hans, C. G. Messing, & W. I. Ausich. 2011. Comatulida. *In* Treatise on Invertebrate Paleontology, Part T, Echinodermata 2 Revised, Crinoidea, vol. 3. University of Kansas Press. Lawrence. p. 70–146.

Hoggett, A. K., & F. W. E. Rowe. 1986. A reappraisal of the family Comasteridae A. H. Clark, 1908 (Echinodermata: Crinoidea), with the description of a new subfamily and a new genus. Zoological Journal of the Linnean Society 88:103–142.

Holland, N. D. 1967. Some observations on the saccules of *Antedon mediterranea* (Echinodermata, Crinoidea). Pubblicazione Stazione Zoologica di Napoli 35:257–262.

Holland, N. D. 1968. The histochemistry and site of synthesis of the globules in the chambered organ of *Antedon mediterranea* (Echinodermata, Crinoidea). Pubblicazione Stazione Zoologica di Napoli 56:264–266.

Holland, N. D. 1969. An electron microscope study of the papillae of crinoid tube feet. Pubblicazione Stazione Zoologica di Napoli 37:575–580.

Holland, N. D. 1970. The fine structure of the axial organ of the feather star *Nemaster rubiginosa* (Echinodermata: Crinoidea). Tissue Cell 2:625–636

Holland, N. D. 1984. Echinodermata: epidermal cells. *In* J. Bereiter-Hahn, A.G. Matoltsy, & K. Sylvia Richards, eds., Biology of the Integument. 1. Invertebrates. Springer. Berlin. p. 756–774.

Holland, N. D. 1988. Fine structure of oocyte maturation in a crinoid echinoderm, *Oxycomanthus japonicus:* a time-lapse study by serial biopsy. Journal of Morphology 198:205–217.

Holland, N. D. 1991. Echinodermata: Crinoidea. *In* A. C. Giese, J. S. Pearse, & V. B. Pearse, eds., Reproduction of marine invertebrates, vol VI, Echinoderms and Lophophorates. Boxwood. Pacific Groove. p. 247–299.

Holland, N. D., & Katsuma Dan. 1975. Ovulation in an echinoderm (*Comanthus japonica*). Experientia 31:1078–1079.

Holland N. D., J. C. Grimmer, & Katherine Wiegmann. 1991. The structure of the sea lily *Calamocrinus diomedeae*, with special reference to the articulations, skeletal microstructure, symbiotic bacteria, axial organs, and stalk tissues (Crinoidea, Millericrinida). Zoomorphology 110:115–132.

Holland, N. D., A. B. Leonhard, & J. R. Strickler. 1987. Upstream and downstream capture during suspension feeding by *Oligometra serripinna* (Echinodermata: Crinoidea) under surge conditions. Biological Bulletin 173:552–556.

Holland, N. D., J. R. Strickler, & A. B. Leonard. 1986. Particle interception, transport and rejection by the feather star *Oligometra serripinna* (Echinodermata: Crinoidea), studied by frame analysis of videotapes. Marine Biology 93:111–126.

Hyman, L. H. 1955. The Invertebrates, vol. 4: Echinodermata. The Coelomate Bilateria. McGraw-Hill. New York. 763 p.

Jangoux, Michel, & M. C. Lahaye. 1990. The attachment complex of the doliolaria larvae of *Antedon bifida* (Echinodermata, Crinoidea). *In* Ch. de Ridder, P. Dubois, M. C. Lahaye, & Michel Jangoux, eds., Echinoderm Research. Balkema. Rotterdam. p. 99–105.

John, D. D. 1939. Crinoidea. British Australia New Zealand (B.A.N.Z.) Antarctic Research Expedition (1929-1931), Zoology and Botany Series B 4(6):1–24.

Kalacheva, N. V., M. G. Eliseikina, L. T. Frolova, & I. Y. Dolmatov. 2017. Regeneration of the digestive system in the crinoid *Himerometra robustipinna* occurs by transdifferentiation of neurosecretory-like cells. Plos One, https://doi.org/10.1371/journal.pone.0182001.

LaHaye, C. A., & N. D. Holland. 1984.Electron microscopic studies of the digestive tract and absorption from the gut lumen of a feather star, *Oligometra serripinna* (Echinodermata), Zoomorphology 104:252–259.

Lahaye, M. C., & Michel Jangoux. 1985a. Functional morphology of the podia and ambulacral grooves of the comatulid crinoid *Antedon bifida* (Echinodermata). Marine Biology 86:307–318

Lahaye, M. C., & Michel Jangoux. 1985b. Post-spawning behaviour and early development of the comatulid crinoid, *Antedon bifida*. Keegan Galway & O'Connor, eds., Echinodermata. Taylor & Francis. London. p. 181–184.

Lamarck, J.-B. M. de 1816. Histoire naturelle des animaux sans vertèbres. Tome second. Paris: Verdière. 568 p.

Linnaeus, Carl. 1758. Systema Naturae per regna tria naturae, secundum classes, ordines, genera, species, cum characteribus, differentiis, synonymis, locis. Editio decima, reformata [10th revised edition] 1:824 p.

Ludwig, Hubert. 1877. Beiträge zur Anatomie der Crinoideen. Zeitschrift für Wissenschaftliche Zoologie 28:255–353 +pl. xii–xix.

M'Andrew, R., & L. Barrett. 1857. List of the Echinodermata dredged between Drontheim and the North Cape. Annals and Magazine of Natural History (2)20:43–46.

Macurda, D. B., Jr., & D. L. Meyer. 1974. Feeding posture of modern stalked crinoids. Nature 247 (5440):394–396.

Macurda, D. B., & D. L. Meyer. 1983. Sea Lilies and Feather Stars: Observations of living crinoids have enriched our ideas about the ecology and behavior of this ancient class of marine invertebrates. American Scientist Vol. 71 4:354–365.

Mashanov, V., O. Zueva, T. Rubilar, L. Epherra, & J. E. García-Arrarás. 2016. Echinodermata. *In* Structure and Evolution of Invertebrate Nervous Systems, A. Schmidt-Rhaesa et al., eds., Oxford University Press. Oxford. p. 665–686.

McClintock, J. B., & J. S. Pearse. 1987. Reproductive biology of the common Antarctic crinoid *Promachocrinus kerguelensis* (Echinodermata: Crinoidea). Marine Biology 96:375–383.

McKenzie, J. D. 1992. Comparative morphology of crinoid tube feet. *In* L. Scalera-Liaci & C. Canicatti, eds., Echinoderm Research. Balkema. Rotterdam. p. 73–79.

Messing, C. G. 1984. Brooding and paedomorphosis in the deep-water feather star *Comatilia iridometriformis* (Echinodermata: Crinoidea). Marine Biology 80:83–91.

Messing, C. G. 2023. World List of Crinoidea. Crinozoa. Accessed through: World Register of Marine Species at: https://www.marinespecies.org/aphia.php?p=taxdetails&id=147423.

Messing, C. G., W. I. Ausich, & D. L. Meyer. 2021. Feeding and Arm Postures in Living and Fossil Crinoids. Treatise on Invertebrate Paleontology, Part T, Revised, Volume 1, Chapter 16. p.1–47.

Meyer, D. L. 1979. Length and spacing of the tube feet in crinoids (Echinodermata) and their role in suspension-feeding. Marine Biology 51:361–369.

Meyer, D. L. 1982. Food and feeding mechanisms: Crinozoa. *In* Michel Jangoux & J. M. Lawrence, eds., Echinoderm Nutrition. Balkema. Rotterdam. p. 25–42.

Mladenow, P. V. 1986. Reproductive biology of the feather star *Florometra serratissima*: gonadal structure, breeding pattern and the periodicity of ovulation. Canadian Journal of Zoology 64:1642–1651.

Mortensen, Tatsuo. 1917. *Notocrinus virilis* n. g., n. sp. a new viviparous crinoid from the Antarctic Sea. Vidensk. Videnskabelige Meddelelser fra Dansk naturhistorisk Forening i Kjøbenhavn 68:205–208.

Mortensen, Tatsuo. 1920. Studies in the development of Crinoids. Papers from the Tortugas Laboratory (Carnegie Institution) 16:1–94.

Motokawa, Tatsuo. 2019. Skin of sea cucumbers: the

smart connective tissue that alters mechanical properties in response to external stimuli. Journal of Aero Aqua Biomechanisms 8(1):2–5.

Nakano, H., T. Hibino, Y. Hara, T. Oji, & S. Amemiya. 2004. Regrowth of the stalk of the sea lily, *Metacrinus rotundus* (Echinodermata: Crinoidea). The Journal of Experimental Zoology Part A: Comparative Experimental Biology 301A:464–471.

Nakano, H., Y. Nakajima, & S. Amemiya. 2009. Nervous system development of two crinoid species, the sea lily *Metacrinus rotundus* and the feather star *Oxycomanthus japonicus.* Development Genes and Evoution 219:565–576.

Nichols, David. 1967. Echinoderms. 3rd edition. Hutchinson and Co., Ltd. London. 200 p.

Nocart, C. 1993. Etude morphologique des saccules chez la comatule *Antedon bifida* (Pennant) (Echinodermata, Crinoidea). Mémoire présenté pour l'obtention du grade de licenciée en Sciences Zoologiques, Université libre Brussels, Belgium.

d'Orbigny, A. D. 1837. Mémoire sur une seconde espèce vivante de la familie des Crinoïdes ou Encrines, servant de type au nouveau genre Holope (*Holopus*). Magasin de Zoologie (7ème année) 10:1–8, pl. 3.

Pennant, Thomas. 1777. British Zoology, vol. IV. Crustacea. Mollusca. Testacea. London. p. i–viii, 1–154, pl. 1–93.

Perrier, Edmond. 1873. Recherches sur l'anatomie et la regeneration des bras de la *Comatula rosacea* (*Antedon rosaceus* Linck). Archives de zoologie expérimentale et générale 2:29–86.

Perrier, Edmond. 1883. Sur un nouveau Crinoïde fixé, le Democrinus Parfaiti, provenant des dragages du Travailleur. Comptes Rendus Académie des Sciences Paris 96:450–452.

Perrier, Edmond. 1886. Mémoire sur l'organisation et le développement de la comatule de la mediterrané (*Antedon rosacea*, Linck). G. Masson. Paris. p. 1–300, pl. I–X.

Pertossi, R. M.,·M. I. Brogger, P. E. Penchaszadeh, & M. I. Martinez. 2019. Reproduction and developmental stages in the crinoid *Isometra vivipara* Mortensen, 1917 from the southwestern Atlantic. Polar Biology 42:807–816.

Pourtalès, Louis F., de. 1869. List of the crinoids obtained on the coasts of Florida and Cuba, by the United States Coast Survey Gulf Stream Expeditions, in 1867, 1868, 1869. Bulletin of the Museum Comparative Zoology, Harvard 1(11):355–358.

Rasmussen, H. W. 1961. A Monograph on the Cretaceous Crinoidea. Der Kongelige Danske Videnskabernes Selskab. Biologiske Skrifter (12):1–428, pl. 1–60.

Reichensperger, August. 1905. Zur Anatomie von *Pentacrinus decorus*. Zeitschrift für wissenschaftliche Zoologie 80:3–35.

Reichensperger, August.1908. Über das Vorkommen von Drüsen bei Crinoiden. Zoologischer Anzeiger. 33: 363–367.

Reichensperger, August. 1912. Beiträge zur Histologie und zum Verlauf der Regeneration bei Crinoiden. Zeitschrift für wissenschaftliche Zoologie 101:1–69.

Rowe, F. W. E., A. K. Hoggett, R. A. Birtles, & L. L. Vail. 1986. Revision of some comasterid genera from Australia (Echinodermata: Crinoidea), with descriptions of two new genera and nine new species. Journal of the Linnean Society of London (Zoology) 86(3):197–277.

Russo, Achille. 1902. Studii su gli Echinodermi. Atti dell' Accademia Gioenia di Scienze Naturali in Catania (Ser. 4) 15(7):1–93, pl. I–III.

Saulsbury, J. 2019. Crinoid respiration and the distribution of energetic strategies among marine invertebrates. Biological Journal of the Linnean Society, 2019. p. XX, 1–15.

Scriba, M. E. L. 2015. Atlas of comparative invertebrate embryology, Vol. 4, Echinodermata I. F. Pfeil Verlag München. Germany. p. 7–33.

Seeliger, O., 1893. Studien zur Entwicklungsgeschichte der Crinoiden. Jahrbücher Abteilung Anatomie und Ontogenie der Tiere 6:161–444.

Steenstrup, J. J. S. 1847. Gebirgsarten und Versteinerungen vom Museum der Kopenhagener Universität. In: GA Michaelis & HF Scherk, Amtlicher Bericht über die 24. Versammlung Deutscher Naturforscher und Aerzte in Kiel 1846. Akademische Buchhandlung. Kiel. p. 117–119.

Teuscher, R. 1876. Beiträge zur Anatomie der Echinodermen. I. *Comatula mediterranea*. Jenaische Zeitschrift für Naturwissenschaft 10:243–262.

Thomson, C. W. 1864. Sea lilies. The Intellectual Observer 6:1–11.

Thomson, C. W. 1872. 2. On the Crinoids of the "Porcupine" Deep-Sea Dredging Expedition. Proceedings of the Royal Society of Edinburgh 7:764–773.

Thomson, C. W. 1876. Notice of new living crinoids belonging to the Apiocrinidae. Journal of the Linnean Society of London, Zoology 13:47–109.

Trotter, J. A., G. Lyons-Levy, D. Luna, T. J. Koob, D. R. Keene, & M. A. L. Atkinson. 1996. Stiparin: A glykoprotein from sea cucumber dermis that aggregates collagen fibrils. [https://www.sciencedirect.com/science/article/pii/S0945053X96901511].

Vail, Lane. 1987. Reproduction in five species of crinoids at Lizard Island, Great Barrier Reef. Marine Biology 95:431–446.

Welsch, Ulrich, Thomas Heinzeller, & J. L. S. Cobb. 1990. Ultrastructure and innervation of ligament connective tissue in *Antedon bifida* and *Decametra spec*. *In* C. de Ridder & others, eds., Echinoderm Research. Balkema. Rotterdam. p. 295–300.

Welsch, Ulrich, Thomas Heinzeller, & N. D. Holland, 1994. Ultrastructure and carbohydrate histochemistry of Reichensperger's organ in *Metacrinus rotundus*. *In* B. David & others, eds., Echinoderms through Time. Balkema. Rotterdam. p. 267–272.

Welsch, Ulrich, A. Lange, R. Bals, & Thomas Heinzeller. 1995. Juxtaligamental cells in feather stars and isocrinids. *In* R. Emson & others, eds., Echinoderm Research, Balkema. Rotterdam. p. 129–135.

Wilkie, I. C. 1979. The juxtaligamental cells of *Ophiocomina nigra* and their possible role in mechanoeffector function of collagenous tissue. Cell Tissue Research 197:515–530.

Wilkie, I. C., M. Candia Carnevali, & J. Trotter. 2004. Mutable collagenous tissue: Recent progress and an

evolutionary perspective. *In* Thomas Heinzeller & J. Nebelsick, eds., Echinoderms: München. Taylor & Francis Group. London. p. 339–349.

Wilkie, I. C., A. Barbaglio, W. M. Maclaren, & M. D. Candia Carnevali. 2010. Physiological and immunocytochemical evidence that glutamatergic neurotransmission is involved in the activation of arm autotomy in the featherstar *Antedon mediterranea* (Echinodermata, Crinoidea). The Journal of Experimental Biology 213:371–379.